UKRAS21 CONFERENCE:

"Robotics at home"

PROCEEDINGS

UKRAS21 Conference Proceedings: 2nd June 2021

UK-RAS NETWORK
ROBOTICS & AUTONOMOUS SYSTEMS

University of Hertfordshire UH

UKRI Engineering and Physical Sciences Research Council

Table of Contents

Introduction

Research Papers

Interactive Session Papers

https://doi.org/10.31256/Ft3Ex7U

#UKRAS21: The 4th UK Robotics and Autonomous Systems Conference

Patrick Holthaus, Farshid Amirabdollahian, Claire Asher, Arthur Richards

On behalf of the Organising and Advisory Committee we take great pleasure in welcoming students, researchers and experts in robotics virtually to #UKRAS21, the 4th UK-RAS Conference for PhD Students & Early-Career Researchers, organised by the EPSRC UK-RAS Network[1] in collaboration with Robot House[2] at the University of Hertfordshire. This exciting virtual event is specifically designed for PhD students and early-career robotics and autonomous systems researchers of the UK-RAS Network and will foster research progress and offer opportunities for networking.

I. Aims

The aim of #UKRAS21 is to promote quality research, networking, and community building for PhD students and practitioners at the frontier of science and technology in intelligent robots and systems, by discussing the latest advancements in this fast growing and exciting field. In the call for papers, we were particularly looking for submissions in areas including:

- Artificial Intelligence and Robotics
- Assistive Technologies and Rehabilitation
- Smart-Home and Robotics
- Virtual and Remote Robotics
- Robotics Research Methods During Social Restrictions
- Novel and Enabling Technologies

II. Topics

This year's theme focuses on *robotics at home*. We have identified three focus areas to examine robotics and autonomous systems within our call for papers that are each covered by an inspiring keynote and four oral presentations from authors of accepted papers: The focus area *robotics for use in the home* considers aspects of rapid prototyping, safety, assisted living, rehabilitation robotics, technology acceptance, and diverse user groups. Keynote speaker Prof. Ana Paiva (Instituto Superior Técnico, University of Lisbon and coordinator of GAIPS at INESC-ID) will talk about the engineering of sociality and collaboration between humans and robots. The oral paper presentations in this area are Exploring Human-Dog Attachment Behaviours and their Translation to a Robotic Platform [1]; Older adults' perceptions of Socially Assistive Robots [2]; Requirements for a home-based rehabilitation device for hand and wrist therapy after stroke [3]; and Robot House Human Activity Recognition Dataset [4].

A second focus area of #UKRAS21 aims to to discuss innovations in delivering robotics research while *working from home*, addressing challenges in remote working, on-line experimentation, digital twinning, or simulation. A keynote talk will be held by Prof. Ana Cavalcanti (Royal Academy of Engineering Chair in Emerging Technologies, University of York) about the RoboStar modelling stack and how to tackle the reality gap. The oral presentations in this area are: Test Framework for a Virtual Competition Testbed [5]; Visually-based Prediction of Artist's Drawing [6]; Design of a Transforming Myriapod Robot for Multimodal Locomotion [7]; and Development of a Teleoperative Quadrupedal Manipulator [8].

In a third focus area, we seek to understand how different robotic and autonomous systems *make themselves at home* by being tailored to suit their respective working environments, such as factories, offshore platforms, power plants, or disaster scenes. We are looking forward to a keynote by Dr Jelizaveta Konstantinova (Ocado Technology) that addresses robots the innovation at Ocado and the SecondHands project. The oral presentations in this area are: An Augmented Reality System for Safe Human-Robot Collaboration [9]; Firefighter Assistance Robot [10]; Small datasets for fruit detection with transfer learning [11]; and A Non-Axisymmetric Parallel Manipulator for Head Stabilisation in Vitreoretinal Surgery [12].

III. Statistics and Format

We have received 35 submissions, of which 12 were accepted as oral presentations in a single track conference format. 17 submissions were invited to produce a brief video clip of their work that we will present in a compilation during the main conference. Authors can then discuss their work with the other delegates in a parallel interactive session, which is our online replacement for the poster session in previous years. We want to thank Claire Asher and Christoph Salge for their dedication in preparing and running the online meeting. In total, we accepted 84% of submissions. Accepted papers are from 22 UK universities and one international collaboration, with ratios shown in Fig. 1. Last year's host institution and this year's host of TAROS[3], the University of Lincoln as well as this year's host, the University of Hertfordshire and King's College London are the most frequent author affiliations.

All papers have received two or more independent reviews from the 40 reviewers that participated in the selection process. The majority of reviews are from the Universities of Hertfordshire, Leeds, Lincoln, and Sheffield Hallam. Fig. 2 depicts all 16 reviewer affiliations.

Patrick Holthaus (University of Hertfordshire) and Farshid Amirabdollahian (University of Hertfordshire) are General Chair and General Co-Chair of #UKRAS21. Claire Asher (UK-RAS Network) and Arthur Richards (Bristol Robotics Lab) are Technical Chair and Programme Chair of #UKRAS21.

[1]https://ukras.org/

[2]https://robothouse.herts.ac.uk/

[3]https://lcas.lincoln.ac.uk/wp/taros-2021/

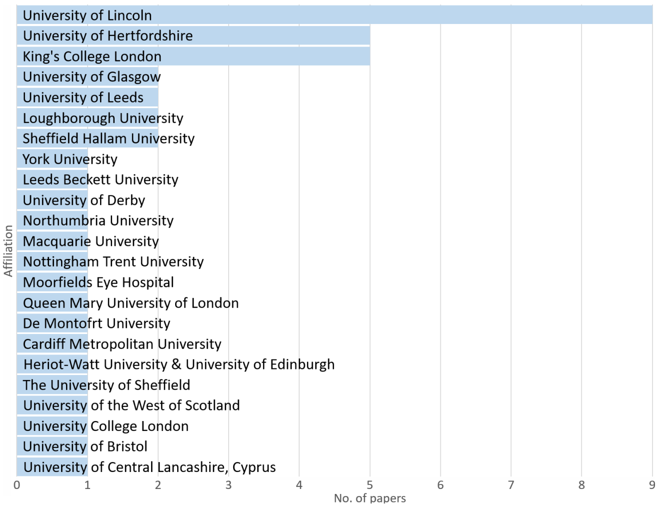

Fig. 1. Distribution of author affiliations

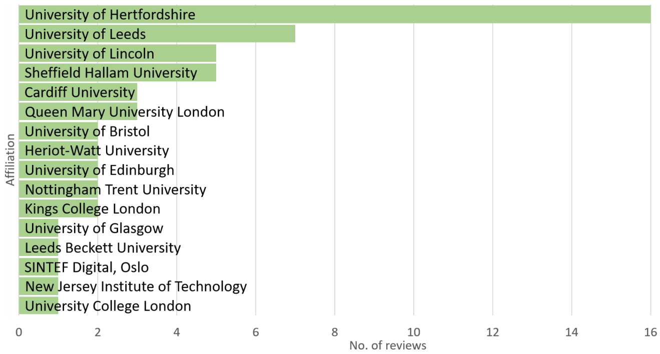

Fig. 2. Distribution of reviewer affiliations

IV. Programme

We would like to express our gratitude for handling the review process and the selection of papers to the members of the programme committee, consisting of Farshid Amirabdollahian, Claire Asher, Frank Förster, Charles Fox, Patrick Holthaus, Gabriella Lakatos, Arthur Richards, Alessandra Rossi, and Christoph Salge.

The committee encouraged authors that are early career researchers to participate in the review process and paired each of them with a more experienced researcher from another institute. We greatly acknowledge the support of 17 reviewers who we consider early career researchers. Additional reviewers were sourced from other UK-RAS member organisations. In total, all submissions have been reviewed by at least two independent reviewers, scoring between 3 (strong accept) and -3 (strong reject), with 0 as borderline. Occasionally, papers were reviewed more than twice, for example where reviewer opinions differed significantly. The conference aims to be inclusive so all papers with average scores of 0 or greater have been accepted.

The 12 highest scoring papers were selected for oral presentation, subject to a limit of no more than one oral presentation per author. Keynotes were invited at the discretion of the programme committee as well established experts within their respective focus area. Awards will be given to the best paper and interactive presentation as selected by a committee comprising programme committee members of #UKRAS21.

We would particularly like to thank Abolfazl Zaraki, Adrian Salazar Gomez, Aidan Scannell, Alessandro Di Nuovo, Amy K. Hoover, Antonia Tzemanaki, Ataollah Ramezan Shirazi, Bente Riegler, Burak Kizilkaya, Catherine Menon, Chengxu Zhou, Christopher Peers, Dan Dai, Elizabeth Sklar, Emanuele De Pellegrin, Emily Rolley-Parnell, Florence Sherry, Hans Natalius, Ildar Farkhatdinov, Ionut Moraru, Junfeng Gao, Karen Archer, Kaspar Althoefer, Leonardo Guevara, Luke Wood, Mark Judge, Maryam Banitalebi Dehkordi, Md Zia Uddin, Mohamad Reza Shahabian Alashti, Mohammad Hossein Bamorovat Abadi, Mohammed Rezwan Rahman, Moustafa Motawei, Mubashir Ahmad, Nicola Camp, Nicola Catenacci Volpi, Robert Richardson, Simon Parsons, Steve Maddock, Vignesh Velmurugan, and Yaniel Carreno for contributing their reviews to the conference.

References

[1] K. Riddoch, E. Cross, and R. Hawkins, “Exploring Human-Dog Attachment Behaviours and their Translation to a Robotic Platform,” in *Proceedings of the 4th UK-RAS Conference: Robotics at Home (#UKRAS21)*, 2021.

[2] N. Camp, J. Johnston, M. Lewis, M. Zecca, K. Hunter, A. D. Nuovo, and D. Magistro, “Older adults’ perceptions of Socially Assistive Robots,” in *Proceedings of the 4th UK-RAS Conference: Robotics at Home (#UKRAS21)*, 2021.

[3] V. Velmurugan, L. Wood, and F. Amirabdollahian, “Requirements for a home-based rehabilitation device for hand and wrist therapy after stroke,” in *Proceedings of the 4th UK-RAS Conference: Robotics at Home (#UKRAS21)*, 2021.

[4] M. H. B. Abadi, M. R. S. Alashti, C. M. Patrick Holthaus, and F. Amirabdollahian, “Robot House Human Activity Recognition Dataset,” in *Proceedings of the 4th UK-RAS Conference: Robotics at Home (#UKRAS21)*, 2021.

[5] L. Wellacott, E. Nault, I. Skottis, A. Colle, S. N. Gowda, P. Nicolay, and E. Rolley-Parnell, “Test Framework for a Virtual Competition Testbed,” in *Proceedings of the 4th UK-RAS Conference: Robotics at Home (#UKRAS21)*, 2021.

[6] C. Jansen and E. Sklar, “Visually-based Prediction of Artist’s Drawing,” in *Proceedings of the 4th UK-RAS Conference: Robotics at Home (#UKRAS21)*, 2021.

[7] F. Sherry and C. Zhou, “Design of a Transforming Myriapod Robot for Multimodal Locomotion,” in *Proceedings of the 4th UK-RAS Conference: Robotics at Home (#UKRAS21)*, 2021.

[8] C. Peers, M. Motawei, R. Richardson, and C. Zhou, “Development of a Teleoperative Quadrupedal Manipulator,” in *Proceedings of the 4th UK-RAS Conference: Robotics at Home (#UKRAS21)*, 2021.

[9] Y. E. Cogurcu and S. Maddock, “An Augmented Reality System for Safe Human-Robot Collaboration,” in *Proceedings of the 4th UK-RAS Conference: Robotics at Home (#UKRAS21)*, 2021.

[10] M. Judge and L. Riches, “Firefighter Assistance Robot,” in *Proceedings of the 4th UK-RAS Conference: Robotics at Home (#UKRAS21)*, 2021.

[11] D. Dai, J. Gao, S. Parsons, and E. Sklar, “Small datasets for fruit detection with transfer learning,” in *Proceedings of the 4th UK-RAS Conference: Robotics at Home (#UKRAS21)*, 2021.

[12] H. Natalius, P. Lambert, L. da Cruz, and C. Bergeles, “A Non-Axisymmetric Parallel Manipulator for Head Stabilisation in Vitreoretinal Surgery,” in *Proceedings of the 4th UK-RAS Conference: Robotics at Home (#UKRAS21)*, 2021.

https://doi.org/10.31256/Xe8Wm4U

An Augmented Reality System for Safe Human-Robot Collaboration*

1st Yunus Emre Cogurcu
Department of Computer Science
The University of Sheffield
Sheffield, United Kingdom
yecogurcu1@sheffield.ac.uk

2nd Steve Maddock
Department of Computer Science
The University of Sheffield
Sheffield, United Kingdom
s.maddock@sheffield.ac.uk

***Abstract*—Closer interaction in Human-Robot Collaboration (HRC) could result in increased worker efficiency in manufacturing situations. However, physical cages often limit this. Our research is investigating the potential for using Augmented Reality (AR) to visualise virtual safety zones, thus replacing real cages. This paper presents initial experiments towards addressing the issues of how to display the safety zones and what size they should be in relation to a robot arm in order to ensure safe working practices.**

***Index Terms*—augmented reality (AR), safety, human-robot collaboration (HRC)**

I. Introduction

Industry standards and practices for human-robot collaboration (HRC) are based on the principle of separating operator and robot work areas and detecting separation violations using sensors or physical cages [10]. However, more flexibility and efficiency could potentially be achieved if there were closer cooperation between human and robot [3], [6]. Augmented Reality (AR) could be used to achieve this by adding virtual safety cages to an environment instead of real cages.

AR in HRC has been investigated in terms of human safety and overall system productivity [7], [10], with [7] concluding that AR is a powerful tool for the visualisation of robot operations and safe areas. Different kinds of virtual safety barrier have been considered, including 2D fields [6], safety curtains [3] and user-configurable barriers (including around the user) [4], along with more general work on how to provide feedback for users [9]. However, the issues of safety zone size in relation to a robot arm and how to display the safety zones remain unresolved. Our paper considers these issues.

The initial experiments we report on use a virtual robot arm. This creates a safe testing environment, allowing quicker, safe feedback on parameter variation, e.g. safety zone size. The system makes use of Robot Operating System (ROS-Industrial) and HoloLens 2 so the work could easily transfer to using a real robot arm (when COVID restrictions allow).

* This work was supported by the Ministry of National Education (Turkey).

II. The System

The system brings together Unity, ROS-Industrial and HoloLens 2. Whilst earlier AR studies made use of HoloLens 1 (e.g.[3], [6]), HoloLens 2 is lighter and more ergonomic that the HoloLens 1, has an increased field of view (FOV) and is now used widely in industry. The Unity real-time engine on Windows 10 is used as the development environment and to deploy HoloLens apps. ROS-Industrial on Linux (Ubuntu 18.04 in our system) is used to control the robot arm. ROS-Sharp [2] is used as the basis for communication between Unity and ROS. A similar ROS-Sharp-based approach is used to communicate between ROS and HoloLens, with the HoloLens used for AR display and user interaction.

The general idea behind our approach to AR is to align a virtual robot arm with a real robot arm using a QR code and some initial user interaction. HoloLens 2 is able to detect QR codes and establish a coordinate system for the QR code object's real-world location. Thereafter ROS commands can be used to keep the real robot arm and the virtual robot arm in sync, with the virtual robot arm being made invisible (a phantom model), but facilitating the addition and HoloLens display of AR information in relation to the real robot arm. The initial tests are done as a simulation, for safety purposes, but the same processes could be used for a real robot arm once the virtual and real robot arms are aligned.

III. Safety Zone Experiments

For the initial experiments, the system is used to control a virtual UR10 robot arm whilst using AR to overlay a safety zone around the robot arm. The kinematic calculations for the trajectory of the robot arm were performed using the ROS MoveIt library. The safety zones are used in detecting proximity violations so that the user is warned and the movement of the robot arm is stopped. The questions to be considered are how large the safety zones should be and how to display them.

The first consideration is safety zone size. However, there is some uncertainty in the published safety standards about size [1]. Four approaches were considered. Safety Zone 1 is a large static safety zone that includes a range of possible points that the robot arm can reach (figures 1a, 1b and 1c show cuboid, cylinder and sphere versions, respectively). Safety Zone 2 is again static and encloses only the volume required for a specific task (figure 1d). Safety Zone 3 is a dynamic volume that grows and shrinks as the robot arm moves (figure 1e). Safety Zone 4 wraps the robot arm in a number of closer-fitting shapes that move with the robot arm (figure 1f).

Safety Zone 1 (cuboid version) is similar to a standard safety cage, keeping the user away from the robot arm for a range of possible tasks. Overall, Safety Zone 1 is the safest approach of the four, but may not produce the most effective HRC. The cuboid version includes dead space that the robot arm never reaches and is perhaps too general depending on how often each of the range of tasks it includes is done. The amount of dead space can be reduced by changing the shape of the safety zone to a cylinder or sphere, as shown in figures 1b and 1c. Safety Zone 2 shrinks the safety zone covering only the zone required for the specific task. This would be equivalent to a physical cage that could be reconfigured, possibly saving on factory floor space. Safety Zones 3 and 4 provide the opportunity to work more closely with the robot arm, but are potentially less safe that the other two static safety zones. A range of factors means that a dynamic safety margin must be considered in each case. The speed of the user and the robot arm become more important. For example, ISO 13855 [8] recommends that if the speed of the operator or user is 2000mm/s and the robot arm speed is 1600mm/s, the safety distance should be greater than 500mm. However, humans are unpredictable, different users may feel safer with larger safety zones than calculated, and robot sensors have latencies that must also be considered. These issues complicate the calculation of safety margins.

The second aspect is how to display the safety zones. This is currently user configurable. Figures 1f and 1g show highlighted edges and enhanced edges, respectively. It is also possible to change the colour used to display the safety zone. Other work [3], [6] does not have this level of user configuration. Red was chosen as the safety zone colour as it is a warning signal in many countries and edge highlighting makes the volumetric space of the safety zone clearer. However, user testing is still required to determine the best way to visualise the safety zones.

The warning message that is displayed when a safety zone is breached by the user. This causes the virtual robot arm to immediately stop moving.

(a) Large static safety zone (cube) to cover a range of robot movements

(b) Cylinder version of figure 1a

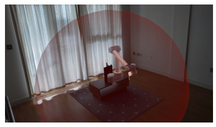

(c) Sphere version of figure 1a

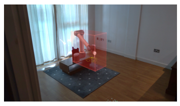

(d) Task-specific static safety zone with edge highlighting

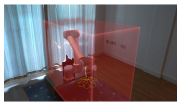

(e) Dynamic safety zone resizing as the robot arm moves

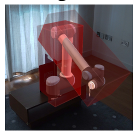

(f) Moving sectional safety zones with edge highlighting

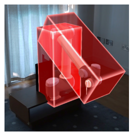

(g) Enhanced edge highlighting for figure 1f

Fig. 1: Safety zone visualisations

IV. Conclusions

We have presented a system that uses Microsoft HoloLens 2 to display AR information in relation to a robot arm. For safety reasons, initial experiments have used a virtual robot arm instead of a real robot arm. Different safety zones are visualised around the robot arm in a range of visualisation styles and a warning is given if the safety zone is violated by the user. The use of safety zones is still an active research challenge [5]. The next steps in our work are to conduct user tests on how best to display safety information and to test the system with a real robot arm. The target system for these experiments will be a spot welding system which currently uses a combination of cage and sensors to separate a user and the robot arm and the spot welding machinery.

References

[1] ISO/TS 15066. Robots and robotic devices – collaborative robots, Geneva, 2016.

[2] Dr. Martin Bischoff. Ros-sharp. https://github.com/siemens/ros-sharp, 2021. [Online; accessed 22 March 2021].

[3] Antti Hietanen, Roel Pieters, Minna Lanz, Jyrki Latokartano, and Joni-Kristian Kämäräinen. Ar-based interaction for human-robot collaborative manufacturing. *Robotics and Computer-Integrated Manufacturing*, 63:101891, 2020.

[4] Khoa Cong Hoang, Wesley P Chan, Steven Lay, Akansel Cosgun, and Elizabeth Croft. Virtual barriers in augmented reality for safe and effective human-robot cooperation in manufacturing. *arXiv preprint arXiv:2104.05211*, 2021.

[5] Eugene Kim, Yoji Yamada, Shogo Okamoto, Mikihiro Sennin, and Hiroki Kito. Considerations of potential runaway motion and physical interaction for speed and separation monitoring. *Robotics and Computer-Integrated Manufacturing*, 67:102034, 2021.

[6] Konstantinos Lotsaris, Nikos Fousekis, Spyridon Koukas, Sotiris Aivaliotis, Niki Kousi, George Michalos, and Sotiris Makris. Augmented reality (ar) based framework for supporting human workers in flexible manufacturing. *Procedia CIRP*, 96:301–306, 2021.

[7] George Michalos, Sotiris Makris, Panagiota Tsarouchi, Toni Guasch, Dimitris Kontovrakis, and George Chryssolouris. Design considerations for safe human-robot collaborative workplaces. *Procedia CIrP*, 37:248–253, 2015.

[8] ISO 13855 – Safety of Machinery. Positioning of safeguards with respect to the approach speeds of parts of the human body, 2010.

[9] CY Siew, AYC Nee, and SK Ong. Improving maintenance efficiency with an adaptive ar-assisted maintenance system. In *Proceedings of the 2019 4th International Conference on Robotics, Control and Automation*, pages 74–78. ACM, 2019.

[10] Valeria Villani, Fabio Pini, Francesco Leali, and Cristian Secchi. Survey on human–robot collaboration in industrial settings: Safety, intuitive interfaces and applications. *Mechatronics*, 55:248–266, 2018.

https://doi.org/10.31256/Nf6Uh8Q

Small datasets for fruit detection with transfer learning*

Dan Dai
LIAT, University of Lincoln
DDai@lincoln.ac.uk

Junfeng Gao
LIAT, University of Lincoln
JuGao@lincoln.ac.uk

Simon Parsons
L-CAS, University of Lincoln
Sparsons@lincoln.ac.uk

Elizabeth Sklar
LIAT, University of Lincoln
ESklar@lincoln.ac.uk

***Abstract*—A common approach to the problem of fruit detection in images is to design a deep learning network and train a model to locate objects, using bounding boxes to identify regions containing fruit. However, this requires sufficient data and presents challenges for small datasets. Transfer learning, which acquires knowledge from a source domain and brings that to a new target domain, can produce improved performance in the target domain. The work discussed in this paper shows the application of transfer learning for fruit detection with small datasets and presents analysis between the number of training images in source and target domains. This investigation is based on three datasets: two containing tomatoes and one containing strawberries. Experimental results indicate that transfer learning can enhance prediction with limited data.**

***Index Terms*—fruit detection, limited datasets, transfer learning, target domain**

I. Introduction

Within the task domain of plant phenotyping, fruit detection is a difficult problem, particularly when trying to identify objects of interest in small image datasets. *Deep learning* is a common approach, using multi-layered *Convolutional Neural Networks (CNNs)* to obtain feature maps, but these networks require sufficient numbers of training examples in order to produce accurate results. *Transfer learning* enables reusing knowledge acquired previously from other tasks or applications and could greatly improve the performance of learning by avoiding various expensive efforts [7].

Recently, several deep learning architectures have been developed from the basic *Region-based CNN (R-CNN)* [4], including *Faster R-CNN* [9], *YOLO* [8] and *Single Shot MultiBox Detector (SSD)* [6]. Most of the machine learning approaches to fruit detection apply these Faster or Mask R-CNN methods [2], [13]. In contrast, transfer learning approaches applied to the agriculture domain mainly focus on identifying plant species [5], classifying pests [12] or diseases [1].

The general principle underlying transfer learning is to take a model trained from data in a *source* domain and adjust this model to a new dataset in a *target* domain. Research in this area has explored the impact of the size of the source dataset and number of labelled examples on the results [1], [2]; but little work has studied these properties in the target domain. The work presented here asks the following questions: Is the size of the source and/or target training sets associated with the accuracy of detection? Is it possible to get the ideal performance in the target domain without carrying out training on large amounts of annotated data (source domain)?

As we already have some knowledge learned from the source domain, therefore it can be saving model training time and resources consumed for the task.

II. Methods

This section presents the basic SSD [6] framework we applied for strawberry and tomato detection, then introduces the transfer learning methods employed. We analyse the relationship between the training dataset size in the source domain and the number of labels in the target domain with respect to the results obtained.

SSD is a one-stage detection system; it eliminates proposal generation and subsequent pixels or feature re-sampling stages, then encapsulates all computation in a single network. This model contains multi-scale feature maps and convolutional predictors for detection, sets default bounding boxes and aspect ratios and allows for different default bounding box shapes in several feature maps to discretize the space of predicted bounding boxes efficiently.

The experiments presented here explore the application of transfer learning for detecting fruits in images. The features learned from a source dataset are transferred to two different new target datasets, each of which may not contain enough training data, due to a paucity of examples or labels. We analyse our results by comparing the accuracy values when transferring from the source to each target, investigating the relationship between these metrics and sizes of the source and target training sets.

(a) T1 (b) T2 (c) SR

Fig. 1. Tomato and strawberry examples in our datasets.

III. Experimental Setup

a) Datasets and Training Parameters: Our experimental data is comprised of three datasets: two different types of tomato (T1, T2) and strawberry (SR). These datasets are collected under different conditions: the strawberry images are all from a polytunnel, whereas the tomato images in T1 are from a garden, showing different growth stages, and the images in T2 are from the Internet.The backgrounds, lighting conditions and other factors differ, so there is some diversity across the data sets. Detailed information about our datasets is shown in Table I and Fig. 1. In our SSD model, the backbone is VGG-16 [11] and is pre-trained with ImageNet [3]. The batch size is 4 and the learning rate is $1e-4$ with the SGD optimizer [10] setting the momentum to 0.9.

TABLE I

NUMBERS OF IMAGES IN OUR DATASETS

Dataset	*Total*	*Training*	*Testing*
T1	496	396 (80%)	100 (20%)
T2	73	59 (80%)	14 (20%)
SR	124	99 (80%)	25 (20%)

b) Transfer learning between tomato and strawberry data sets: Our goal is to quantify the influences of the numbers of training images in the source (T1) and target domains (SR or T2). The number of training images are randomly partitioned as follows: into four parts for the source domain, T1[1]; into twelve parts for SR[2]; and into seven parts for T2[3]. The number of images in each test set (SR and T2) is almost 20% of each total. Table II shows the results of transferring the T1 model to different sized datasets of SR and T2 images. Results are also shown graphically in Fig 2. For comparison, we also trained SSD models with the SR and T2 datasets (3000 iterations). The mAP values we obtained for these models are 0.354 and 0.789, respectively.

TABLE II

RESULTS OF TRAINING ON SR AND T2 AND SELECTED MAP RESULTS FOR TRANSFER LEARNING FROM DIFFERENT-SIZED T1 DATASETS TO SR AND T2 (BEST PERFORMANCE IN EACH ROW IN BOLD)

Training/test	mAP	Training/test	mAP
(SR) (99/25)	0.354	(T2) (59/14)	0.789

Source (T1) (training/test)	Target	0	10	50	60(59)[1]	90	Avg
62(49/13)	SR	0.076	0.299	**0.393**	0.383	0.380	0.3363
	T2	0.779	0.739	**0.796**	0.788	– [2]	0.7714
124(99/25)	SR	0.108	0.274	0.350	**0.394**	0.338	0.3154
	T2	0.798	0.794	**0.813**	0.764	–[2]	0.7904
248(198/50)	SR	0.067	0.334	0.359	**0.401**	0.381	**0.3368**
	T2	0.827	0.764	0.827	**0.829**	–[2]	**0.7961**
496(396/100)	SR	0.052	0.304	0.303	0.378	**0.380**	0.3240
	T2	0.810	0.759	**0.838**	0.811	–[2]	0.7933
Avg	SR	0.0758	0.3027	0.3513	**0.3890**	0.3698	
	T2	0.8035	0.7640	**0.8186**	0.7980	–[2]	

[1] 60(59) means 60 training images for SR and 59 for T2.

[2] – refers to the fact that T2 has fewer training images (i.e. <90)

If we use the source model without any re-training (i.e. number of target training images is 0), as the number of training images in T1 increases, fruit detection performance in SR decreases. This is because of the feature difference between strawberry and tomato: with more source data training, features learned by the model are more related to tomatoes. In contrast, detection accuracy for T2 improves as the source dataset size increases. We also find that T2 provides better detection results if we do not use any images to re-train the source model.

Examining the relation between the numbers of training images in the source and target datasets, the best average performance is with $\mathsf{T1}=248$. For T2, the average results are better than training on the target domain only ($0.7961 > 0.789$). As the size of the source training dataset increases, the detection results in the target domain seem to reach a saturation state. This suggests that we don't need to train and label large amounts of data in the target domain in order to get high performance, thus saving model training time and resources consumed for the task. Indeed, judging from the current results, using a target dataset that is almost half the size of the source dataset achieves high detection performance.

[1]The four partitions of the T1 dataset each contain {62,124,248,496} images, respectively.

[2]The twelve partitions of the SR dataset each contain {0,5,10,20,30,40,50,60,70,80,90,99} images, respectively.

[3]The seven partitions of the T2 dataset each contain {0,5,10,20,40,50,59} images, respectively.

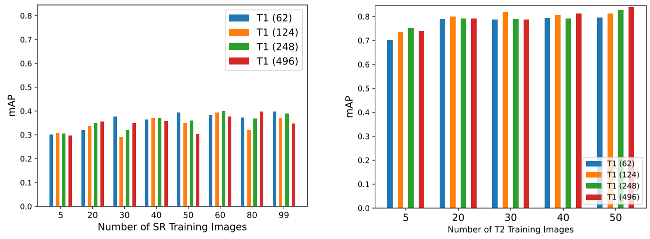

Fig. 2. Results of transfer learning from T1 to SR (left) and T2 (right). mAP is shown for different numbers of images.

IV. SUMMARY AND NEXT STEPS

We applied transfer learning to fruit detection in limited datasets and analysed the impact of the number of the training images in the source and target domains. Next, we will consider how to reduce the features distribution differences between the source and target domains to improve detection performance, discuss and explain the effects of transfer from small samples to large data sets.

REFERENCES

[1] J. G. A. Barbedo. Impact of dataset size and variety on the effectiveness of deep learning and transfer learning for plant disease classification. *Computers and Electronics in Agriculture*, 153, 2018.

[2] S. Bargoti and J. Underwood. Deep fruit detection in orchards. In *IEEE Intl Conf on Robotics and Automation (ICRA)*, 2017.

[3] J. Deng, W. Dong, R. Socher, L.-J. Li, K. Li, and L. Fei-Fei. Imagenet: A large-scale hierarchical image database. In *IEEE Conf on Computer Vision and Pattern Recognition (CVPR)*, 2009.

[4] R. Girshick and J. Donahue. Rich feature hierarchies for accurate object detection and semantic segmentation. In *IEEE Conf on Computer Vision and Pattern Recognition (CVPR)*, 2014.

[5] A. Kaya, A. S. Keceli, C. Catal, H. Y. Yalic, H. Temucin, and B. Tekinerdogan. Analysis of transfer learning for deep neural network based plant classification models. *Computers and Electronics in Agriculture*, 158, 2019.

[6] W. Liu, D. Anguelov, D. Erhan, C. Szegedy, S. Reed, C.-Y. Fu, and A. C. Berg. SSD: Single shot multibox detector. In *European Conference on Computer Vision (ECCV)*. Springer, 2016.

[7] S. J. Pan and Q. Yang. A survey on transfer learning. *IEEE Trans on Knowledge and Data Engineering*, 22(10), 2009.

[8] J. Redmon and A. Farhadi. Yolov3: An incremental improvement. *arXiv preprint arXiv:1804.02767*, 2018.

[9] S. Ren, K. He, R. Girshick, and J. Sun. Faster R-CNN: Towards real-time object detection with region proposal networks. In *Advances in Neural Information Processing Systems*, 2015.

[10] H. Robbins and S. Monro. A stochastic approximation method. *The Annals of Mathematical Statistics*, 22(3), 1951.

[11] K. Simonyan and A. Zisserman. Very deep convolutional networks for large-scale image recognition. *arXiv preprint arXiv:1409.1556*, 2014.

[12] K. Thenmozhi and U. S. Reddy. Crop pest classification based on deep convolutional neural network and transfer learning. *Computers and Electronics in Agriculture*, 164, 2019.

[13] Y. Yu, K. Zhang, L. Yang, and D. Zhang. Fruit detection for strawberry harvesting robot in non-structural environment based on Mask-RCNN. *Computers and Electronics in Agriculture*, 163, 2019.

https://doi.org/10.31256/Yo6Ds5M

Firefighter Assistance Robot

Lewis Riches
School of Built Environment, Engineering and Computing
Leeds Beckett University
Leeds, UK
l.riches6426@student.leedsbeckett.ac.uk

Dr Mark Judge
School of Built Environment, Engineering and Computing
Leeds Beckett University
Leeds, UK
m.s.judge@leedsbeckett.ac.uk

***Abstract*—This work sets out to explore the supporting role an intelligent robotics system might play in gathering and processing the initial data from fire incidents. Initial findings from this developing project indicate that having a continually updating map of internal conditions improves accuracy of route planning and potentially the ability of crews to reach casualties and stabilise the building with increased efficiency.**

***Index Terms*—Firefighting Robot, Field Robotics, Planning, Mapping, Simulation**

I. Introduction

Cognitive load theory suggests that too much stimuli offered at one time can cause key information to be missed [1]. The maximum capacity of the short-term memory has now been found to be only 4±1 pieces of information at one time [2]. Fire incidents are complex environments at which it is essential for crews to have as much information as possible, including during approach and upon arrival at the scene. Duty of care to preserve life (both crew and casualties) is the overriding priority, along with considerations for the environment and building. Existing protocol [3] states that, when a major fire incident is declared, a human command structure can be set up. Such a structure allows for the decision making and processing of stimuli to be spread across a large body of personnel reducing cognitive load on an individual. Along with a command structure, the technique of sectorisation can be used to divide large buildings into smaller sections, further reducing the amount of stimuli one team or individual needs to process. However, there is limited information and preparation opportunities whilst the crews are en route. UK Government statistics show the average response time to a fire incident, within the UK, is 8 minutes and 49 seconds [4]. Thus, the time after arrival is used to formulate a plan to tackle the incident, often using paper maps and further witness testimony. By creating supportive intelligent robotic systems, containing layout, construction and internal hazard information, the 8 minute response time could be better used to develop and evaluate a plan(s) for the incident.

II. Computer Simulation

Whilst there is much work taking place in the field of physical firefighter assistance robotics [5][6][7], due to the scale of such projects, together with the COVID19 global-pandemic situation, it was decided that all initial research work would be conducted using computer simulation software. Simulation software allows for the generation of digital models of real-world objects and environments. These digital models provide researchers the ability to change any detail of the model allowing for full flexibility of the environments to make them as realistic and accurate as possible and create any scenarios of the environment required. To enable this realism the software requires a physics engine to apply real world physics to the models generated [8].

TABLE I
Simulation software requirments

Functional Requirments	Non-Functional Requirments
Accurate Physics Engine	Easy to use interface
Realistic 3D renderer	Simple documentation
Real-time playback	Low impact on computer resources
	C, Ros and Matlab Support

Table I summarises the main requirements of the simulation software to be used for this project, along with optional requirements of supporting C++ or Python. The packages considered for this work were: Webots [9], Gazebo [10] and CoppeliaSim [11]. In order to determine the most appropriate of these, Multiple Criteria Decision Analysis (MCDA) [12] was used. Table II shows the results of the analysis, leading to the use of Webots for this work.

TABLE II
MCDA results

Criteria	***Rank***	***Weight***	**Score**		
			Gazebo	***Webots***	***CoppeliaSim***
Controller	1	40	80	200	200
Physics Engine	2	30	150	150	150
User interface	4	10	20	50	20
3D renderer	3	20	60	80	60
Total		100	310	480	430

III. Implementation

As an initial proof of concept, the A* algorithm [13] was chosen as the search method to be used since it employs a heuristic based search. A* was chosen over other algorithms such as simultaneous localisation and mapping (SLAM) [14] due to its capacity as an informed search approach, which allows it to analyse a map and plot the quickest route. For this research, the system will be provided with an initial structural outline of the building, which will be given in the form of a binary occupancy map [15]. Real world implementation could use CCTV [16], drones [17], ad-hoc networks interacting with smart devices [18] or building information modelling [19] to generate the occupancy map but for this research this was provided using a graphical user interface to mark the outline on a grid. Initial route planning was performed on this occupancy map. Once the system was following the planned route, it was able to use LiDar [20] and distance sensors to update the map with potential hazards encountered, replanning to avoid obstacles. When the system reaches its target location it then provides a final updated version of the binary occupancy.

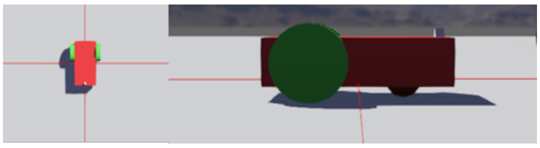

Fig. 1. Scenario Overviews

A straightforward robotics test system was modelled and used in this first phase of the project. To sense the external environment the system uses four distance sensors. Their trajectories are shown by the red lines in figure 1. Additionally a 360 degree lidar sensor was used. For internal sensing, the system has two motor encoders one for each wheel along with inertial units for sensing roll, pitch, and yaw.

IV. Execution and Results

Each scenario was completed in Webots and all files and maps provided were generated ahead of time and were not included in the execution speeds recorded. As this is early-stage work, 3 simple scenarios have been executed. Each scenario defined a start (green square) and target point (red square) with obstacles (black square) and available space (white square). Each scenario was given the initial map shown in Fig2 A and the final updated maps are shown in Fig 2 A, B and C with the robot's path shown by the yellow path. Definitions of the three scenarios are also shown below.

- Scenario 1 – Static environment, no obstacles (Fig2 A).
- Scenario 2 – Static environment, one obstacle (Fig2 B).
- Scenario 3 – Static environment, two obstacles (Fig2 C).

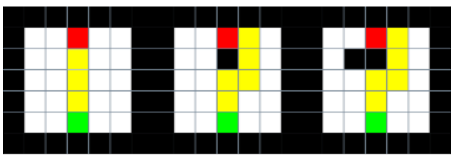

Fig. 2. Scenario Overviews

TABLE III
Simulation Results

Scenario	Execution Times	Observation
Scenario 1	20s	Reached target sqaure
Scenario 2	49s	Reached target sqaure
Scenario 3	49s	Reached target sqaure

V. Conclusion and Future Work

Early findings (Table III) suggest a continually updating map of an internal structure and hazards could expedite decision making, locate trapped civilians, identify fire sources, potential hazards and structural defects by passing this information to inbound fire crews. Execution times show the robot can quickly move to its target location while simultaneously mapping its environment and re-planning its route when required. To further analyse the benefit this robot could provide, further simulation testing will be completed in realistic environments. Interrogation of simulation results can provide evidence of whether the system can efficiently map a large complex environment but also complete the mapping before fire crews arrive on the scene (8 minutes and 49 seconds). To test the full impact this system could have on reducing cognitive load, virtual reality (VR) could be used to put firefighters in realistic situations but with no risk to life.

References

[1] P. Chandler and J. Sweller, "Cognitive Load Theory," Cogn. Instr., vol. 8, no. 4, pp. 293–332, 1991.
[2] N. Cowan, "The magical number 4" Behav. Brain Sci., vol. 24, no. 1, pp. 87–114, 2001
[3] London Fire Brigade, "Incident Command." https://www.london-fire.gov.uk/about-us/services-and-facilities/techniques-and-procedures/incident-command/
[4] Home Office, "Response times to fires" 2020.
[5] A. Han, "Meet the Robot Firefighter That Battled the Notre Dame Blaze," Apr. 17, 2019. https://www.popularmechanics.com/technology/robots/a27183452/robot-firefighter-notre-dame-colossus/
[6] M. Stewart, "LAFD Debuts the RS3" Oct. 13, 2020. https://www.lafd.org/news/lafd-debuts-rs3-first-robotic-firefighting-vehicle-united-states
[7] J. Penders et al., "A robot swarm assisting a human fire-fighter," Adv. Robot., vol. 25, no. 1–2, pp. 93–117, 2011
[8] T. Erez, Y. Tassa, and E. Todorov, "Simulation tools for model-based robotics" Proc. - IEEE Int. Conf. Robot. Autom., pp. 4397–4404, 2015
[9] O. Michel, "WebotsTM: Professional Mobile Robot Simulation," vol. 1, no. 1, pp. 39–42, 2004
[10] N. Koenig and A. Howard, "Design and use paradigms for Gazebo" 2004 IEEE/RSJ Int. Conf. Intell. Robot. Syst., vol. 3, pp. 2149–2154, 2004
[11] Coppelia Robotics, "versionInfo," 2020 https://www.coppeliarobotics.com/helpFiles/en/versionInfo.html
[12] UK Government, "Multi-criteria analysis manual" 2009. https://www.gov.uk/government/publications/multi-criteria-analysis-manual-for-making-government-policy.
[13] P. Hart, N. Nilsson, and B. Raphael, "A Formal Basis for the Heuristic Determination of Minimum Cost Paths," IEEE Trans. Syst. Sci. Cybern., vol. 4, no. 2, pp. 100–107, 1968
[14] J. J. Leonard and H. F. Durrant-Whyte, "Simultaneous map building and localization for an autonomous mobile robot," in Proceedings IROS '91:IEEE/RSJ Int. Workshop Intel. Robots '91, pp. 1442–1447.
[15] H. Moravec and A. Elfes, "High resolution maps from wide angle sonar" Proc. 1985 IEEE Int. Conf. Robot. Autom, vol. 2, pp. 116–121
[16] P. Gomes, P. Santana, and J. Barata, "A vision-based approach to fire detection," Int. J. Adv. Robot. Syst., vol. 11, pp. 1–12, 2014.
[17] E. Yanmaz, S. Yahyanejad, B. Rinner, H. Hellwagner, and C. Bettstetter, "Drone networks," Ad Hoc Networks, vol. 68, no. September, pp. 1–15, 2018.
[18] A. Boukerche and R. W. L. Coutinho, "Smart Disaster Detection and Response System" Proc. - IEEE Symp. Comput. Commun., pp. 1102–1107, 2018.
[19] C. Eastman, "Outline Building Description System" p. 23, 1974.
[20] Y. Li and J. Ibanez-Guzman, "Lidar for Autonomous Driving" IEEE Signal Process. Mag., vol. 37, no. 4, pp. 50–61, 2020

https://doi.org/10.31256/Yi5Od4A

A Non-Axisymmetric Parallel Manipulator for Head Stabilisation in Vitreoretinal Surgery

Hans Natalius
Med Physics and Biomedical Eng Dept.
University College London
London, United Kingdom
hans.natalius.16@ucl.ac.uk

Patrice Lambert
Biomedical Eng and Imaging Sciences
King's College London
London, United Kingdom
patrice.lambert@kcl.ac.uk

Lyndon da Cruz°
Institute of Ophthalmology
University College London
London, United Kingdom
0000-0002-7695-6354

Christos Bergeles°
Biomedical Eng and Imaging Sciences
King's College London
London, United Kingdom
0000-0002-9152-3194

***Abstract*—A non-axisymmetric parallel manipulator headrest design was previously proposed to counter patient head motion during ophthalmic surgery, and a non-motorized prototype was built. Custom linear actuators were designed, and installed to the headrest manipulator prototype in preparation for kinematic performance test. An inverse kinematic-based control algorithm was implemented, and initial kinematic testing was done. Finally, the future plans for the research are briefly explained.**

***Index Terms*—parallel robots, medical robots and systems, actuation and joint mechanisms**

I. Introduction

Involuntary patient head motion is one of the biggest obstacles in achieving efficacy in stem cell implantation [1], [2] and gene vector delivery under local anaesthesia. The precision required to target thin retinal layers, of micrometer dimensions, is several orders of magnitude below the motion caused by patient head repositioning. During anterior segment ophthalmic surgery, for example, involuntary patient head motion can be as much as 11 mm [3]. Most researches that aim to mitigate head movement had focused on how to constraint the head, with examples such as the head fixation device for iRAM!S robot [4] and the Granular-Jamming Headband [5]. On the other hand, other approaches, such as countering head motion, were rarely explored. A non-axisymmetric headrest manipulator proposed for this purpose was in the early stages of research, with a non-motorized prototype alongside its inverse kinematic, statics and performance analysis were presented in [6]. The current paper presents motorisation and control considerations for an updated robot prototype towards evaluating its kinematics performance.

II. Mechanism Design

We summarise the manipulator design explained in depth in [6]. The manipulator comprised 3 planar linear prismatic actuator pairs, that were arranged in a non-axisymmetric manner. The non-axisymmetric arrangement was used to provide a space for the patient's neck, as the patient's head was positioned within end-effector perimeter to fulfil system height requirement, as mentioned in [6]. Meanwhile, the 6 actuators allow for translation and rotation along all axes. This design allows for easier control, due to the patient's head located closer to the end-effector center of mass. In the current paper, the linear struts embedded in [6] have now been swapped for linear actuators. To fulfil dimensional constraint requirements, 6 custom linear-prismatic actuators with stroke lengths of 150 mm, 160 mm, and 200 mm were used.

This research was supported by Sir Michael Uren Foundation and University College London Overseas Research Scholarship. Christos Bergeles and Lyndon da Cruz equally contributed to this research.

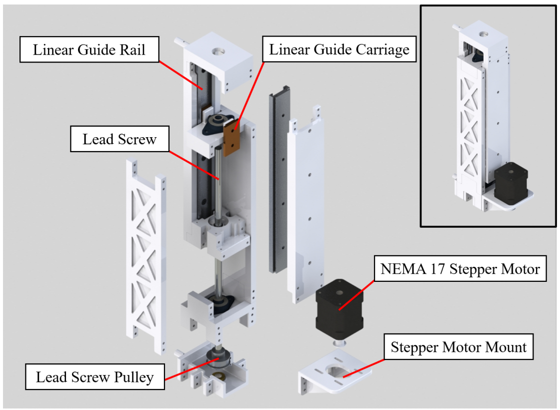

Fig. 1. Custom linear-prismatic actuator construction and final assembly.

Lead screws were used within the custom prismatic actuators to allow actuator extension and retraction motion, whilst linear guide rails were mounted parallel to the lead screw to constraint the actuators from rotational motion. NEMA 17 stepper motors were mounted to the actuator using 3D printed custom motor mounts. The motor mounts feature several slots, which allow the belt tension to be adjusted by moving the motor along the slots. The motor mounts were designed to

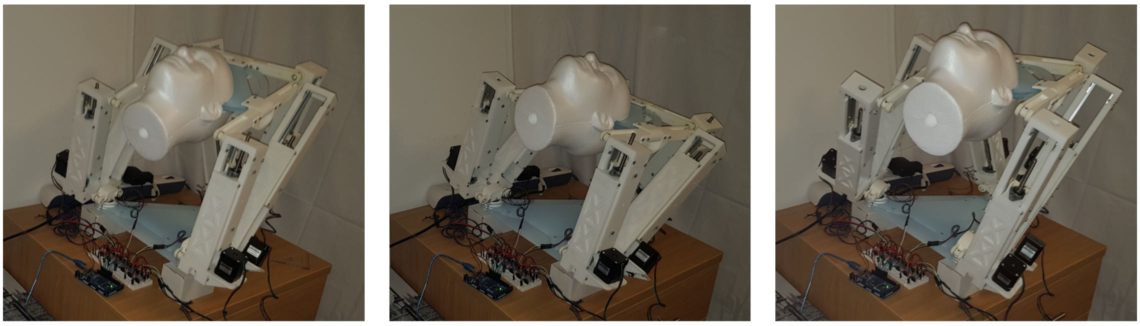

(a) (b) (c)

Fig. 2. Manipulator prototype, with the end-effector positioned in several different positions (X, Y, Z) and orientations (θ_x, θ_y, θ_z) relative to the origin, (a) [0, 0, 320, 0°, 15°, 5°], (b) [−50, 50, 290, −5°, −5°, 5°], and (c) [50, 50, 360, 5°, 5°, 5°].

be replaceable, to account for the need to use motors with different specifications in further steps of the research. The stepper motors were connected to the lead screws via belt-pulley system with 2 : 1 reduction ratio. Lead screw and motor position within the actuator were arranged to give minimum actuator height when the actuator is in fully-retracted state. Fig. 1 shows the construction of the linear actuators.

Six A4988 stepper motor drivers were used to control the stepper motors, and Arduino Mega2560 was used to provide input to the motor drivers. The manipulator inverse kinematic model, which was briefly explained in [6], was implemented in MATLAB to compute the length of each actuator when provided the desired end-effector pose. The resulting actuator lengths were then compared with the current actuator lengths, and the actuator value differences were sent to the Arduino through serial communication using Simulink.

To avoid the risk of damaging the manipulator, each of the parallel manipulator actuator needed to be associated with specific actuator values. Therefore, the manipulator prototype was tested by positioning the end-effector on random combination of positions and orientations within the manipulator workspace. The position and orientation of the end-effector were expressed in mm and degrees respectively, relative to the global origin located at the manipulator base.

III. Results

The assembled manipulator prototype, equipped with motorized linear actuators, is shown in Fig. 3, with point O being the manipulator global origin.

The actuator setup mentioned in Section II was proven to be able to move the end-effector to several different poses. In addition to positions, these poses can also include orientations relative to all 3 Axes. Some of these poses are shown in Fig. 2. Furthermore, the manipulator did not break when the end-effector moves, which proved that inverse kinematic based control system works well. The prototype manipulator also fulfilled the workspace requirement mentioned in [6].

IV. Future Work

This paper detailed the initial steps taken to prepare the non-axisymmetric headrest manipulator prototype for kinematic performance test. The next step of this work will be to evaluate and quantify the performance of the motorized headrest manipulator using optical tracking of the end-effector. Closed loop control will be implemented in a patient-head motion simulation scenario, and the end-effector design will be updated to accommodate a surgical pillow.

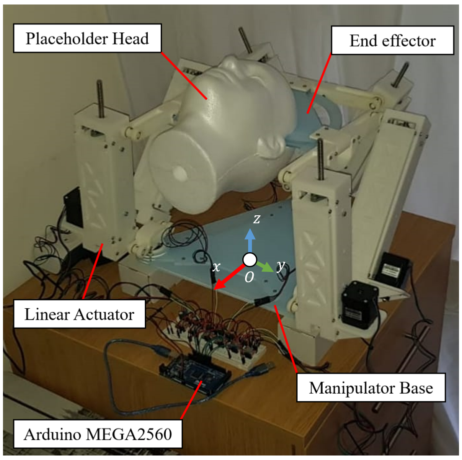

Fig. 3. Manipulator prototype, with a proxy head on the end-effector.

References

[1] L. da Cruz et al., ”Phase 1 clinical study of an embryonic stem cell–derived retinal pigment epithelium patch in age-related macular degeneration”, Nature Biotechnology, vol. 36, no. 4, pp. 328-337, 2018.
[2] ”REP1 Gene Replacement Therapy for Choroideremia”, Clinicaltrials.gov. https://bit.ly/37MLG5N. [Accessed: 02 December 2019].
[3] K. Brogan, B. Dawar, D. Lockington and K. Ramaesh, ”Intraoperative head drift and eye movement: two under addressed challenges during cataract surgery”, Eye, vol. 32, no. 6, pp. 1111-1116, 2018.
[4] K. Huang et al., ”A flexible head fixation for ophthalmic microsurgery”, 2017 Chinese Automation Congress (CAC), 2017.
[5] R. Wirz, R. Lathrop, I. Godage, J. Burgner-Kahrs, P. Russell and R. Webster, ”Can coffee improve image guidance?”, Medical Imaging 2015: Image-Guided Procedures, Robotic Interventions, and Modeling, 2015.
[6] H. Natalius, P. Lambert, M. Tiwari, L. da Cruz and C. Bergeles, ”Design, Static and Performance Analysis of a Parallel Robot for Head Stabilisation in Vitreoretinal Surgery”, Mechanisms and Machine Science, pp. 169-179, 2020.

https://doi.org/10.31256/Iq9Ki4X

Test Framework for a Virtual Competition Testbed

Liam Wellacott*, Emilyann Nault†, Ioannis Skottis‡ ***Alexandre Colle§, Shreyank N Gowda¶,
Pierre Nicolay‖, and Emily Rolley-Parnell**
Heriot-Watt University & University of Edinburgh
Edinburgh, United Kingdom
Email: *lw88@hw.ac.uk, †en27@hw.ac.uk, ‡i.skottis@ed.ac.uk, §ac385@hw.ac.uk, ¶s1960707@ed.ac.uk,
‖pon1@hw.ac.uk, **emily.rolley-parnell@ed.ac.uk
***The following authors are ordered alphebetically
Code: https://github.com/LiamWellacott/CDT2019-ERL
Video: https://www.youtube.com/watch?v=RoxGla2P-uY&ab_channel=ColleAlexandre

***Abstract*—Virtual environments have been utilised in robotics research as a tool to assess systems before deploying them in the field. The COVID-19 pandemic has brought about additional motivation for the development of virtual benchmarks in order to aid in safe and productive development. In-person robotics competitions have also halted, thus limiting the scope of opportunities for students and researchers. We implemented the structure of a service robotics competition into an extendable and adaptable virtual scoring environment. The competition challenges the state of the art in home service robotics by presenting realistic household tasks for robots to complete. The virtual environment provides a foundation for competition teams to assess their systems when accessing the physical environment is not possible. We believe that utilising virtual environments as a means of assessment will lead to other benefits such as increased access and generalisation.**

***Index Terms*—Robotic Competitions, Benchmarking, Simulation, Human-Robot Interaction**

I. Introduction

Competitions are an important tool for pushing the state of the art in robotics applications. They also provide new researchers with practical skills and knowledge used throughout their career. Hosting physical competitions has not been possible during the COVID-19 pandemic. This has highlighted the need for tools which allow teams to continue their work regardless of access to the physical competition environment.

In this work we target the European Robotics League Consumer Service Robots competition (ERL Consumer for short). Teams are challenged with performing realistic household tasks for an older adult, Granny Annie. The competition is normally hosted at locations across Europe with accredited testbeds designed to appear like a typical small apartment. The competition organisers provide a handbook which describes the tasks and scoring criteria. Additionally, functional benchmarks provide a method to assess a team's solution in a single capability (e.g. natural language understanding). Both the tasks and functional benchmarks are performed across a three-day period. They are partially automated, but require human intervention for purposes such as setting up objects in the environment.

To our knowledge, there is no automated virtual environment where teams can test their system against the ERL competition tasks and functional benchmarks. We identified this gap first-hand when attempting to produce our own competition entry while working under the restrictions of the COVID-19 lockdown in the UK. In this paper we present our virtual benchmark for the ERL Consumer competition.

II. Background

Robotics competitions have made a shift to becoming more virtual, which has only increased in prominence since the start of the COVID-19 pandemic. Some competitions such as the SpaceRobotsChallenge have opted to use simulation since sending competition robots to space would be infeasible/unreasonable. In recognition of the disruptive nature of the COVID-19 pandemic, other competitions have shifted towards virtual platforms such the VirtualRobotX competition. More recently other competitions have announced virtual competitions entries such as 2021 RoboCup@Home and 2021 RoboCup Rescue.

In the context of service robotics, OpenRobotics, in collaboration with Hitatchi, created a virtual robotics competition called ServiceSim [1]. The competition's focus is HRI in an office environment. In an effort to facilitate research in the field of social robotics and specifically the learning of social norms (e.g. proxemics), Pimentel and Aquino-Junior [2] have developed a virtual environment with a scoring mechanism using ROS, Gazebo and OpenAI. Most recently, SEAN by Nathan Tsoi *et al.* [3] developed a virtual world with the focus on the development and evaluation of algorithms for social navigation (dynamic conditions such as simulated pedestrians, cars, etc.).

Robotics competitions are not only important for robotics research, but also are used to educate and engage students. A good example of this is the competition RoboCupJunior [4]. Virtual environments can grant students access to state of the art equipment in cases where it otherwise would not have been possible.

III. Virtual Benchmark

The virtual benchmark is a system for testing ROS-based ERL Consumer competition solutions in an automated virtual environment. When the user starts the benchmark, the *simulation environment*, which has been configured for a given *scenario*, is launched. The user's competition solution performs the task and notifies the *virtual referee* upon completion. The referee evaluates the task performance and returns a score.

The *simulation environment* is a Gazebo world designed with the same furniture and overall dimensions as the physical Heriot-Watt University Robotic Assisted Living Testbed (RALT) (Fig. 1). To configure the world for a particular scenario, we utilise the large number of Gazebo-compatible object models available online (e.g. boxes of food, standing human). Each scenario is built using a separate `roslaunch` file which describes the positions of the objects as well as the starting position of the robot. As in the physical competition, the team has time to ensure the robot is fully initialised before the scenario begins.

Fig. 1. The virtual RALT Gazebo world

To start the scenario, the user launches the *virtual referee*, which is based on the Referee, Scoring and Benchmarking Box (RSBB) used in the ERL Consumer competition. In addition to its role in scoring and scenario monitoring, the RSBB provides a single interface for smart home features through which the robot can interact with devices in the home. Importantly, the virtual referee employs the same ROS topics used in the RSBB in the physical competition, meaning teams don't have to change their solution to interact with our referee. Once the user launches the referee, a start signal is sent to the robot which contains the scenario context. The scenario context could be:

- The smart doorbell has been activated and the robot must greet the visitor.
- Granny Annie has used her smart tablet to "summon" the robot to her.
- Granny Annie makes a natural language request.

The virtual referee then waits for the robot to signal it has completed the task. Once the signal is received, the state of the environment (using gazebo model states) is examined to provide a score for the run.

The virtual benchmark contains the following *scenario*, a simplified version of the ERL Consumer competition task "catering for Granny Annie's comfort". Granny Annie summons the robot through the smart tablet and requests the cracker box from the kitchen. The robot must interpret this command and retrieve the box. Once the task is completed, the robot notifies the referee and receives a score of two for (1) removing the box from the kitchen island and (2) placing the box next to Granny Annie.

The virtual benchmark is designed to be extended with additional test scenarios, which requires two steps to set up. Firstly, the user must configure the world state by producing a new `roslaunch` file to describe the objects and starting location for the robot. Secondly, the user must add the scenario logic to the virtual referee. This can be accomplished by extending the existing referee with the start signal and end logic, reusing the topics and services already in place.

The virtual benchmark does not rely on a particular robot or software solution to be compatible. The only requirement is the ROS interface, which is also true for the physical competition. Currently the virtual benchmark is configured for the RALT environment and Tiago robot. However, the `roslaunch` file can be reconfigured to use another environment/robot and reuse the virtual referee scenario logic freely. This means that it is possible to test your solution across multiple competition testbeds to assess generalisation capability [5].

IV. Conclusion and Further Work

Implementing automatic scoring benchmarks provides a potential tool for holding robotics competitions virtually. They can also be applied to other similar competitions such as RoboCup@Home. The tasks and functional benchmarks provide obvious candidates for developing further scenarios, but we can also create new situations to bridge the gap in complexity between benchmark and task. Finally, incorporating elements of noise (e.g. human models active in the environment) and uncertainty (e.g. sensor readings) can help improve generalisability through making the virtual testbed more similar to a real world environment.

Looking beyond COVID-19, virtual benchmarks provide milestones and test cases for team's systems, thus providing a means for developers to test their system without physical access. They can help improve the generalisation of a system by making it easy to test across many virtual benchmarks. Finally, we believe automation of the environment set up will allow teams to spend more time focusing on their strategy, ultimately leading to more innovative systems.

References

[1] "Service robot simulator," https://www.openrobotics.org/blog/2018/5/22/service-robot-simulator, accessed: 2021-04-07.

[2] F. Pimentel and P. Aquino Junior, "Simulation system for learning of social rules using gazebo and openai gym," in *III Brazilian Humanoid Robot Workshop and IV Brazilian Workshop on Service Robotics*, 01 2020, pp. 79–83.

[3] N. Tsoi, M. Hussein, J. Espinoza, X. Ruiz, and M. Vázquez, "Sean: Social environment for autonomous navigation," in *Proceedings of the 8th International Conference on Human-Agent Interaction*, 2020, pp. 281–283.

[4] A. Eguchi, "Robocupjunior for promoting stem education, 21st century skills, and technological advancement through robotics competition," *Robotics and Autonomous Systems*, vol. 75, pp. 692–699, 2016.

[5] "Isr testbed simulated environment," https://github.com/socrob/mbot_simulation_environments, accessed: 2021-04-07.

https://doi.org/10.31256/Rq9Yg6I

Visually-based Prediction of Artist's Drawing

Chipp Jansen[1]
[1]*Dept of Engineering*
King's College London, UK
chipp.jansen@kcl.ac.uk

Elizabeth I Sklar[1,2]
[2]*Lincoln Institute for Agri-food Technology*
University of Lincoln, UK
esklar@lincoln.ac.uk

***Abstract*—This paper describes recent work in the development of a co-creative human-robot drawing system, which observes an artist's drawing process in real-time. Using the data gathered in a recent pilot study, a series of models were trained in order to recover the current state of the artist's drawing behaviour and pen attributes from a multi-camera multi-perspective set-up, aligned to a "ground truth" dataset obtained from a drawing tablet. Experiments, carried out with two computer vision models based on a CNN architecture, form a baseline for future, more sophisticated models.**

***Index Terms*—human-robot collaboration, co-creative drawing, computer vision, deep learning, sketch-based computing**

I. Introduction

Visual artists enjoy a large economy of creative digital tools to produce their work. However, as result of a recent study into co-creative artistic workflows [1] , we have found a desire for a more fluid transition between digital and analog media (e.g. pen and ink on paper), as artists often use physical media for initial idea exploration. Here, we investigate vision-based methods to understand artists' activity (e.g. are they currently drawing or not?) and output (e.g. predicting the pen position on the page) while drawing; and to understand which inputs (e.g. camera positions) are most useful for this modelling.

II. Background

Computer graphics and human-computer interaction have a rich literature on sketch-based computing and interaction via digital interfaces such as drawing tablets [2]. Neural network approaches to model sketching, such as the *sketch-rnn* model [3] (and the availability of large-scale drawn datasets, e.g. *QuickDraw!* [4]) have inspired many co-creative drawing systems [5]–[7]. Some of these co-creative systems respond to artists working with analog media and capture the drawing process for reflective post-processing [8], [9]. However, none of these systems build a real-time model of what the artist is currently drawing or their behaviour. In addition, artists and illustrators still use physical media as part of their workflow and desire a more fluid way of capturing their drawings [10], a feature which is currently lacking.

III. Models and Experiments

a) Set-up: We have developed a research prototype comprising multiple cameras that observe an artist's drawing surface: 3 RGB cameras (overhead, oblique right and left), 1 front facing depth camera (with RGB and infrared cameras integrating into a depth image). The artist draws on paper on top of a drawing tablet which records the position (x and y coordinates) and pressure of the drawing pen [11]

b) Data: In early 2020, we conducted a drawing data gathering study involving 13 professional and student illustrators who were prompted to engage in two drawing exercises: (i) observational drawing of a still-life; and (ii) drawing from imagination or memory. Here we utilise data from both drawing exercises for 5 participants, independently, to produce two types of datasets with corresponding models: *activity* and *pen_position*. The examples in each dataset are comprised of 6 temporally correlated images[1], which are resized to a fixed resolution (80×60 pixels) and labelled using the corresponding drawing tablet data as ground truth.

The *activity* dataset examples are labeled with a 3-class *pen_state* variable ("drawing", "hovering", "away") and two binary classes *is_drawing* and *is_present* based on the pen state. Each *activity* dataset had 2500 examples sampled at even intervals (200ms). The *pen_state* dataset had 3500 examples sampled only when the artist was drawing and are labeled with the normalised pen position: $(x, y) = ([0, 1], [0, 1])$.

c) Models: Each model takes 6 camera images as input (from individual sources or in combination). Each image is fed independently through a sequence of *Convolutional Neural Network (CNN)* layers, to be concatenated in a single layer that fully connected to output variables. There are three flavours of the *activity* model based on the variables: *pen_state*, *is_present* and *is_drawing*. The drawing model produces normalised pen position (as above). Models were built and trained using *Tensorflow*[2], with an 80/20 training/validation split on the datasets, using an ADAM optimiser with a learning rate of 0.01, for 30 epochs each.

d) Experiments: We experimented with 7 different combinations of input images (single individual image input and all images), on the three flavours of *activity* models and the *pen_state* model. Each model was trained and evaluated independently with a corresponding user-session dataset.

Research is supported through an EPSRC DTP Studentship "Collaborative Drawing Systems", Grant Reference EP/N509498/1

[1]4 RGB images for each camera, the infrared and depth image from the depth camera

[2]https://www.tensorflow.org/

IV. Results and Discussion

Figure 1 shows the results for the three flavours of the *pen_state* model, broken down by the different input image combinations, between which there are little differences. Overall, the predicting the *is_present* variable is the most accurate (mean 93.5%, std 2.9%, n=70), followed by the predicting the *is_drawing* variable (mean 73.3%, std 5.8%, n=70) and the ternary *pen_state* activity variable (mean 68.2%, std 6.9%, n=70). This suggests that the models are better able to predict whether the artist is present than drawing. This makes sense when one considers how visually close the drawing and hovering state are, and that the pen tip is often visually occluded from the image view.

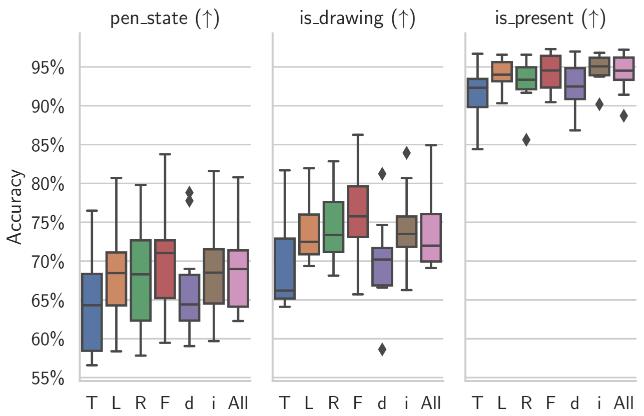

Fig. 1. Accuracy of *activity* models (*L-R*) *pen_state* (ternary), *is_drawing* (binary), is present (binary). Each error bar summarises 10 drawing sessions for the input images: (**T**)op, (**L**)eft, (**R**)ight, (**F**)ront (with (**d**)epth and (**i**)nfrared component), (**All**) six images combined as input.

Figure 2 shows the mean squared error (MSE) for the x and the y component of the *pen_position* model. Overall, the MSE for x (mean 0.0022, std 0.0064, n=70) was lower than y (mean 0.0032, std 0.0078, n=70). The combined MSE (mean 0.0054, std 0.0137, n=70), the model's training metric, was highest. There seems to be little difference amongst the RGB cameras (T, L, R, and F), while the individual depth (d) performs worse, and the individual infrared (i) has an outsized comparative variance. However, the combined images (All) yield a far better result than the individuals.

V. Summary and Future Work

We have shown that using a CNN architecture with camera images we can (1) predict activity and pen position across different artists and; (2) predict using all input sources and pairs of input sources. For predicting pen position, the combination of images performed better than individuals, where (surprisingly) they did not for predicting activity.

One limitation here is that each model is trained specifically for a user and drawing exercise. The rationale here would be that a co-creative system would train a model specific to an artist, and perhaps starting from a more general model. However, there are opportunities for future work in training

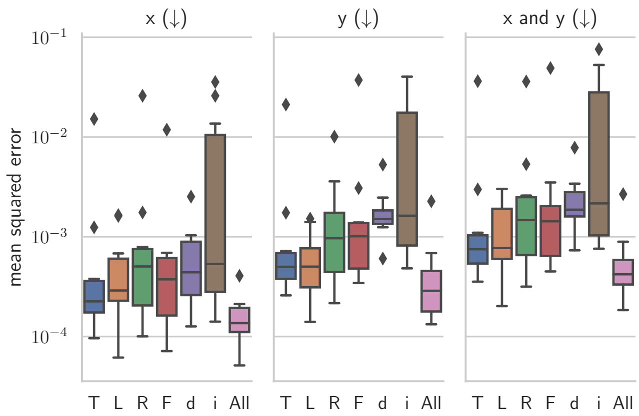

Fig. 2. Mean Squared Error (MSE) (log scale) *pen_position* models (*L-R*): x, y and combined $x + y$, Each error bar summarises 10 drawing sessions for the input images (same as Figure 1).

a generalised model as well as for *transfer learning* – how does one artist's model fair when evaluated on another artist's model? Or, how do models trained on observational drawing differ than that of the same artist drawing from imagination?

Further work in investigating advantages of different combinations of inputs are possible and would be more broadly applicable toward the human-robotic interaction research community, when considering the best view of a mobile camera for a robot when observing detailed human work, such as drawing, medical surgery or small electronics assembly.

In our work of human-robotic collaboration, our aim is for these models to contribute towards a framework for a co-creative drawing system, which is aware of the activity of the artist and what they are drawing based on visual input. Such a framework would benefit the co-creative computation community, and provide a basis to evaluate different co-creative approaches within the same context.

References

[1] C. Jansen and E. Sklar, "Exploring co-creative drawing workflows," *Frontiers in Robotics and AI*, vol. 8, p. 92, 2021.

[2] J. Jorge and F. Samavati, *Sketch-Based Interfaces and Modeling*. Springer Science & Business Media, Dec. 2010.

[3] D. Ha and D. Eck, "A Neural Representation of Sketch Drawings," *arXiv:1704.03477 [cs, stat]*, May 2017.

[4] J. Jongejan, H. Rowley, T. Kawashima, J. Kim, and N. Fox-Gieg, "Quick, Draw!" https://quickdraw.withgoogle.com/, 2016.

[5] P. Karimi, M. L. Maher, N. Davis, and K. Grace, "Deep Learning in a Computational Model for Conceptual Shifts in a Co-Creative Design System," *arXiv:1906.10188 [cs, stat]*, Jun. 2019.

[6] J. E. Fan, M. Dinculescu, and D. Ha, "Collabdraw: An Environment for Collaborative Sketching with an Artificial Agent," in *C & C*, Jun. 2019, pp. 556–561.

[7] C. Oh, J. Song, J. Choi, S. Kim, S. Lee, and B. Suh, "I Lead, You Help but Only with Enough Details," in *CHI*, Apr. 2018, pp. 1–13.

[8] V. Cabannes, T. Kerdreux, L. Thiry, T. Campana, and C. Ferrandes, "Dialog on a canvas with a machine," *arXiv:1910.04386 [cs]*, Oct. 2019.

[9] P. Fernando, J. Weiler, S. Kuznetsov, and P. Turaga, "Tracking, Animating, and 3D Printing Elements of the Fine Arts Freehand Drawing Process," in *TEI*, 2018, pp. 555–561.

[10] C. Jansen and E. Sklar, "Co-creative Physical Drawing Systems," in *ICRA-X Robotic Art Program at ICRA*, 2019.

[11] ——, "Co-creative drawing with a robot," in *UK-RAS*, 2020.

https://doi.org/10.31256/Mj3Lt6M

Design of a Transforming Myriapod Robot for Multimodal Locomotion

Florence Sherry
School of Mechanical Engineering
University of Leeds
Leeds, United Kingdom
mn17fes@leeds.ac.uk

Chengxu Zhou
School of Mechanical Engineering
University of Leeds
Leeds, United Kingdom
C.X.Zhou@leeds.ac.uk

***Abstract*—This paper describes the design and simulation verification of a multimodal locomotion system on a myriapod robot which is able to walk on uneven terrain and roll on flat ground. The proposed design aimed to reduce actuation while maintaining power efficiency on both flat and uneven terrain. A mathematical approach was utilised to determine key parameters. A simulation study was conducted to verify the kinematics and dynamics of the system, modelling the locomotion of the robot while walking and during its transformation to rolling on flat ground.**

***Index Terms*—multimodal locomotion, myriapod robot, legged locomotion, transforming robot**

I. Introduction

Multi-terrain mobile robots have increased utility when compared to traditional dedicated mobile robots [1]. However, multi-terrain robots often require complex locomotion systems with a large number of actuators, which puts constraints on size, weight, efficiency and cost. Wheeled locomotion is effective on flat terrain but struggles on uneven terrain. Legged locomotion is suited to uneven terrain but requires an increased complexity for coordinated control [2]. Myriapod robots are a form of legged locomotion based on centipedes and millipedes which have demonstrated the capacity for reduced actuation due to flexible body couplings, which allow passive adaption to the ground profile [3]. The large number of legs ensures stability without the need for complex control systems. However, myriapod systems are slow on flat terrain which makes them unsuitable for applications within buildings, homes and warehouses. Previous complex legged robots such as [4] have been able to increase their velocity on flat terrain by transforming to a wheel form, which is propelled forward by "spare" legs. The proposed design utilises this approach while maintaining the simplicity offered by a myriapod platform, utilising only 2 motors for transformation and forward locomotion both in legged form and wheeled form.

II. Kinematics Design

The Myriapod robot walks in a millipede form on uneven terrain and transforms to a wheel on flat terrain. A central drive shaft runs down the body of the millipede, powered by a single motor. Worm gears on the drive shaft transfer torque to the legs via a spur gear on the leg axle. The drive shaft is split into sections connected by universal-joints (U-joints), allowing an offset angle between drive shaft sections which is limited by the geometry of the body casings, see Fig. 1. A cable runs through each body section and is attached to a second motor. When the cable is wound in it pulls the body into the wheel form, consecutive body cases fit into one another, securing their position. When the robot is in wheel form the legs continue to rotate propelling it forward. The legs on either side of each body sections are in phase with one another. Consecutive leg pairs are out of phase with one another by an acute phase angle. This is a metachronal walking gait which is used by millipedes [5]. In walking form this gait results in a vertical undulation of the body.

Fig. 1: Partial physical prototype of the proposed myriapod.

TABLE I: Key form parameters. n=16 is the number of leg sets, c=2 is the number of legs sets contacting the ground, d=0.072 m is the distance between adjacent leg roots and s=0.01 m is safety margin distance between leg tips

Parameter	Derived Equation	Value
Maximum body section offset angle ($Q_{\max}$) in degrees	$Q_{\max} = \frac{360}{\pi}$	22.50°
Phase angle delay between adjacent legs (θ) in degrees	$\theta = c \cdot \left(\frac{360}{n}\right)$	56.25°
Vertical length of the leg (R) in meters	$R = \frac{d-s}{\left(2\sin\frac{\theta}{2}\right)\left(2-\cos\frac{Q_{\max}}{2}\right)}$	0.06 m
Length of the whole robot (L) in meters	$L = n \cdot d$	1.15 m
Wheel form diameter (D_w) in meters	$D_w = \frac{L}{\pi}$	0.37 m

The parameters seen in Table I, were necessary to size the robot. The speed of the walking gait is characterised by [6] as

$$V_m = \frac{2R\sin\frac{\theta}{2}}{t_g} \tag{1}$$

where V_m is the velocity of the walking millipede in the direction of travel, calculated to be 0.058 m/s and t_g is the

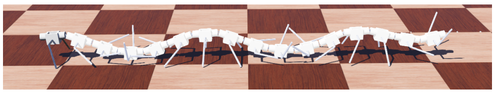

Fig. 2: The myriapod robot walking in millipede form[1].

time the leg is in contact with the ground in seconds. See Table 1 for R and θ.

III. Simulation

A motion study was conducted to validate the design and to evaluate whether rolling increased velocity on flat terrain.

A. Simulation Setup

Webots™ from Cyberbotics Ltd was used to produce 2 simulations, one modelling the walking in millipede form Fig. 2 and one modelling its transformation from millipede to wheel form and rolling locomotion Fig. 3. Limits on computation power meant modelling simplifications were necessary. Leg rotation was modelled with a motor powering each leg set. This neglects the variation of shaft angular velocity resulting from the use of consecutive U-joints. The robot was modelled travelling forward on a flat arena, as a result there were no forces acting which would cause lateral movement. Therefore U-joints were modelled as hinge joints only allowing vertical rotation. Lateral movement of the robot would indicate simulation errors. The transformation was achieved by modelling motors at these hinges. The control code for the transformation activated these motors consecutively to replicate the behaviour of a cable wound from one end by a motor.

B. Results

The position of the 8^{th} body section was tracked in the x, y and z direction over a period of 35 seconds. The direction of travel is positive x, the positive y direction is the vertically upward and z is the lateral direction. In millipede form the locomotion behaved as expected, the average velocity in the direction of travel was 0.067 m/s. During the transformation to rolling simulation there are 4 main phases of movement in the recorded data see Fig. 4a. Phase 1 is the transformation period, seen in Fig. 3 with a duration of 4 seconds. Phase 2 is stable forward rolling, ending at 10 seconds. Phase 3 is rocking, a period of forward and backward rolling, causing the anomaly on Fig. 4b. Phase 3 was caused by the leg rotation which propels the roll, becoming out of phase with the rolling cycle. A protruding leg halts rotation and causing a backwards roll. Uncoordinated rocking continues until the wheel reaches a stationary position at 25 seconds and the legs begin propelling it forward again. Phase 4 is another period of stable forward rolling. The stable rolling speed was approximately 0.35 m/s this was 5.22 times faster than the walking speed of 0.067 m/s. The overall speed during the 35 seconds was 0.19 m/s. During the transformation to rolling simulation there was an unexpected displacement in the z direction, indicating computational errors in the simulation.

[1]Video of Fig. 2 and Fig. 3 is available at https://youtu.be/TCx6ydXqHts/

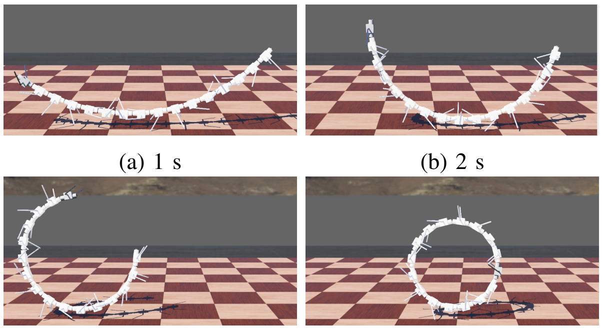

(a) 1 s (b) 2 s

(c) 3 s (d) 4 s

Fig. 3: The myriapod robot transforming from (a) (b), (c) to (d) rolling.

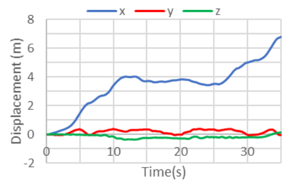

(a) Displacements in x, y, z w.r.t time.

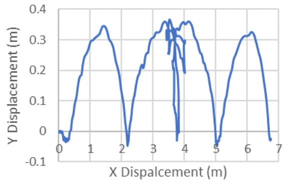

(b) Forward displacement w.r.t vertical displacement.

Fig. 4: Displacements of the myriapod robot's 8^{th} body section from transforming to wheel form to forward rolling.

IV. Conclusion

A transforming myriapod robot has been designed with increased efficiency on flat terrain while maintaining minimally actuated systems. Simulations confirmed that rolling did increase the velocity of locomotion on flat terrain. However, the leg frequency is not currently optimised for continuous propelled rolling. To achieve this, it is necessary to determine the ideal relationship between the walking gait frequency of the millipede and the rolling cycle of the wheel form. The simulation validated the locomotion style not the transformation system. The modelling simplifications mean the simulation velocities are likely an overestimation.

References

[1] Adarsh R S, and M.M. Dharmana, "Multi-terrain multi-utility robot", Procedia Computer Science, vol.133, pp.651-659, 2018.
[2] R. Siegwart *et al.*, "Introduction to autonomous mobile robots", Cambridge: MIT Press, 2011.
[3] D. Koh, *et al.*, "Centipede robot for uneven terrain exploration: Design and experiment of the flexible biomimetic robot mechanism", IEEE BioRob, 2010, pp.877-881.
[4] Festo AG & Co. KG, "BionicWheelBot", 2018. [Online]. Available: https://festo.com/group/en/cms/13129.htm. [Accessed: 2021-04-05].
[5] J. Sathirapongsasuti, *et al.*, "Walking with a millipede", Intel ISF, 2004.
[6] A. Garcia, *et al.*, "Understanding the locomotion and dynamic control for millipedes: Kinematic analysis of millipede movement", ASME SMASIS, 2015, pp.1-10.

https://doi.org/10.31256/Hy7Sf7G

Development of a Teleoperative Quadrupedal Manipulator

Christopher Peers, Moustafa Motawei, Robert Richardson and Chengxu Zhou

***Abstract*—This paper outlines the design and operation of a teleoperated quadrupedal robot enhanced with a manipulator arm and gripper. Using the mobile quadruped platform Laikago, a ViperX 300 robot arm and a wearable inertia based motion capture system, a low-cost robot was assembled capable of hybrid robot and manipulator control to allow seamless and intuitive human to robot interface. Vision for the user is provided through a 3D camera mounted at the front and a stereo camera mounted on the robot arm end-effector. The robot is fully controllable using a wearable inertial based motion capture suit. To verify the functionality of the whole system prior to testing on the real robot, physical simulations were conducted and successfully demonstrated the capabilities of the proposed teleoperation framework.**

***Index Terms*—quadruped robot, manipulator, legged robot, teleoperation**

I. Introduction

Teleoperation has been an important aspect of robotics as it allows for tasks that require the accuracy of a human operator to be completed whilst forgoing the need of having the operator be physically present. The benefits of teleoperated robotics extends to tasks that are also too dangerous for humans to be present as well as for tasks that are located in impossible or difficult to reach environments.

The extent of legged robot teleoperation has typically consisted of a simple joystick, however, when a legged robot must complete complex manipulation tasks, there lacks an intuitive control method able of allowing a difficult task to be completed in a short time frame with minimal errors. Existing legged robots such as the ANYmal have demonstrated that it is possible to combine a robotic arm and a quadruped platform to perform simple manipulation tasks [1]. However, performing these tasks requires the operator to switch between controlling either the quadruped robot or the arm, which would result in difficulty when dealing with complex situations. A method of overcoming this issue has recently been shown using the Boston Dynamics Spot and dynamic grasping [2]. This method however cannot be used for complex or delicate tasks that require teleoperation due to the degree of automation used.

A solution to this is to adopt a different control method that allows for a wider range of human input. A method that has been explored is the use of Inertial Measurement Unit (IMU) motion capture to control robots. Several insights have shown that it is possible for both the high and low level control of a robot to be generated through the use of various IMU embedded devices to a high enough degree of accuracy required for manipulation. One example is the use of a wearable inertia based motion capture system to control the high-level walking motion of a bipedal robot where the commands stemmed from the feet positions [3]. Another example is the use of gesture controls from hand and arm mounted IMUs to control the high-level motions of a wheeled robot [4]. Through the use of an arm-mounted IMU-embedded device, a 7 Degree of Freedom (DoF) robot was reliably teleoperated [5]. The use of teleoperation and the accuracy and robustness of a wearable inertia based motion capture system is demonstrated thoroughly through the development of a dementia-care robot [6]

Authors are with the School of Mechanical Engineering, University of Leeds, Leeds, UK. {ll14c4p, el17m3m, r.c.richardson, c.x.zhou}@leeds.ac.uk

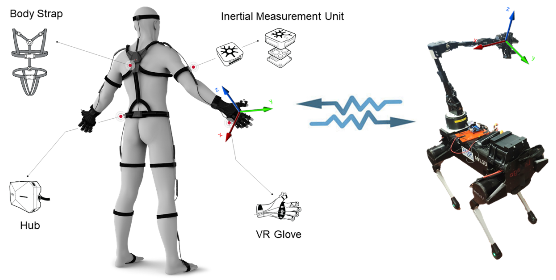

Fig. 1. The developed teleoperative system consists of a wearable inertial motion capture suit (left) and a quadrupedal manipulator (right).

As illustrated in Fig. 1, the developed teleoperative system is composed of the wearable inertia based motion capture system which is worn by the operator and the quadrupedal manipulator, of which is composed of the ViperX 300 robotic arm and the Laikago quadruped robot. The Laikago from Unitree is a small, low-cost quadrupedal robot capable of locomotion via a single trotting gait. The ViperX 300 is a lightweight 5 DoF robotic arm. The need for a higher DoF robot arm was alleviated due to the extra DoF gained by the legged mobile platform. There were no visual sensors mounted on the original Laikago or robot arm. In this paper, the control system allowing the wearable inertia based motion capture system to communicate with the teleoperative system will be outlined along with the simulation test results. The fully developed system will allow the operator to control both the quadruped robot and the manipulator simultaneously.

II. Hardware Overview

A. Hardware Design

The main goal was to minimise the extra load caused by mounting the arm on the Laikago to ensure locomotion is as stable as possible and also to provide enough sensory data to make operation easier. To make the robot arm more suitable for mounting onto the Laikago, the base was redesigned to be more compact and the aluminium box-section lengths of the arm were replaced with carbon fibre rods. These changes reduced the overall weight of the arm from 4.1 kg to 2.6 kg. The Laikago possesses two parallel carbon fibre rods as

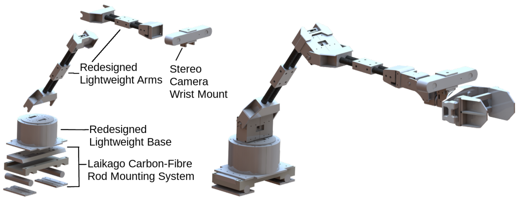

Fig. 2. Labelled exploded view (left) of the redesigned and additional parts assembly, and (right) whole robot arm assembly.

mounting locations where two 3D-printed parts could fix the robot arm and the 3D camera to the Laikago. A 3D camera is mounted on the front of the Laikago, on top of the onboard computer, allowing the user to have a wide field of vision when teleoperating the robot. A stereo camera is mounted on the modified wrist link of the end-effector. The 3D camera will allow the teleoperator to assess the surroundings of the robot and allow for safer locomotion without the need of moving the robot arm to gain visual feedback. The stereo camera output will allow for manipulation tasks which require a greater degree of accuracy to be performed, such as cutting wires or carrying liquids. A labelled diagram of each redesigned part and mounting system along with a rendered full assembly of the robotic arm is illustrated in Fig. 2.

B. Teleoperation Control System

The human body motion is captured by a wearable motion capture system, Perception Neuron, which provides stable and accurate human body segments pose estimations. The accompanied SDK could read whole skeleton data including fine finger movements and broadcast to ROS through *rosserial* protocol. Since the human master and the robot are kinematically dissimilar, therefore, directly connecting them at joint levels is not feasible. Relative scaled pose is then connected between the human hand and the robot gripper, where at time t, their relation is described as

$$\boldsymbol{x}_{sd}^{t} = \boldsymbol{x}_{sd}^{0} + \boldsymbol{\mu}(\boldsymbol{x}_{m}^{t} - \boldsymbol{x}_{m}^{0}), \tag{1}$$

where $\boldsymbol{x} = [x, z, \theta_{\text{yaw}}]$ are the (x) sagittal and (z) vertical displacements and (θ_{yaw}) rotation about the vertical axis, subscripts "m" refers to the master, "s" to the slave, and "d" to a desired value. Superscript "0" refers to the initial timing where both end effectors are connected. We use the VR gloves' readings to detect the hands' closures as the trigger to move the robot. Specifically, the left glove's closure triggers the left hand movements for controlling the legged mobile base, and the right glove's closure connects the master's right hand to the gripper. $\boldsymbol{\mu}$ is used to scale the motions between the master and the robot. Note that the orientation is not scaled, thus $\mu_{\text{yaw}} = 1$.

III. Simulation

To validate the developed teleoperative robotic system, we firstly performed simulation studies. A customized URDF was created that combines both the Laikago and ViperX 300 models and loaded into PyBullet, the Python bindings of the widely used physics simulation engine Bullet. With this environment, the feasibility of the control schemes and performance of the robot could be accurately judged. The Laikago's walking pattern generation is adopted from a bipedal gait generator [7] and the legged manipulator's joint commands are solved using a QP-based whole body controller [8].

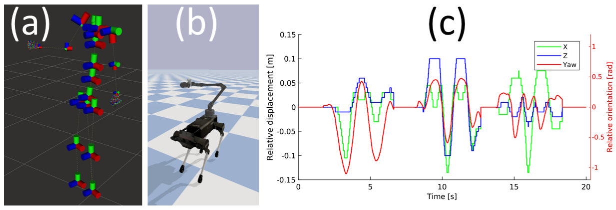

Fig. 3. Teleoperation validated in simulation. (a) Sensed human model. (b) Simulated quadrupedal manipulator. (c) Relative pose sent to the robot. (https://youtu.be/J8xHjMD8-vA/)

As a proof of concept, the initial simulation was carried out only for teleoperating the robot arm while the quadruped was walking in place. The results are shown in Fig. 3. The human master was moving only the right arm about the vertical axis and along the front, vertical directions, respectively. The relative pose from the motion capture data was sent to the robot only during the master's right hand was closed. This strategy is quite intuitive and its successful enabling and disabling of the robot arm's motion can be seen from Fig. 3(c). We could also observe that, though the human master endeavoured to move every time along only one direction, there were inevitable coupled motions sent to the robot. Extra effort is needed to improve this for fine operations.

IV. Conclusion

A robot capable of seamless teleoperated movement and manipulation with the use of a wearable inertial motion capture device is presented. The hardware layout and design of the overall robot was discussed along with modifications to optimise the robot for teleoperation. The robot was thoroughly tested in a simulation environment. The wearable inertia based motion capture system was shown to be a robust method of controlling the robot in a seamless fashion. The robot was shown to be capable of performing teleoperated tasks from within the simulated environment. Further work includes the fully finished assembly of the robot in real life, along with real life testing through various manipulation scenarios.

References

[1] C. D. Bellicoso *et al.*, "ALMA - Articulated locomotion and manipulation for a torque-controllable robot", IEEE ICRA, 2019.
[2] S. Zimmermann *et al.*, "Go Fetch! - Dynamic grasps using Boston Dynamics Spot with external robotic arm", IEEE ICRA, 2021.
[3] S. Kim *et al.*, "A walking motion imitation framework of a humanoid robot by human walking recognition from IMU motion data", IEEE-RAS Humanoids, 2009.
[4] S. Shin *et al.*, "Controlling mobile robot using IMU and EMG sensor-based gesture recognition", BWCCA, 2014.
[5] C. Yang *et al.*, "Neural learning enhanced teleoperation control of Baxter robot using IMU based motion capture", ICAC, 2016.
[6] H. Lv *et al.*, "Teleoperation of collaborative robot for remote dementia care in home environments", IEEE JTEHM, vol. 8, pp. 1-10, 2020.
[7] C. Zhou *et al.*, "Overview of gait synthesis for the humanoid COMAN", Journal of Bionic Engineering, 14(1), 2017, pp. 15–25.
[8] C. Zhou *et al.*, "A Generic optimization-based framework for reactive collision avoidance in bipedal locomotion", IEEE CASE, 2016.

https://doi.org/10.31256/Bw7Kt2N

Robot House Human Activity Recognition Dataset

Mohammad Hossein Bamorovat Abadi, Mohammad Reza Shahabian Alashti, Patrick Holthaus,
Catherine Menon, and Farshid Amirabdollahian

***Abstract*—Human activity recognition is one of the most challenging tasks in computer vision. State-of-the art approaches such as deep learning techniques thereby often rely on large labelled datasets of human activities. However, currently available datasets are suboptimal for learning human activities in companion robotics scenarios at home, for example, missing crucial perspectives. With this as a consideration, we present the University of Hertfordshire Robot House Human Activity Recognition Dataset (RH-HAR-1). It contains RGB videos of a human engaging in daily activities, taken from four different cameras. Importantly, this dataset contains two non-standard perspectives: a ceiling-mounted fisheye camera and a mobile robot's view. In the first instance, RH-HAR-1 covers five daily activities with a total of more than 10,000 videos.**

***Index Terms*—Human Activity Recognition, Dataset.**

I. Introduction

In recent years, neural networks and machine learning methods have been successfully adopted for many recognition tasks in computer vision [1]. The nature of such algorithms entails that they are dependent on a high number of labelled samples depicting the relevant entity or situation. This means they are most successful when used with large datasets that are specific to the problem domain. The number of such datasets is growing rapidly [2], leading to more accurate human activity recognition models. However, most of these datasets are gathered from YouTube or outdoor environments and do not cover indoor everyday activities. As a direct consequence, these existing datasets are not ideal for human activity recognition (HAR) in the growing application domain of companion robotics and home care technologies. Therefore, we present a dataset that is suitable for human activity recognition in companion robotics scenarios. In particular, we aim to use the dataset to generate deep neural network models that are able to either use a single perspective or a fusion of multiple cameras to improve the accuracy of HAR.

II. Related Work

HAR datasets can typically be characterised based on scene properties, such as protagonist (individual or group), activity (daily activities, sports, . . .), environment (indoor or outdoor), or situation (controlled or spontaneous) and camera properties, such as data type (RGB or RGB-D), dynamics (static, moving), perspective, etc. [1], [13]. In this section, we will review the most popular RGB-based HAR video datasets and provide a brief overview of their properties in Table I.

The first publicly available datasets that contain daily activities are *KTH* [12] and *Weizmann* [11]. The low number of individual actions for each activity and the strictly controlled environment with soft background from a single perspective limit their utility in deep learning approaches. The UCF datasets, e.g. *UCF101* [8], by contrast, consist of videos that are captured from various YouTube sources without controlling the environment. *YouTube-8M* [5], of similar nature, is the largest HAR dataset so far with more than 8 Million videos in 4716 activities. The number of classes and videos in both datasets are versatile enough to be used for deep learning; however, using YouTube videos means there is no fixed view of the activities. *INRIA XMAS* [10] is the first HAR dataset that contains multiple different viewpoints, including a top-view camera in a controlled environment, while *MuHAVi* [9] is a dataset containing 8 views with 17 classes of activities. The controlled environment, lack of a dynamic perspective and the low number of videos are shortcomings of *INRIA XMAS* in our application domain. Likewise, the low number of actions (238) and controlled environment are drawbacks of *MuHAVi*. *Charades* [6] is a two-perspective dataset that includes 157 classes and 9,848 videos of daily indoor activities. *Sports-1M* [7] is one of the largest datasets, with more than one Million videos of 487 sports activities in a real-world environment that contains noisy backgrounds and a dynamic camera perspective that follows a ball or a group of people. *Moments in Time* [4] is another large recent dataset that includes more than 1 Million three-second videos labelled in 339 classes. *HACS* [3] is another new large HAR dataset with 1.5 Million videos of 200 activities. In summary, the above HAR datasets can not be adequately applied to the domain of companion robotics for the following reasons:

Fig. 1: Example activities of the dataset from all perspectives.

All authors are with the School of Physics, Engineering, and Computer Science, University of Hertfordshire, College Lane, Hatfield, AL10 9AB, UK. Corresponding author's email: m.bamorovat@herts.ac.uk

TABLE I: Overview of popular RGB-based HAR datasets and their properties.

Name	Year	Videos	Activities	Fixed Views	Environment	Situation	Dynamics	Perspective
HACS [3]	2019	1,550,000	200	-	Indoor/Outdoor	Uncontrolled	Static	Side
Moments in Time [4]	2019	1,000,000	339	-	Indoor/Outdoor	Uncontrolled	Static	Side
YouTube-8M [5]	2016	8,000,000	4,716	-	Indoor/Outdoor	Uncontrolled	Static	Side
Charades [6]	2016	9,848	157	2	Indoor/Outdoor	Controlled	Static	Side
Sports-1M [7]	2014	1,133,158	487	-	Indoor/Outdoor	Uncontrolled	Static/Moving	Side
UCF101 [8]	2012	13,320	101	-	Indoor/Outdoor	Uncontrolled	Static	Side
MuHAVi [9]	2010	238	17	8	Indoor	Controlled	Static	Side
INRIA XMAS [10]	2006	390	13	5	Indoor	Controlled	Static	Side/Top
Weizmann [11]	2005	90	10	1	Outdoor	Controlled	Static	Side
KTH [12]	2004	599	6	1	Outdoor	Controlled	Static	Side

- Daily activities: Most of the datasets are captured in mixed in-/outdoor scenarios or from random sources and are therefore do not represent repetitions of specific human daily activities. There is only cone ontrolled dataset of daily in-/outdoor activities.
- Dynamic perspective (robot view): In assistive robotics scenarios (c.f. [14]), the robot viewpoint is a crucial element. That is, the robot needs to have a good understanding of the situation and the activities a human might be engaged in while focusing on the human with its camera. With the exception of *Sports-1M*, which does not contain any daily indoor activities, there are no other datasets containing dynamic viewpoints.
- Redundancy: Companion robots may not be always engaged in direct interaction with a human but may still require information about the human's current activity to function efficiently (c.f. [14]). In these situations it might be necessary to obtain this information from an external camera. Of the above mentioned datasets, only three consider multiple perspectives.

III. RH-HAR-1 Dataset

To address the specific requirements of HAR in the assistive robotics domain and to overcome the drawbacks presented in Section II, we are currently generating the first version of the *Robot House Human Activity Recognition* dataset (*RH-HAR-1*) at the University of Hertfordshire. It consists of videos of a person in a home environment who is engaged in daily activities at different times and in various situations. Activities recorded so far are walking, drinking, sitting down, standing up and reaching for an object, cf. Figure 1. The dataset includes a dynamic perspective from a robot's point of view that is following the person plus a top-view perspective using an omnidirectional ceiling camera. In total, the activities are being recorded with four different RGB cameras from the following perspectives: I. front (static) II. back (static) III. ceiling (static, fish-eye), and IV. robot (dynamic). Each scene lasts between two and four seconds and is recorded with 30 fps. The ceiling camera is recorded at 512×486 pixels, all other cameras at 640×480. The resulting cut scenes are time-synchronised and organised by class (activity), totalling more than 10,000 short videos.

[1]Accessible at uhra.herts.ac.uk

IV. Conclusion and Future Work

In this paper we have presented *RH-HAR-1*, a dataset containing video scenes of indoor daily activities. It makes use of four different synchronised perspectives including a dynamic one from a robot's viewpoint and an overview from the ceiling to address the specific challenges of activity recognition in assistive robotics scenarios. Once completed, we will make the dataset available on the University of Hertfordshire Research Archive[1]. We plan to later extend the number of activities and increase the variety of actions in each class to cover more everyday situations and increase the dataset's versatility.

References

[1] L. M. Dang, K. Min, H. Wang, M. J. Piran, C. H. Lee, and H. Moon, "Sensor-based and vision-based human activity recognition: A comprehensive survey," *Pattern Recognition*, vol. 108, p. 107561, 2020.

[2] F. Caba Heilbron, V. Escorcia, B. Ghanem, and J. Carlos Niebles, "ActivityNet: A Large-Scale Video Benchmark for Human Activity Understanding," in *CVPR*. IEEE, 2015, pp. 961–970.

[3] H. Zhao, A. Torralba, L. Torresani, and Z. Yan, "HACS: Human Action Clips and Segments Dataset for Recognition and Temporal Localization," in *ICCV*. IEEE, 2019, pp. 8668–8678.

[4] M. Monfort, A. Andonian, B. Zhou *et al.*, "Moments in Time Dataset: One Million Videos for Event Understanding," *IEEE Transactions on Pattern Analysis and Machine Intelligence*, vol. 42, no. 2, pp. 502–508, 2019.

[5] S. Abu-El-Haija, N. Kothari, J. Lee *et al.*, "Youtube-8m: A large-scale video classification benchmark," in *arXiv:1609.08675*, 2016.

[6] G. A. Sigurdsson, G. Varol, X. Wang, A. Farhadi, I. Laptev, and A. Gupta, "Hollywood in homes: Crowdsourcing data collection for activity understanding," in *ECCV*. Springer, 2016, pp. 510–526.

[7] A. Karpathy, G. Toderici, S. Shetty, T. Leung, R. Sukthankar, and L. Fei-Fei, "Large-scale Video Classification with Convolutional Neural Networks," in *CVPR*. IEEE, 2014, pp. 1725–1732.

[8] K. Soomro, A. R. Zamir, and M. Shah, "Ucf101: A dataset of 101 human actions classes from videos in the wild," *arXiv:1212.0402*, 2012.

[9] S. Singh, S. A. Velastin, and H. Ragheb, "Muhavi: A multicamera human action video dataset for the evaluation of action recognition methods," in *AVSS*. IEEE, 2010, pp. 48–55.

[10] D. Weinland, R. Ronfard, and E. Boyer, "Free viewpoint action recognition using motion history volumes," *Computer vision and image understanding*, vol. 104, no. 2-3, pp. 249–257, 2006.

[11] L. Gorelick, M. Blank, E. Shechtman, M. Irani, and R. Basri, "Actions as space-time shapes," *IEEE transactions on pattern analysis and machine intelligence*, vol. 29, no. 12, pp. 2247–2253, 2007.

[12] C. Schuldt, I. Laptev, and B. Caputo, "Recognizing human actions: a local svm approach," in *ICPR*. IEEE, 2004, pp. 32–36.

[13] Y. Kong and Y. Fu, "Human action recognition and prediction: A survey," *arXiv:1806.11230*, 2018.

[14] F. Amirabdollahian, R. O. D. Akker, S. Bedaf *et al.*, "Accompany: Acceptable roboticS COMPanions for AgeiNg Years - Multidimensional Aspects of Human-System Interactions," in *HSI*. IEEE, 2013, pp. 570–577.

https://doi.org/10.31256/Ub8Vp6N

Older adults' perceptions of Socially Assistive Robots

Nicola Camp
Department of Sport Science
Nottingham Trent University
Nottingham, UK
nicola.camp@ntu.ac.uk

Martin Lewis
School of Human Sciences
University of Derby
Derby, UK
m.lewis@derby.ac.uk

Kirsty Hunter
Department of Sport Science
Nottingham Trent University
Nottingham, UK
kirsty.hunter@ntu.ac.uk

Daniele Magistro
Department of Sport Science
Nottingham Trent University
Nottingham, UK
daniele.magistro@ntu.ac.uk

Julie Johnston
Department of Sport Science
Nottingham Trent University
Nottingham, UK
julie.johnston@ntu.ac.uk

Massimiliano Zecca
Wolfson School of Mechanical, Electrical and Manufacturing Engineering
Loughborough University
Loughborough, UK
m.zecca@lboro.ac.uk

Alessandro Di Nuovo
Department of Computing
Sheffield Hallam University
Sheffield, UK
a.dinuovo@shu.ac.uk

Abstract— **Socially assistive robots (SARs) may have many benefits for older adults, including assisting in physical health interventions and reducing loneliness. However, the way in which they are perceived by older adults is unclear. This study aimed to understand some of these perceptions through semi-structured interviews. These revealed that there is a current lack of knowledge about SARs, and limited acceptance of them in terms of having them in the home. Despite this, some potential advantages were identified, although some participants did not perceive a need for such new technology. Future research should identify new design strategies to address participants' concerns and better match their needs.**

Keywords— Older adults, SAR acceptance, Barriers

I. Introduction

Socially assistive robots (SARs) are robotic technology platforms with audio, visual, and movement capabilities. Their purpose is to create friendly and effective interaction with a human user with the additional aim of giving assistance to the user and achieving measurable progress in their quality of life, often related to motivation, rehabilitation, or learning [1]. It is important to note that SARs are both platforms for interventions as well as interventions in and of themselves; they can learn and engage socially with individuals while also presenting interventions to users similar to mobile apps (e.g. skills training, health tracking). They can engage users across multiple sensory options, most often including sound, sight, and touch, which can create multiple modalities for the delivery of content or interactions, depending on user preferences or personal physical abilities [2]. Robot-led psychometric assessment could have many advantages, such as wider availability, test standardization and assessor neutrality, while providing higher engagement and usability to people with limited digital literacy [3].

Although research with SARs is still in its infancy, there have been positive participant responses to SARs assisting in physical health interventions related to increasing exercise with the elderly [4] and improved cardiac rehabilitation through self-reported usefulness of SARs to assist in the completion of rehabilitation tasks [5]. Social robots can provide a solution for the ageing population challenge, especially to reduce social isolation and loneliness [6]. These advanced systems could provide continuous support in a variety of daily activities, thus, enabling older people to live independently at home for longer. However, little is known about how older adults perceive SAR technology [7], or if they would be willing to accept the technology in their own homes. As they are the target audience for many of these systems, it is important to understand whether older adults consider SAR technology to be beneficial for them, and what they would use SAR technology for. This study aimed to contribute to this understanding through semi-structured interviews.

II. Method

Data collection: Semi-structured interviews were conducted with 33 individuals, aged between 55-82 years (M=67.6 years, SD=7.4), and consisting of men (n=15) and women (n=18), using online video call software (Facebook messenger, WhatsApp, Zoom, Microsoft Teams) depending on the participants choice. A semi-structured interview guide was developed. Participants were shown images of a human-based and an animal-based design of SAR and asked broad questions to encourage discussion, including: "Which design is best and why?", "How could these robots be useful to you?", "What barriers (if any) may exists to introducing this technology into the homes of older adults?"

Data analysis: Data was analysed using a realist thematic analysis approach [8]. We identified 4 key themes: existing knowledge of social robots, factors that influence acceptance of social robots, potential advantages, and potential barriers.

III. Results

Existing Knowledge

Overall, 55% of interview participants had some existing knowledge of SARs (Fig. 1), however, most explained that this was very limited and based on media coverage where they "*might see a news item about something like this*".

Influencing factors

The design of the robot was one of the most influential factors, with 70% of participants stating they would have a human design and 33% accepting the animal design (Fig. 1). However, only 6% would have either design now (Fig. 1), with the rest stating that they would consider one in the future. The idea of "*need*" was highlighted as key influencing factor for this, for example, one person stated that "*I'd have one if I felt I needed it or if it was a definite help*".

Several people stated that the animal design seemed "*less intrusive*", "*less intimidating*" and "*potentially more user friendly*" than the human design. However, it was suggested that the animal design was less suitable due to the increased risk of falling, and that "*having more things moving about just increases the risk of you falling*".

Advantages

Assistance with Activity of Daily Living (ADL) performance was the most frequently perceived advantage to having a SAR within the home, particularly in relation to household activities, or "*simple chores*", for example, one participant stated that "*I'm sure that in the house of the future, tasks that become onerous as you get older, washing up and basic tasks… and lifting and shifting things, you know… That may be a great help as you lose your musculature"*

Many people stated that it would be "*nice just to have as a companion in the first instance. You know, somebody to talk to*" because "*if you're sat here on your own day in and day out, to have something like that, I should think, could save your sanity*", which highlights the importance of company as a potential advantage.

Barriers

One of the main barriers to social robot acceptance is a perceived lack of need for the technology, and the idea that social robots are a "*novelty*" that would "*wear off very quickly*". For example, one participant stated that "*From the novelty point of view, yes but erm I don't see any real use for it",* with another echoing this idea, "*I don't see that having a robot there to talk to me is really going to help massively*"

Several people also raised the issue that people may become "over-reliant" on SARs, resulting in reduced movement and an increase in sedentary behaviour. This idea was summarized by one participant as "*we might all become bone-idle and never do anything and you'd just atrophy"* with another stating that "*they might make you become lazy instead*".

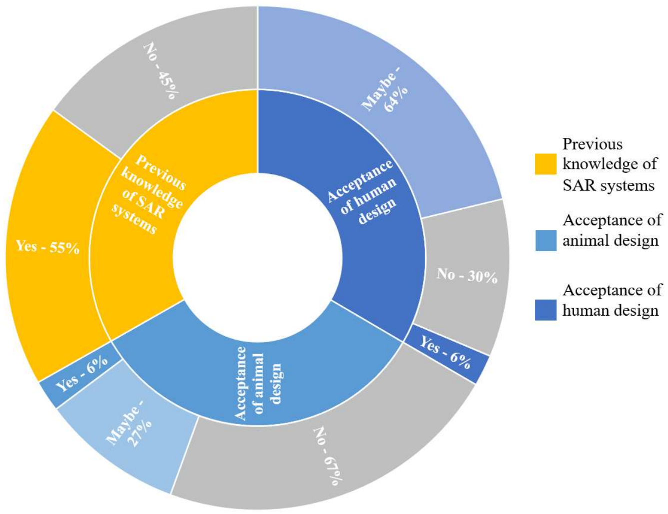

Figure 1) Previous knowledge and current acceptance of SAR technology among UK older adults

IV. Discussion

This study aimed to understand older adults' perceptions of SARs. Many suggested that they would be willing to have a SAR in their own home if they felt they needed one and were able to identify some advantages of them; however only 6% would consider either design now. There are several potential reasons for this, one being the lack of existing knowledge, and therefore a potential lack of awareness surrounding the capability of SARs. For many participants, "*company*" was highlighted as a key advantage to SARs in the home, with many commenting that the animal-like design is, "*less intrusive*". However, humanoid robots include support for complex functionalities such as dexterous manipulation, advanced navigation and, moreover, a natural, more intuitive interface, which can overcome some of the difficulties currently experienced especially by the elderly, thanks to the multimodality of stimulation given by them. One of the key barriers was a perceived "*lack of need*", which may also highlight that people aren't aware of how physically helpful a SAR could be.

Future designs of SAR should include an element of encouraging movement, especially if they are focused towards older adults who, as a group, are known to have high levels of sedentary behaviour. Several participants raised the issue of "*over-reliance*" as a barrier to them accepting a SAR into their home. Therefore, by ensuring that some form of activity is actively encouraged by the SAR, it is possible that they will become more accepted. Equally, a focus on reablement technology would be beneficial to help avoid the over-relance issue.

Overall, this study shows that older adults perceive SARs to be potentially helpful, especially in relation to providing company for those living alone. Future work should look to highlight the potential benefits of SARs for older adults, especially to supporting physical tasks within daily life. This may be achieved with new participatory design strategies that involve the user from the beginning to create robots with customisable services that will better match the user requirements and needs.

References

1] Feil-Seifer D, Mataric M. Defining socially assistive robotics. 2005 Presented at: 9th International Conference on Rehabilitation Robotics; 2005; Chicago p. 465-468.

[2] Causo A, Vo G, Chen I, Yeo S. (2015) Design of robots used as education companion and tutor. Robotics Mechatronics:75-84.

[3] Di Nuovo, A.; Varrasi, S.; Lucas, A.; Conti, D.; McNamara, J.; Soranzo, A. (2019) Assessment of Cognitive skills via Human-robot Interaction and Cloud Computing. J. Bionic Eng., 16, 526–539.

[4] Fasola J, Mataric M. A socially assistive robot exercise coach for the elderly. J Hum Robot Interact 2013;2(2):1.

[5] Kyong IK, Freedman S, Mataric M, Cunningham M, Lopez B. A hands-off physical therapy assistance robot for cardiac patients. 2005 Presented at: 9th International Conference on Rehabilitation Robotics; 2005; Chicago.

[6] Robinson, H., MacDonald, B., Kerse, N., Broadbent, E.: The Psychosocial Effects of a Companion Robot: A Randomized Controlled Trial. Journal of the American Medical Directors Association. 14, 661–667 (2013).

[7] Camp, N., Lewis, M., Hunter, K., Johnston, J., Zecca, M., Di Nuovo, A., & Magistro, D. (2021). Technology used to recognize activities of daily living in community-dwelling older adults. International Journal of Environmental Research and Public Health, 18(1), 163.

[8] Wiltshire, G. & Ronkainen, N. (In Press) A realist approach to thematic analysis: making sense of qualitative data through experiential, inferential and dispositional themes. Journal of Critical Realism

https://doi.org/10.31256/Xw5Aj7Q

Requirements for a home-based rehabilitation device for hand and wrist therapy after stroke

Vignesh Velmurugan, Luke Wood, Farshid Amirabdollahian

***Abstract*—Recovering hand function to perform activities of daily living (ADL), is a significant step for stroke survivors experiencing paresis in their upper limb. A home-based, robot mediated training approach for the hand allows the patient to continue their training independently after discharge to maximise recovery at the patient's pace. Developing such a hand/wrist training device that is comfortable to wear and easy to use is the objective of this work. Using a user-centred design approach, the first iteration of the design is based on the requirements derived from the users and therapists, leading to a first prototype. The prototype is then compared and evaluated against the required features. This paper highlights the methodology used in the process of validating the design against our initial brief.**

***Index Terms*—Rehabilitation, hand, wrist, requirements, orthosis**

I. Introduction

Motor function deficits in the upper limb are prevalent in 80% of stroke survivors [1]. Normal hand function is expected to perform Activities of Daily Living (ADL), and hence its training alongside the proximal segments helps to improve functional recovery [2].

Most conventional post-stroke rehabilitation takes place in the form of a one to one session in a clinical environment. In conditions like the ongoing pandemic, the patient must be able to continue training without direct contact at their own home. Robot-aided rehabilitation helps to achieve this by allowing the user to train for a longer duration, several times a day, without fatigue caused by travelling to and from the clinic. Thus the user would be able to train at a higher intensity which has shown to improve recovery of arm function [3]. Remote supervision also increases productivity and reduces the pressure on the health care system.

The objective of this research is to design a home-based rehabilitation device for the hand and wrist that facilitates active initiation and execution of movements. In this paper, we discuss the different user requirements of such a device and the methods of evaluation to verify that the prototype iterations meets these requirements.

II. Design Methodology

A cooperative approach involving users at every stage is adopted in the design of this device. Firstly, a review of the state of the art identified several contemporary works that focus on post-stroke training of wrist and fingers such as Gloreha [4], Hand of Hope [5], Saebo Flex [6], and SCRIPT SPO [7]. In engaging with the potential users, the SCRIPT researchers used methods such as focus groups and cultural probes to develop persona based scenarios. These scenarios helped to formulate a set of requirements that the potential users expect in such devices. These requirements serve as the basis for our first design iteration. The resulting prototype will be subject to two formative and a summative evaluation phases involving the potential users and therapists. Therefore, the user is an active participant within the design cycles.

All authors are with the School of Physics, Engineering, and Computer Science, University of Hertfordshire, College Lane, Hatfield, AL10 9AB, UK. Corresponding author's email: v.velmurugan@herts.ac.uk

III. User Requirements

In the first phase of our design process, a review of the state of the art involving task analysis, exclusion audit and studies by the SCRIPT consortium helped to form a comprehensive but non-exhaustive list of requirements. In this section, we discuss these requirements and their methods of evaluation.

Fig. 1. Early prototype showing the device's independence from changing CoRs of the index finger during flexion and extension

A. Functional requirements

1) **Adjustable functional assistance.**
Patients with hemiparesis experience hyperflexion (increased involuntary flexion) in their hand joints, often leaving them with a closed fist and fully flexed wrist. They require assistance with extension to overcome the hyperflexion. The magnitude of assistive forces required, depends on user's motor deficit and varies with training due to the underlying recovery. Based on therapists' feedback, a maximum extension force and torque of $10\,\mathrm{N}$ and $1.5\,\mathrm{Nm}$ can be applied at the fingertips and wrist respectively. Using the spring's stiffness and joint angle feedback, achieving this requirement can be verified using a force sensor as described in [8].
2) **Range of motion for Activities of Daily Life.**
The device should allow for training over the entire range of motion (RoM) required to perform ADL as established from the literature (Table. I).

TABLE I
RoM TO PERFORM ADL

	Wrist	Fingers			Thumb	
		MCP	PIP	DIP	MCP	PIP
Flexion	70°	90°	100°	80°	100°	80°
Extension	60°	0°	10°	0°	0°	10°
Abduction	20°	25°			50°	
Adduction	30°	0°			0°	

3) **Does not hinder any of the natural range of motions of the joints.**
The device should not block any unassisted(Abduction/Adduction) DoF required to perform ADL (Table. I). This ensures that using the device does not lead to muscle atrophy.
This and the previous requirement (No 2.) will be evaluated by measurement of the joint angle using a goniometer and a data glove.
4) **Self-aligning centre of rotation (CoR).**
The CoR of the joints varies with hand movement. Misalignment between the CoR of the user's joints and those of the device would lead to the user's discomfort. Hence the device/orthosis needs to allow for alignment with the hand's CoR (Fig. 1). Our design eliminates this concern using a flexible interaction element.
5) **Measurement of finger and wrist motion.**
Measurement of the flexion and extension angles of the fingers and wrist is necessary for the user and the therapists to monitor the training progress. These measurements can also be used to control therapeutic interactive games. These have been shown to improve user's motivation. SCRIPT researchers evaluated the repeatability of their joint angle measurement using four different standardised grip sizes. We aim to evaluate our prototype using the same approach and a goniometer.
6) **Accommodate different hand dimensions.**
A device that is customised to the user's hand-size is preferred since a mismatch in dimensions leads to discomfort and render it bio-mechanically inefficient. Hence the design has to adapt to different hand dimensions. A qualitative evaluation regarding any discomfort while training, involving multiple users with different hand sizes will be used to validate this.
7) **Visual and tactile transparency**
Wearable hand devices often block fingers' tactile sensing and restrict the visibility of the hand. The ability to observe grasping and movement of the fingers and wrist and feel the tactile features of the interacting object adds to this sensory stimulation and neural modulation potential. The functional element, achieving tactile and visual feedback is considered within the design cycles, while usability elements are subjectively evaluated.

B. Usability requirements

8) **Ease of donning/doffing.**
This is one of the most significant requirements of all, since the users experience deficits in their motor function. Therefore, the design should allow the user to don/doff independently with ease.
9) **Safe to use at home.**
Given the absence of a clinician's supervision, the device should pose no risk of injury to the user and the family members.
10) **Smaller space requirement and increased mobility.**
Based at home, the device should occupy less space to ensure use-as-needed. Location flexibility could reduce mental/emotional fatigue which in turn could lead to longer training duration.
11) **Require relatively less technical proficiency to operate.**
Easy, infrequent and short procedures for setting up, operating and troubleshooting helps with maintaining the motivation levels of the user.

Given the subjective nature of these requirements (Nos 7-11), a qualitative evaluation involving clinicians and stroke survivors with Likert scale questionnaires will be used to study the usability of the device. This requirement analysis showed the significance of wearability and usability in user's acceptance and hence required a major part of our focus.

IV. CONCLUSION

A prototype has been developed according to the above mentioned requirements and is ready to be evaluated against them. The results of this formative evaluation will help to update both the design and the underlying initial set of requirements. The resulting second iteration of the prototype will undergo further evaluation involving potential users, to validate its functionality and usability.

REFERENCES

[1] A. Schwarz, C. M. Kanzler, O. Lambercy, A. R. Luft, and J. M. Veerbeek, "Systematic review on kinematic assessments of upper limb movements after stroke," *Stroke*, vol. 50, no. 3, pp. 718–727, 2019.
[2] H. I. Krebs, B. T. Volpe, D. Williams, J. Celestino, S. K. Charles, D. Lynch, and N. Hogan, "Robot-aided neurorehabilitation: a robot for wrist rehabilitation," *IEEE transactions on neural systems and rehabilitation engineering*, vol. 15, no. 3, pp. 327–335, 2007.
[3] G. Kwakkel, "Intensity of practice after stroke: More is better," *Schweizer Archiv fur Neurologie und Psychiatrie*, vol. 160, no. 7, pp. 295–298, 2009.
[4] A. Borboni, M. Mor, and R. Faglia, "Gloreha—hand robotic rehabilitation: Design, mechanical model, and experiments," *Journal of Dynamic Systems, Measurement, and Control*, vol. 138, no. 11, 2016.
[5] N. Ho, K. Tong, X. Hu, K. Fung, X. Wei, W. Rong, and E. Susanto, "An emg-driven exoskeleton hand robotic training device on chronic stroke subjects: task training system for stroke rehabilitation," in *2011 IEEE international conference on rehabilitation robotics*. IEEE, 2011, pp. 1–5.
[6] J. F. Farrell, H. B. Hoffman, J. L. Snyder, C. A. Giuliani, and R. W. Bohannon, "Orthotic aided training of the paretic upper limb in chronic stroke: results of a phase 1 trial," *NeuroRehabilitation*, vol. 22, no. 2, pp. 99–103, 2007.
[7] F. Amirabdollahian, S. Ates, A. Basteris, A. Cesario, J. Buurke, H. Hermens, D. Hofs, E. Johansson, G. Mountain, N. Nasr *et al.*, "Design, development and deployment of a hand/wrist exoskeleton for home-based rehabilitation after stroke-script project," *Robotica*, vol. 32, no. 8, pp. 1331–1346, 2014.
[8] S. Ates, C. J. Haarman, and A. H. Stienen, "Script passive orthosis: design of interactive hand and wrist exoskeleton for rehabilitation at home after stroke," *Autonomous Robots*, vol. 41, no. 3, pp. 711–723, 2017.

https://doi.org/10.31256/Pm5De6C

Exploring Behaviours Percieved as Important to the Human-Dog Bond and their Translation to a Robotic Platform

Katie A. Riddoch
Institute of Neuroscience and Psychology, University of Glasgow
Glasgow, Scotland
k.riddoch.1@research.gla.ac.uk

Dr. Roxanne D. Hawkins
Division of Psychology, University of the West of Scotland
Paisley, Scotland
roxanne.hawkins@uws.ac.uk

Prof. Emily S. Cross
Department of Cognitive Science Macquarie University
Sydney, Australia
emily.cross@mq.edu.au

***Abstract*— To facilitate long-term engagement with social robots, robots can be modelled on 'successful' social animals – specifically, pet dogs. Unfortunately, scientific understanding is limited to qualities of dogs that are 'liked', opposed to behaviours that facilitate and maintain the human-dog bond. To better understand dog behaviours that are important for building bonds between owner and pet, we collected open-ended responses from dog owners (n=153). Thematic analysis identified 7 behaviour categories: the importance of 1) attunement, 2) communication, 3) consistency and predict-ability, 4) physical affection, 5) positivity and enthusiasm, 6) proximity, and 7) shared activities. We consider the feasibility of translating dog behaviours into a robotic platform, and potential barriers moving forward. In addition to providing insight into important behaviours for human-dog bonding, this work provides a springboard for those hoping to implement dog behaviours into animal-like agents, avatars, and robots.**

Keywords—dog behaviour, social robots, biomimetics, human-animal interaction, HRI, HAI

I. Introduction

Loneliness (defined as the subjective feeling that one lacks social support or companionship) is a public health issue growing in importance and urgency due to population ageing [1], social media influences, and most recently, pandemic-induced social isolation measures. In an attempt to reduce loneliness and its many associated consequences (e.g., cardiovascular disease, depression, and suicidal thoughts) a range of technological solutions are being developed [1, 2]. It has been proposed that the ability of social robots to analyse and respond to aspects of human behaviour make them a candidate solution for addressing loneliness in some contexts [3]. To sidestep the complexities, expense, and high expectations associated with developing humanoid robots to take on these roles, robot developers are increasingly drawing inspiration from other 'successful' social animals [3,4].

In western cultures, pet dogs can provide a source of comfort and companionship, and ownership can benefit a person's mental health and wellbeing [5]. As a result, studying human-dog attachment, and implementing dog behaviours into robots, might help us create artificial systems that provide similar benefits [6]. It has further been suggested that by creating systems that resemble dogs, we could encourage greater acceptance of social robots - allowing users to reap the benefits of dog-ownership long-term [4, 7] while minimising the costs and risks of looking after living animals.

Several studies have examined pet dog behaviours and their applicability to social robots [4-7], with a focus on qualities and behaviours which are 'liked' (e.g., smartness, friendliness, attentiveness). We argue that liked behaviours could be different to those which are important to bonding – such as how we might like, but not have a strong bond with, a household appliance. To gain clarity regarding this distinction, and to ensure future developments are grounded in a rich and informative evidence base, we asked dog owners which behaviours they perceived to be important to the bond they share with their dog.

Method

Participants

In total, 283 individuals accessed the online study. After the removal of incomplete datasets and incorrect responses (n=130), 153 complete datasets remained. All participants were dog owners over the age of 18 years, and the majority identified as female (female: n= 123, male: n=4, non-binary: n=1). All study procedures were approved by the University of Glasgow College of Science & Engineering Ethics Committee (#300190287). Study procedure and sample size estimation (n=128) were pre-registered on the Open Science Framework: https://bit.ly/3dhdH9h. All data were anonymised and will be stored for 10 years, and then deleted.

Procedure

On the online survey platform (www.qualtrics.com) participants read an information sheet, provided virtual informed consent, and were given the option to provide an email address (entering them into a prize draw to win one of five £25 gift cards). Finally, after completing a series of questionnaires (out of the scope of this report), participants were asked to describe behaviours of their dog, according to the following instruction: "Please describe things that your dog does that you really like. Specifically, behaviours that you think are crucial to the bond you have with your dog."

Qualitative Data Analysis

Data were analysed using Thematic Analysis using NVivo software (v.12), following a rigorous six-step method [8]. This is a widely used inductive method of qualitative analysis that involves familiarisation with the data, followed by classification of recurring ideas into codes. These codes are grouped into broader themes, which are then discussed by independent coders. In this study, two coders (one analysing the full dataset, and the other analysing a randomly selected subset [20%, n=31]) agreed on 7 data-driven themes.

II. Results

The coders agreed on 7 key themes: the importance of 1) attunement, 2) communication (verbal and non-verbal), 3) consistency & predictability, 4) physical affection, 5) positivity & enthusiasm, 6) proximity, & 7) shared activities.

1. *Attunement*

Numerous owners mentioned how their dogs alter their behaviour in response to the owner's routine (n=17) or emotional state (n=37). E.g., the dog will display physical affection just prior to the owner waking or will provide physical affection when the owner is experiencing a low mood, appearing to pick up on their emotional cues.

2. *Communication*

Many owners (n=88) mentioned the importance of their dog expressing their needs to them. Accounts included examples of vocal behaviour and body language (e.g., through eye contact, by presenting toys, or through the use of nudging body parts or vocalisations). Additionally, owners stressed the importance of their dog consistently listening and responding to their voice commands or gestures.

3. *Consistency and Predictability*

The importance of consistency was a common report (n=68), specifically in terms of enthusiasm, positivity, obedience, and emotional awareness (e.g., consistently expressing joy on their owners return). Inconsistency was also reported as being desirable (n=20) – e.g., variability in play behaviour, and the dog expressing independence.

4. *Physical Touch*

Many owners (n=86) mentioned the importance of physical touch initiated by the dog – e.g., the dog resting a body part (e.g., head, paw, whole body) on the owner, or giving the owner "kisses", "hugs", and "cuddles".

5. *Positivity and Enthusiasm*

Many owners (n=51) mentioned that when they arrive home, their dog approaches them at the door and expresses one (or a combination) of the following: erratic tail wagging, wiggling of their body, leaping into their arms, jumping up and around excitedly, or bringing a toy.

6. *Proximity*

Owners (n=18) mentioned the importance of their dog physically following them (e.g., from room to room), physically touching the owner whilst co-sleeping (n=48), and generally remaining in close proximity while at home or out on walks (n=18). The owners perceive this behaviour as resulting from love, loyalty, or the owner being a perceived source of nurturance or protection.

7. *Shared Activities*

Many owners (n=100) mentioned playing (e.g., games, training, general playful behaviours) and how the dog's perceived enjoyment of activities was important for bonding. People also mentioned the importance of affection and 'checking in' behaviours whilst walking together (n=43).

III. DISCUSSION

By using open-ended questions, we gathered rich detail about specific behaviours (7 core themes) perceived as important for the human-dog bond. While many of the behaviours could be implemented in a robot, significant gaps in our knowledge remain, which will result in barriers to implementation. Further exploration of these behaviours would be an important next step. For example, many participants expressed that "cuddling" is important, but they did not specify what "cuddling" consists of. To translate such behaviours into a robotic platform, we will need a fuller understanding of the individual components of the dog behaviour. Our online study design prevented us from asking follow-up questions, but future research can build on these findings.

Future work could use video and motion capture technology to further classify dog behaviours and owner reactions. Incorporating rigorous qualitative methods could also facilitate insights regarding anthropomorphic attributions, and the role that individual preferences play. By conducting controlled mixed-methods experiments with robotic dogs, it should also be possible to manipulate the presentation of dog behaviours and determine desirable behavioural boundaries - e.g., in terms of intensity, frequency, or duration of behaviour.

Conducting further research, to better understand how preferred dog behaviours can (or cannot) be successful modelled onto dog-like robotic systems, stands to greatly inform our understanding of the costs and benefits of dog-like social robots in psychosocial interventions.

IV. CONCLUSION

This study provides detailed insights into dog behaviours perceived as important for maintenance of the human-dog bond. We recommend that next steps focus on exploring the nuances of these behaviours, and testing the applicability and feasibility of programming such behaviours into dog-like robots. Exploring users' reactions and engagement via quantitative and qualitative methods will be important evaluation strategies.

ACKNOWLEDGMENT

E.S.C. gratefully acknowledges research funding from the European Research Council under the European Union's Horizon 2020 Research and Innovation Programme (GA 677270) and the Leverhulme Trust (PLP-2018-152).

REFERENCES

[1] Leigh-Hunt, N., Bagguley, D., Bash, K., Turner, V., Turnbull, S., Valtorta, N., & Caan, W. (2017). An overview of systematic reviews on the public health consequences of social isolation and loneliness. *Public health*, *152*, 157-171.

[2] Miller, E., & Polson, D. (2019). Apps, avatars, and robots: the future of mental healthcare. *Issues in mental health nursing*, *40*(3), 208-214.

[3] Prescott, T. J., & Robillard, J. M. (2020). Are Friends Electric? The Benefits and Risks of Human-Robot Relationships. *iScience*, 101993.

[4] Miklósi, Á., Korondi, P., Matellán, V., & Gácsi, M. (2017). Ethorobotics: A new approach to human-robot relationship. *Frontiers in psychology*, *8*, 958.

[5] Sable, P. (2013). The pet connection: An attachment perspective. *Clinical Social Work Journal*, *41*(1), 93-99.

[6] Krueger, F., Mitchell, K. C., Deshpande, G., & Katz, J. S. (2021). Human–dog relationships as a working framework for exploring human–robot attachment: a multidisciplinary review. *Animal Cognition*, 1-15.

[7] Konok, V., Korcsok, B., Miklósi, Á., & Gácsi, M. (2018). Should we love robots?–The most liked qualities of companion dogs and how they can be implemented in social robots. *Computers in Human Behavior*, *80*, 132-142.

[8] Braun, V., & Clarke, V. (2019). Reflecting on reflexive thematic analysis. *Qualitative Research in Sport, Exercise and Health*, *11*(4), 589.

https://doi.org/10.31256/Os6Aw4Y

Human activity recognition in RoboCup@home: Inspiration from online benchmarks

Mohamad Reza Shahabian Alashti, Mohammad Hossein Bamorovat Abadi, Patrick Holthaus, Catherine Menon, and Farshid Amirabdollahian

***Abstract*—Human activity recognition is an important aspect of many robotics applications. In this paper, we discuss how well the RoboCup@home competition accounts for the importance of such recognition algorithms. Using public benchmarks as an inspiration, we propose to add a new task that specifically tests the performance of human activity recognition in this league. We suggest that human-robot interaction research in general can benefit from the addition of such a task as RoboCup@home is considered to accelerate, regulate, and consolidate the field.**

***Index Terms*—Human activity recognition, robotics competitions, benchmarks.**

I. Introduction

It is likely that technological progress will soon result in a greater prevalence of robots and intelligent systems within human living and working environments. Robots are thereby expected to assist people in their daily life, for example, by helping with the housework or serving food. Many applications benefit from a sophisticated robot perception that is able to detect human activities [1]. This entails learning, recognition, and potentially prediction of human postures, gestures, actions, and emotions in real-world scenarios. Our work investigates the current role of human activity recognition (HAR) in the *RoboCup@Home* competition [2] and identifies a benefit of adding a task that emphasises benchmark of HAR in human-robot interaction (HRI). We thus propose to introduce a new task in *RoboCup@Home* that is inspired by established activity recognition benchmarks.

II. RoboCup@home Competition

RoboCup is a global project to advance progress in artificial intelligence and robotics. Besides its flagship league RoboCupSoccer, it has established a number of other competitions that are not related to football but evolve around other robotics application domains. One of these competitions, the *RoboCup@Home* league, is focusing on HRI in everyday situations at home and in other indoor spaces to promote and foster the development of service and assistive robotics [3]. Robots must autonomously solve a wide range of tasks to support the human in their activities such as navigation in unknown environments, people recognition, object picking and placing, or verbal interaction. Prior to each year's competition, a predefined set of up around 20 tasks is designed by a technical committee to evaluate the robot's abilities. The exact set varies and is published in the annual rulebook [2]. In this paper we focus on those tasks that are related to HAR.

All authors are with the School of Physics, Engineering, and Computer Science, University of Hertfordshire, College Lane, Hatfield, AL10 9AB, UK. Corresponding author's email: `m.r.shahabian@herts.ac.uk`

TABLE I
Overview of HAR tasks in RoboCup@Home

Year	Task	Activity
2009	Who Is Who?	Waving
	Enhanced Who Is Who?	Waving
	Shopping Mall	Pointing
	Demo Challenge (In the bar)	Waving
2010, 2011	Who Is Who?	Waving
	Enhanced Who Is Who?	Waving
	Shopping Mall	Pointing
2012	Who Is Who?	Waving
2013	Emergency Situation	Fire event
2014	Emergency Situation	Fall over, waving
	Technical Challenge: People Activity Detection	Standing, Sitting, Laying, Confused, Happy, Bored
2015	Robo-Nurse	Waving, fall, sit, walk
	Wake me up test	human awakening
	Demo Challenge	Learning actions on-the-fly
2016	Navigation Test	Crowd
	Demo Challenge	Learning actions on-the-fly
2017	Cocktail Party	Waving
	Navigation Test	Crowd
	E2GPSR	Describing a person
	Demo Challenge	Learning actions on-the-fly
2018	Cocktail Party	Rising and waving
	Navigation Test	Crowd
	Person and Speech Recognition	Crowd, waving, rising, standing, siting, laying
	E2GPSR	describing a person
	Tour guide	Waving
	Demo Challenge	Learning actions on-the-fly
2019	Hand Me That	Pointing
	Stickler for the Rules	Littering
2020	What is That?	Nodding

A. Human Activity Recognition in RoboCup@Home

A glimpse at rulebooks[1] of the 2009 to 2020 competitions illustrates that most tasks are in HRI and object detection and recognition, while only a small number of tasks test HAR-related functions. Table I lists all tasks that include human activities from every year's rulebook from 2009 to 2020. With the exception of 2014, in which the technical challenge was explicitly dedicated to identify what people present and do, there is no explicit identification of HAR tasks in this league at all. More than half of of the tasks that contain any activity recognition can be solved by recognising waving gesture as a signal for the robot to continue its operation. Likewise, pointing, nodding and rising were usually required only at specific points in time and not as general function where the robot would need to distinguish between different set of activities during a longer period of interaction or observation.

[1]Online resource: robocupathome.org/rules

Crowd identification and asking them to move away were actions needed to accomplish the *Navigation Test* from 2016 to 2018. Some state-of-art recognition challenges, such as describing a person and learning actions from demonstrations have been introduced in the *Enhanced Endurance General Purpose Service Robot (E2GPSR)* task and the *Demo Challenge*. In these two tasks, no team has yet achieved the maximum score. In 2017 and 2018, for example, none of the teams attempted the *Demo* challenge and the highest achieved score in *E2GPSR* these years was 70 out of 250 in the open platform competition [4]. The recognition of individual, very specific events like a dropping blanket, littering, or a fire hazard were a part of some tasks. The detection of general human activities such as falling, sitting, walking, lying, and awakening were only essential in *Emergency Situation* (2014), *Robo-Nurse* (2015), and *Person and Speech Recognition* (2018).

III. Activity recognition benchmarks

A wide range of HAR benchmarks has been developed to compare the performance of activity recognition algorithms on standardised datasets. The recognition is thereby typically vision- or sensor-based, or a combination of the two.

A. Sensor-based Benchmarks

The *OPPORTUNITY* challenge is an example for the use of public benchmarks for sensor-based activity recognition [5]. A wide range of locomotion models and gestures were collected using onboard robot sensors, and environmental sensors. These were classified by *k-NN, NCC, LDA and QDA* techniques then evaluated using standard approaches such as *Weighted F-measure, Area under the ROC curve* and *Misalignment measures*. The *HASC Challenge*, orchestrated by Nagoya University [6], is also similar and involves data collected from a large number of subjects by 20 teams. The *BSN Contest* [7], was a competitive benchmark based on body-attached sensors. The *BDA Challenges*[2], which aim to recognize daily physical activity from phone sensors, are another example of HAR competitions that aim to recognise six basic activities.

B. Vision-based Benchmarks

Although many research groups have prepared datasets, only some of these are designed to evaluate the accuracy. *ActivityNet* [8], for example, is an international challenge on activity recognition that have been held since 2016 in conjunction with the CVPR conference. It includes a diverse set of tasks each emphasising a different aspects of activity recognition to develop the visual perception of videos and natural human language. Three challenges were based on *ActivityNet*'s own dataset and some other tasks were based on other large-scale activity and action datasets, including Kinetics, AVA, ActEV, HACS, and ActivityNet Entities. The *SPHERE* challenge [9] is another activity recognition competition in the context of a smart environment utilising data including RGB-D, accelerometer, and environment sensor. Two main challenges are predicting posture and daily living activities with the aim of creating a reliable model to enhance physical well-being. The *VISUM challenge*[3] is third benchmark that uses the *KTH dataset* with six type of human actions (walking, jogging, running, boxing, hand clapping and hand waving).

IV. Suggestions for Improving RoboCup@Home

Inspired by these publicly available benchmarks, we propose to include a new task in the competition that puts an exclusive focus on general HAR to further advance activity recognition in HRI and further acknowledge its importance in the field. We suggest to add a task that accounts for both types of HAR benchmarking, vision- and sensor-based. Ideally, the task would combine the use of the robot's integrated sensors and sensors from a smart environment to facilitate a competition within an interactive scenario. Motion detectors, door sensors, wearables (e.g. smartwatches) or cameras could be used to gather information about a person to recognise postures and activities in different locations. Moreover, we propose a complementing online simulation, which could alleviate hassles and costs. The task could, for example, be set in an assistive robotics scenarios where HAR plays a crucial role.

V. Conclusion

We reviewed tasks in *RoboCup@Home* and revealed that activity recognition only plays a limited role within this competition. We also provided an overview of activity recognition benchmarks in home environments to use as an inspiration to better account for the importance of HAR in HRI. With this background, we proposed a task for *RoboCup@Home* that focuses on HAR benchmarking. Using a combination of vision and other sensors, this task will allow to evaluate activity recognition during interaction to further advance HRI research.

References

[1] T. Kumrai, J. Korpela, T. Maekawa, Y. Yu, and R. Kanai, "Human activity recognition with deep reinforcement learning using the camera of a mobile robot," in *2020 IEEE International Conference on Pervasive Computing and Communications (PerCom)*, 2020, pp. 1–10.

[2] D. Holz, J. Ruiz-del Solar, K. Sugiura, and S. Wachsmuth, "On RoboCup@Home: Past, Present and Future of a Scientific Competition for Service Robots," in *Robot Soccer World Cup*. Springer, 2014.

[3] F. Jumel, "Advancing Research at the RoboCup@Home Competition," *Robotics & Automation Magazine*, vol. 26, no. 2, pp. 7–9, 2019.

[4] M. Matamoros and M. Luz, "Robocup@home scoring history," github/RoboCupAtHome/AtHomeCommunityWiki/wiki/Scores, 2018.

[5] R. Chavarriaga, H. Sagha, A. Calatroni, S. T. Digumarti, G. Tröster, J. d. R. Millán, and D. Roggen, "The Opportunity challenge," *Pattern Recognition Letters*, vol. 34, no. 15, pp. 2033–2042, 2013.

[6] N. Kawaguchi, N. Ogawa, Y. Iwasaki, K. Kaji, T. Terada, K. Murao, S. Inoue, Y. Kawahara, Y. Sumi, and N. Nishio, "HASC Challenge," in *Augmented Human International Conference*, 2011, pp. 1–5.

[7] M. Giuberti and G. Ferrari, "Simple and robust BSN-based activity classification," in *International Symposium on Applied Sciences in Biomedical and Communication Technologies*, 2011, pp. 1–5.

[8] F. Caba Heilbron, V. Escorcia, B. Ghanem, and J. Carlos Niebles, "ActivityNet: A Large-Scale Video Benchmark for Human Activity Understanding," in *Conference on Computer Vision and Pattern Recognition*. IEEE, 2015, pp. 961–970.

[9] N. Twomey, T. Diethe, M. Kull, H. Song, M. Camplani, S. Hannuna, X. Fafoutis, N. Zhu, P. Woznowski, P. Flach, and I. Craddock, "The SPHERE Challenge: Activity Recognition with Multimodal Sensor Data," *arXiv preprint arXiv:1603.00797*, 2016.

[2] Online competition: kaggle.com/c/bda-2020-physical-activity-recognition

[3] Online competition: kaggle.com/c/visum-activity-recognition

https://doi.org/10.31256/If7Nm5Z

Affordable Robot Mapping using Omnidirectional Vision

Mohammad Hossein Bamorovat Abadi, Mohammad Reza Shahabian Alashti, Patrick Holthaus,
Catherine Menon, and Farshid Amirabdollahian

***Abstract*—Mapping is a fundamental requirement for robot navigation. In this paper, we introduce a novel visual mapping method that relies solely on a single omnidirectional camera. We present a metric that allows us to generate a map from the input image by using a visual Sonar approach. The combination of the visual sonars with the robot's odometry enables us to determine a relation equation and subsequently generate a map that is suitable for robot navigation. Results based on visual map comparison indicate that our approach is comparable with the established solutions based on RGB-D cameras or laser-based sensors. We now embark on evaluating our accuracy against the established methods.**

***Index Terms*—Visual Sonar, Omnidirectional Vision, Visual Mapping.**

I. INTRODUCTION

Mobile robots require a navigation algorithm to move in a goal-directed manner. A good understanding of the environment is thereby key for a successful navigation. There are many methods of obtaining this information, such as using a variety and combination of sensors as input. Most popular solutions include a laser range finder to generate highly accurate maps for simultaneous localisation and mapping (SLAM), cf. [1]. However, lasers that provide a high scanning rate often cost more than £1,000 and are not always feasible. However, lasers that provide a high scanning rate often cost more than £1,000. There are other affordable solutions that use, for example, RGB-D cameras to provide the navigation system with input. However, these are usually limited in their field of view due to the opening angle. Our approach, by contrast, uses a single omnidirectional RGB camera capable for gathering information about the entirety of the robot's surroundings. Our research further identifies a metric for generating a map from the input image using a visual sonar approach to find obstacles around the robot. Data from visual sonar sensors is used to determine a metric distance between the robot and these obstacles. These distances are then used to generate a map that a robot can use for navigation.

II. PREVIOUS WORK

Our approach builds on top of existing work that uses monocular vision instead of a laser sensor to find the obstacles around a robot with the help of edge detection and so-called visual sonars [2]. This approach has been modified to be used with an omnidirectional vision system [3]. It has also been extended to determine a free path by varying the number of sonar beams to identify their ideal range and shape [4]. The method can enable robot navigation when using an enhanced model that uses three individual sonars to the left, right, and front of the image to detect obstacles and another one to determine a free path simultaneously [5].

All authors are with the School of Physics, Engineering, and Computer Science, University of Hertfordshire, College Lane, Hatfield, AL10 9AB, UK. Corresponding author's email: m.bamorovat@herts.ac.uk

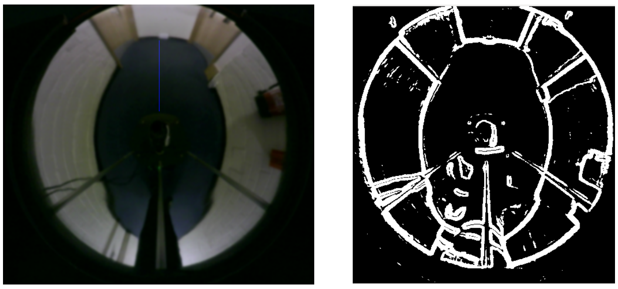

(a) Visual Sonar Beam (b) Sobel Edge detection

Fig. 1: (a) Omnidirectional image with a visual sonar. (b) Result of the edge detection and thresholding algorithm.

III. METHOD

One key characteristic of the previous approach is that it is non-metric. In comparison, we present an omnidirectional vision system for mobile robot navigation that generates a metric map. Our method consists of two steps: (A) visual preprocessing to find edges that represent obstacles and to calculate the sonar beams and (B) a fitting step to relate the pixel distance to real-world lengths.

A. Visual processing

First, a sobel operator is used to detect edges in the image. We further apply a black and white threshold to remove noise (cf. Fig. 1b). In parallel, we use an algorithm to identify and mask surface reflections to prevent them from being incorrectly identified as obstacles [4]. We then generate visual sonar beams that measure distances to obstacles comparable to normal sonar technology. Instead of using acoustic signals, visual sonar works on the preprocessed image and results in pixel-based distances [6]. That is, the beams originate at the centre of the image and extend outwards until they reach an edge. Figure 1a shows an example beam (blue) on an omnidirectional image.

B. Sonar Fitting

In this section we present a novel method to calculate the metric distance between robot and obstacles, taking into account the pixel-based characteristics of visual sonar. Each sonar beam forms a vector of visual sonar consisting of a group of pixels. The length of this vector is the number of pixels. For instance, the sonar between robot and the wall in Figure 1a has a length of 158 pixels. This distance corresponds to a metric length, which can be identified using the robot's odometry, i.e. by moving the robot around between defined places. A relationship can be found using a fitting method that relates changes in the robot's position to changes in the pixel distance that originates from the visual sonar. Since all visual sonars start from the centre of the omnidirectional image, a single sonar sensor can be considered alone to identify this relationship, which can then be used for the other sensors. A dense calibration is necessary to find the correlation function d between the sonar pixels and their real-world distance. We have designed a routine that begins with the robot placed sufficiently close to a wall so that the sonar vector's first pixel can be detected. The robot is then moved back. Information is gathered from the odometry to obtain a real-world distance and from the visual sensor for a change in pixel distance. We then use the fitting method above to determine the metric distance from the visual sensor, obtaining from this fitting method an equation that takes pixel input and outputs the metric distance.

IV. Evaluation

We replaced the RGB-D sensor of a TurtleBot2e[1] with an RGB camera-based solution (<£50) to evaluate our approach under realistic circumstances, cf. [4]. We also mounted a rotating DS-01 laser (£150) as a high-precision alternative to compare the mapping results. Our experiments, all of which were performed at University of Hertfordshire's Robot House, consisted of two parts: calibration and mapping.

A. Calibration

A successful calibration is the prerequisite for applying our approach to a robot's navigation system. We, therefore, performed a series of tests moving the robot backwards at different speeds. Each of these tests has been repeated 10 times to gather odometry data and sonar pixel lengths. Results indicate that the most reliable data is obtained from a calibration with a slowly moving robot (velocity: 0.0 angular, $-.05$ linear) without any obstacles in front. Moreover, a straight robot movement with minimal deviations from its path led to optimal results. Figure 2 shows the result of fitting of a polynomial using one of the most reliable calibration routines. The function $d(x)$ describes the relation between the distance d in cm and the visual sonar length x in pixels:

$$\begin{aligned} d(x) = (0.0125 * x^7) + (0.0552 * x^6) + (0.0533 * x^5) \\ -(0.0910 * x^4) - (0.1683 * x^3) + (0.0784 * x^2) \\ +(0.4732 * x) + 0.5147 \end{aligned}$$

B. Mapping

With the function d and the visual sonar, we can calculate metric distances that can be used in mapping. Figure 3 shows a map that has been generated using SLAM[2] to use our visual sonar approach. As a comparison, red colour indicates the mapping of the same area that has been recorded with the high-precision laser. The visual sonar method has generated a map that is not as precise as the one generated with a laser and contains some artifacts but it is suitable for navigation tasks as we were able to successfully use it for driving the robot.

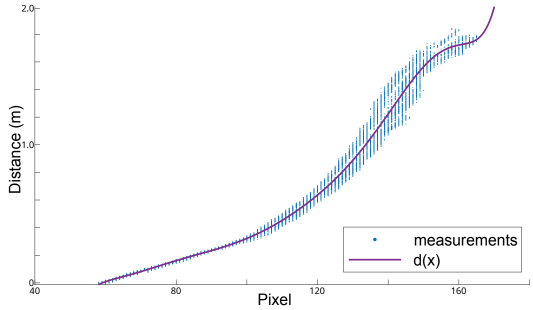

Fig. 2: Calibration and polynomial odometry fitting d

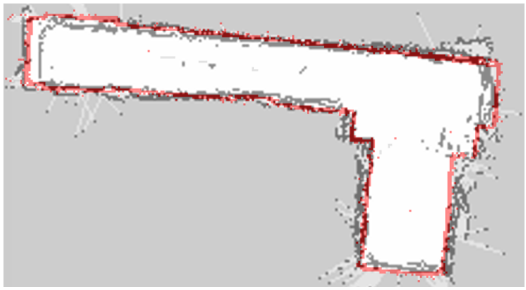

Fig. 3: Mapping result with laser comparison in red

V. Conclusion

We have presented a novel method for calculating the metric distance between a robot and obstacles based on a visual sonars. It correlates pixels from an omnidirectional image and the robot's odometry by fitting a function that determines the relationship between the sonar's length in pixels and a real-world distance. We have demonstrated that this method produces comparable results visually. For future work, we aim to revise the edge detection algorithm and plan to integrate regression learning to further improve results. Moreover, we plan a study to compare the approach's performance to other methods and technologies, such as RGB-D cameras and laser sensors and to calculate their precision and computation time.

References

[1] Y. D. Yasuda, L. E. G. Martins, and F. A. Cappabianco, "Autonomous visual navigation for mobile robots: A systematic literature review," *ACM Computing Surveys*, vol. 53, no. 1, pp. 1–34, 2020.

[2] S. Lenser and M. Veloso, "Visual sonar: Fast obstacle avoidance using monocular vision," in *Intelligent Robots and Systems*, 2003, pp. 886–891.

[3] B. Bonev, M. Ángel Cazorla Quevedo, and F. E. Ruiz, "Robot navigation behaviors based on omnidirectional vision and information theory," *Journal of Physical Agents*, vol. 1, no. 1, 2007.

[4] M. H. Bamorovat Abadi, M. Asghari Oskoei, and A. Fakharian, "Mobile robot navigation using sonar vision algorithm applied to omnidirectional vision," in *AI & Robotics (IRANOPEN), 2015*. IEEE, 2015, pp. 1–6.

[5] M. H. Bamorovat Abadi, M. A. Oskoei, and A. Fakharian, "Side sonar vision applied to omni-directional images to navigate mobile robots," in *Iranian Congress on Fuzzy and Intelligent Systems*, 2017, pp. 97–102.

[6] M. H. Bamorovat Abadi and M. Asghari Oskoei, "Effects of mirrors in mobile robot navigation based on omnidirectional vision," in *Intelligent Robotics and Applications*. Springer, 2015, pp. 37–48.

[1]A platform specification can be found at turtlebot.com/turtlebot2

[2]We used the standard ROS gmapping suite from wiki.ros.org/gmapping

https://doi.org/10.31256/Gy2Wm9H

A Call for Stronger Privacy Protections to Promote the Development of Ethical Domestic Robots

Chloe Haden
Hertfordshire Law School
(University of Hertfordshire)
Hatfield, Hertfordshire
C.Haden@herts.ac.uk

Farshid Amirabdollahian
School of Physics, Engineering and Computer Science
(University of Hertfordshire)
Hatfield, Hertfordshire
F.Amirabdollahian2@herts.ac.uk

Abstract— **The sale of service robots for personal and domestic is expected to rapidly increase in coming years. Growing concerns are raised towards the lack of clarity towards ethical and security safeguards within Data Protection Regulation for these products, particularly relating to privacy. With domestic robots having access to once historically protected spaces, it is imperative that legal rules keep up with technological advancements and the issues they pose to individuals and their rights. Respectively, this paper calls for stronger privacy protections to promote and encourage the development of ethical domestic robots.**

Keywords— Privacy, Data Protection, Safeguards, Artificial Intelligence, Robotics

I. Introduction

Artificial Intelligence (AI) and robotics is an ever-growing field in modern history, with the Internet of Things (IoT) offering additional support for better domestic robots [1]. Robots are equipped with the ability to sense, process and act. Particularly for domestic robots, that have access to individual's private homes, the risks to privacy have raised concern [2]. As stated by Calo, the potential to compromise devices in the home is not a new problem, but the difference with robotics is the ability to move and manipulate, as well as record and relay information [3].

To begin, this paper aims to assess the implications to privacy in reflection of the progression of domestic robots through use of conceptual research, to identify how privacy protections could be strengthened. In review of the General Data Protection Regulation (GDPR) [4], this paper aims to contribute by providing recommendations for a future framework for AI and robotics, including domestic robots, to ensure not only accountability to developers, but also the strongest of protections to individual's and their rights.

The recommendations proposed in this paper should be viewed in light of some limitations, however, though use of a combined doctrinal and research-based methodology, the data discussed is consistent, reliable and precise. The suggestions intend to be considered as fundamental research, with the intention of reducing privacy concerns through the drawing together of ideas and research from different disciplines.

II. The Development of Domestic Robots

Already, domestic robots that manage household chores, provide social company, entertainment and education are successful in the consumer market, and are viewed to soon be a commonplace in individual's homes.

A. iRobot's Roomba

The iRobot's series of Roomba autonomously vacuums and mops floors, using AI to create floorplans of the house, and mapping efficient routes for future use [5]. Companion and domestic Robots which are capable of connecting to the IoT within the home creates the possibility of unprecedented access to individual houses by law enforcement, civil litigants and hackers [3], or through sales to third parties [6].

B. Amazon's Ring 'Always Home' Cam

In 2020, Amazon's company Ring unveiled an autonomous indoor security camera, which has the ability to fly through chosen, personalised paths of the user's house which is streamed to the user's app [7]. Although Ring claim the new product was designed at privacy in the forefront, it is currently vague to what extent Ring, or Amazon themselves will have access to the data, and what purposes it will be used for, raising serious privacy concerns.

C. Companion Robots

Companion robots raise specific concerns due to the high level of interaction with their users, particularly those that are designed to collect human-centered data such as biometric data and respond to user's physical needs and emotions through the use of AI algorithms [8]. It is imperative that the highest level of privacy protection exists not only at the forefront of the design stage for these robots, but also throughout their life-cycle.

III. The General Data Protection Regulation

The General Data Protection Regulation (GDPR) [4] was implemented in 2018 to strengthen protections to individual's personal data. Personal data is defined in Article 4 of the GDPR [4] as any information that relates to an identifiable person, by reference to an identifier such as a name, location data, online identifier or other listed factors. The processing of special categories of data, which include biometric data, are given stronger protections under Article 9 of the GDPR [4].

It is clear that companion robots that process personal data would be subject to the GDPR safeguards. However, as stated by the ICO, data about a house will not, by itself, constitute personal data, unless that data can be linked to the relevant owner [9], which blurs the lines when considering domestic devices such as the previously discussed Roomba and Ring security camera as well as upcoming companion robots. It is also unclear whether inferences to individual users drawn from non-personal data are protected under the GDPR [10], further reflecting the lack of clarity in this area.

It is essential that obligations are placed on those who deploy and develop robotics to ensure the strongest of privacy protections. With the rise of the IoT and AI and Robotics, it is inevitable that eventually, a specific framework addressing these challenges will be introduced. The White Paper on AI [11] makes an attempt at this, but has been heavily criticised for its lack of scope and minimal consideration for transparency [12]. To ensure AI and robotics are developed and deployed consistently with ethical and human-centric approaches at the forefront, it is imperative that future legislation addresses these matters in depth.

IV. Recommendations

Stronger privacy protections and safeguards are particularly important in relation to domestic robots, which have unprecedented access to individual's private homes, heightening privacy risks and implications. Although companies and organisations may claim their products and services satisfy privacy standards and that data protection is guaranteed, evidence in recent years arguably proves otherwise, particularly for the largest of companies, who prominently deploy and develop AI and robotic technology.

Amazon and Google were fined in 2020 for noncompliance with the GDPR by the French Data Protection Authority [13], and more specifically related to AI and robotics, privacy concerns were raised in 2018 when a US Judge demanded Amazon Echo recordings for evidence in a double murder investigation [14]. Again in 2020, a lawsuit was filed against Amazon's company Ring, in which privacy and security concerns were raised by the Courts [15].

This reflects that company and organisational guarantee to consumers is not enough, making it essential that future legislation efficiently enforces such companies to develop and design products with privacy and ethical implications at the forefront, to ensure the strongest protections to individuals and their rights, and to allow the benefits of these technological advancements reach their potential.

A. *Regular Updates*

Domestic robots in particular, that once bought are not within direct contact of developers, need to be subject to regular updates that are easily accessible to users and available to be installed remotely. An obligation for regular updates to be issued would ensure available products preserve and improve their abilities, whilst keeping the devices in compliance with standards ensuring that individuals and their rights remain sufficiently protected. To ensure updates are installed to products, a time requirement could also potentially be placed on users to ensure compliance.

B. *Awareness and Education*

There is a need to raise awareness and educate users on the implications of these products, and with possible requirements for transparency, in addition to sufficient redress methods for machine decisions, public trust and acceptance could increase, consequently increasing opportunities for AI and robotic developers. For domestic robots in particular, more awareness needs to be raised in relation to third-party use of data, and the associated risks and implications. This could be achieved through obligations, which could be placed on developers to inform and educate users before having access to their products, perhaps through a series of videos and related questions.

C. *Human Right and Data Protection Impact Assessments*

Under Article 35 of the GDPR [5], a Data Protection Impact Assessment (DPIA) must be completed where a type of processing, particularly using new technologies is used. This paper calls for a more thorough assessment including broader human right considerations, especially for domestic robots, and that such assessments and monitoring of products take place regularly throughout the system's life cycle.

V. Conclusion

It is inevitable, given the rapid progression of AI and robotics that technological advancements will continue to grow, presenting new and additional challenges. It is imperative that future legislation ensures clear and sufficient safeguards to individuals, and efficiently tackles the novel complexities of this technology. As discussed, privacy by-design, regular updates, more thorough and regular assessments, and an increase to user awareness and education of products is essential to achieve a future of ethical domestic robots.

References

[1] International Federation of Robotics, *Press Release,* Oct. 2020. Accessed on: Mar. 22, 2021 [Online]. Available: https://ifr.org/ifr-press-releases/news/service-robots-record-sales-worldwide-up-32

[2] L. Urquhart, D. Reedman-Flint, N. Leesakul, "Responsible Domestic Robots: Exploring Ethical Implications of Robots in the Home" *Journal of Information, Communication and Ethics in Society*, Vol. 17(2), pp 246-272, 2019

[3] R. Calo, "Robots and Privacy", in *Robot Ethics: The Ethical and Social Implications of Robotics*, P. Lin, G. Bekey, and K. Abney, Eds. Cambridge: MIT Press, 2010

[4] Council Regulation (EC) 2016/679 on the protection of natural persons with regard to the processing of personal data and on the free movement of such data, and repealing Directive 95/46/EC (General Data Protection Regulation) OJ L119/1

[5] iRobot Website, "Roomba", Accessed on: Mar. 24, 2021 [Online]. Available: https://www.irobot.co.uk/roomba

[6] J. Wolfe, "Roomba Vaccum Maker iRobot Betting Big on the 'Smart' Home", Jul. 24, 2017, Reuters, Accessed on: Mar. 22, 2021 [Online]. Available: https://www.reuters.com/article/us-irobot-strategy-idUSKBN1A91A5

[7] J. Siminoff, "Introducing Ring Always Home Cam: An Innovative New Approach to Always Being Home", Sep. 24, 2020, Ring LLC, Accessed on: Mar. 22, 2021 [Online]. Available: https://blog.ring.com/2020/09/24/introducing-ring-always-home-cam-an-innovative-new-approach-to-always-being-home/

[8] L.F. Carver, "Robopets: Using Technology to Monitor Older Adults Raises Privacy Concerns", Mar. 19, 2020, The Conversation, Accessed on: Mar. 23, 2021 [Online]. Available: https://theconversation.com/robopets-using-technology-to-monitor-older-adults-raises-privacy-concerns-132326

[9] Information Commissioner's Office, "Determining What is Personal Data", p.12, Accessed on: Mar. 23, 2021 [Online]. Available: https://ico.org.uk/media/for-organisations/documents/1554/determining-what-is-personal-data.pdf

[10] A. Chatzimichali, R. Harrison, and D. Chrysostomou, "Toward Privacy-Sensitive Human-Robot Interaction: Privacy Terms and Human-Data Interaction in the Personal Robot Era", *Paladyn, Journal of Behavioural Robotics,* Vol. 12, pp. 160-174, 2021

[11] European Commission, *White Paper on Artificial Intelligence – A European Approach to Excellence and Trust COM(2020),* Feb. 19, 2020.

[12] European Data Protection Supervisor, *EDPS Opinion on the European Commission's White Paper on Artificial Intelligence – A European approach to excellence and trust* (Opinion 4/2020), Jun. 19, 2020.

[13] CNIL, "Cookies: Financial Penalty of 35 Million Euros Imposed", Dec. 10, 2020, Accessed on: Mar. 23, 2021 [Online], Available: https://www.cnil.fr/en/cookies-financial-penalty-35-million-euros-imposed-company-amazon-europe-core

[14] *State of New Hampshire v Timothy Verrill*, *Search Warrant* (Docket No. 219-2017-CR-072), Accessed on: Mar. 24, 2021, Available: https://www.documentcloud.org/documents/5113287-Timothy-Verrill-order-for-Amazon-Echo-data.html

[15] United States District Court Central District of California, *Ashley Lemay, Dylan Blakeley, Tania Amador, and Todd Craig & Others v Ring LLC* (1/03/20) Case No. 2:20-cv-074

https://doi.org/10.31256/Qv4Tp7H

Towards Localisation of Remote Centre of Motion and Trocar in Vitreoretinal Surgery

Jeremy Birch, Kawal Rhode, Christos Bergeles
King's College London
London, United Kingdom
jeremy.birch@kcl.ac.uk

Lyndon Da Cruz
Moorfields Eye Hospital
London, United Kingdom

***Abstract*—Minimally-invasive robot-assisted surgery often uses instruments that are pivoted about a trocar. For precise and safe control, the instrument's remote centre of motion (RCM) is required to match the trocar insertion point. In cases where there are free-moving body parts, such as the eye in vitreoretinal surgery, RCM and trocar locations can deviate, making estimation techniques challenging. This work addresses this by developing a hardware solution that can concurrently track the RCM and trocar locations for vitreoretinal surgery tools. A solution was developed that consisted of two miniature cameras, an inertial measurement unit and tool-mounting brackets for the Alcon surgical forceps. The system was designed and prototyped using additive manufacturing. A bench setup was used to carry out initial qualitative validation. On-going work will improve the first prototype and then move towards developing a robust RCM and trocar position estimation algorithm.**

***Index Terms*—Robot-Assisted surgery, Vitreoretinal Surgery**

I. Introduction

Vitreoretinal surgery consists of procedures carried out within the interior of the eye and on the retina. To insert the specialised surgical tools an incision has to be made in the sclera. A trocar, which is an access port placed in the incision, provides strain relief and prevents trauma around the wound. Surgeons manoeuvre the surgical tools using the trocar as a fulcrum without putting extraneous lateral forces on it. Research is being conducted into instrumented hand-held tools [1] and robot-assisted surgery [2], [3] to tackle some of the challenges encountered during surgery such as the manipulation of frail tissue like the retina without causing permanent damage or hand tremors which makes it difficult to handle tissue at a miniature scale. This will allow for the delivery of new regenerative therapies to the minuscule layers of the retina, which otherwise would be impossible to do manually.

Surgical tool control requires accurate information on the location of the remote centre of motion (RCM) and of the point of insertion into the trocar. These locations are used to enable pivoting around the trocar (when both points are aligned) and to detect misalignment when eye rolling is not desired, as in that case harmful lateral forces are being exerted on the trocar's walls that may lead to tissue damage, astigmatism or lens tear. Current research [4], [5] either requires for the manual setting of the trocar position or assumes that it is the same as the RCM. This is not always the case for freely moving body parts, such as the eye, that deform due to body movement or force exerted by the instruments. A method to estimate and compare both the positions of the RCM and the point of insertion into the trocar is needed.

This work aims to fulfil this requirement, specifically for the use on co-manipulated vitreoretinal surgery robots with passive wrists where the direction of the surgical tool is decoupled from its controlled axial joint rotation. Two miniature cameras were mounted on the front of the tool to visually locate the trocar position. An inertial measurement unit (IMU) was mounted on the rear of the tool to capture its pose and estimate the RCM. Having these two positions allows for their comparison in real-time. Furthermore, this system will enable the compilation of a comprehensive first of its kind dataset, allowing for future research on topics including instrument localisation or robot learning from surgeon movements in vitreoretinal surgery.

The following article describes the design and prototyping of the system, showcased in Fig.1 that will be used as a platform for further research. The system was designed around the Alcon surgical forceps, a popular tool used by surgeons for vitreoretinal surgery.

II. Electronic System Design

The electronic system comprises of two miniature cameras that connect to a PC, an IMU that relays its measurements to a micro-controller using Serial Peripheral Interface (SPI), which in turn is connected via serial link to the PC.

Two cameras were needed for depth perception, to provide visual localisation of the trocar. The cameras had to be as small as possible so as to not get in the way of the forceps being handled. They also required a good enough resolution to locate the trocar. For this reason the Enable Inc., minnieScope-XS camera was chosen. It has a diameter of 1.4mm, a maximum resolution of 1 Megapixel, is sterilisable and conforms to ISO 10993-1:2009 (general biocompatibility).

An IMU was chosen to capture the pose of the forceps. These have a small footprint, are low-cost and can be placed on the surgical instrument itself. Using other methods like electromagnetic or optical tracking would not work for this application as line of sight cannot be kept at all times and they would require additional bulky equipment that would

This project has been funded by EPSRC Doctoral Training Partnership allocation to King's College London and an ERC Starting Grant [714562].

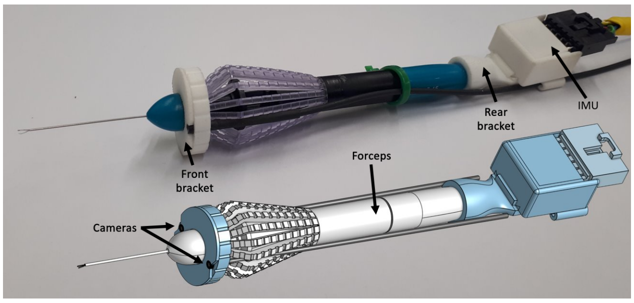

Fig. 1. Final design prototype assembled on the Alcon surgical forceps (top) with the corresponding 3D-CAD design (bottom).

affect surgical workflow. A wired rather than a wireless IMU was chosen due to the additional size and weight that a battery and antenna would impose on the IMU compartment. The SEN-13762 breakout board from Sparkfun, containing an InvenSense MPU-9250 IMU, was chosen due to it being of low-cost, incorporating a 3-axis magnetometer and having good gyroscope noise performance.

The Texas Instruments EK-TM4C1294XL micro-controller development board was chosen because the software library to connect to the particular IMU was available and required minimal modification. Its purpose was to relay to the PC the pose measurements sent to it by the IMU.

III. Mounting System Design

Taking into consideration the ergonomics, weight distribution and feedback from our clinical collaborator, a 3D-CAD model was created (Fig. 1). This consisted of two brackets, one that would be mounted at the front of the forceps and the other at the rear. The front bracket held the cameras by using a rotating mechanism that locked in place when fully turned, wedging the cameras in some grooves. The rear bracket held the IMU compartment, which could slide onto the bracket and lock in place, allowing the IMU to be covered in a drape and be reused or replaced if damaged without having to dispose of the entire prepared tool. The brackets would be glued onto the forceps, being easy to complete in the 30 minutes preparation time before surgery, thus removing the need to have a mounting mechanism. There are a number of bio-compatible adhesives that could be used, for example the Intertronics Opti-tec 5006 adhesive.

The design was 3D printed and assembled to ensure all parts fitted properly (Fig. 1). To evaluate whether the camera placement was adequate to capture enough of the eye for the trocar position estimation algorithm, a surgery setup was employed, consisting of the assembled brackets and camera on the forceps, together with a Bioniko eye and face phantom. A video was recorded using the mounted camera with the forceps inserted into the trocar, whilst moving it the same way as during surgery. From the video it was confirmed that there was an adequate viewing angle, being able to see all of the eye and the surrounding area of the face.

IV. IMU Verification Tests

A verification test was performed to observe the behaviour of the IMU rotation values, whilst in motion. The IMU was strapped onto the handle of an Entact 7 DoF haptic device, which would provide the ground truth values. Three 15-minute tests were performed whilst the haptic device's handle was manually rotated. Results showed a very noisy signal with errors ranging from $0°$ to $360°$, this was caused by two factors. Firstly, noise was injected into the signal by the cable being constantly tugged when rotating the forceps. Secondly, the IMU was strapped onto a metal handle connected to a moving metal frame. The metal frame would keep intersecting the magnetometer's magnetic field causing disturbances in the measurements, a known problem with magnetometers [6]. While this is not expected to be a problem when the IMU is mounted on the plastic forceps, it limited our capability to experimentally evaluate the system attached to a haptic device.

V. Conclusions and Further Work

This paper presents the successful development and verification of the hardware that will be used for the localisation of a surgical tool's RCM and the point of insertion into the trocar, during co-manipulated robotic vitreoretinal surgery. The assembled prototype will be used as a platform for further work to be carried out on the project.

During the verification tests, the IMU measurements were found to be noisy. It was concluded that this was caused by the cables and the connectors being pulled during use of the forceps. To prevent this, it is recommended to switch to a wireless IMU, which can connect directly to the PC. The slight increase in size and weight of the system would not affect the handling of the forceps and would also remove the need of a micro-controller. It is also recommended that the magnetometer should be calibrated in situ and should not be mounted on top of metal to prevent errors in the rotation.

Further work will consist of developing the algorithms that will estimate the RCM and trocar locations. These two points will be used as part of the control system of the co-manipulated robot to warn the surgeon when there in an unintentional misalignment between the two points.

References

[1] B. Gonenc *et al.*, "Towards robot-assisted vitreoretinal surgery: force-sensing micro-forceps integrated with a handheld micromanipulator," in *IEEE ICRA*, 2014, pp. 1399–1404.

[2] M. D. De Smet *et al.*, "Robotic assisted cannulation of occluded retinal veins," *PLoS ONE*, vol. 11, no. 9, 2016.

[3] E. Vander Poorten *et al.*, "Robotic retinal surgery," in *Handbook of Robotic and Image-Guided Surgery*, Elsevier, 2020, pp. 627–672.

[4] J. Smits *et al.*, "Setup and method for remote center of motion positioning guidance during robot-assisted surgery," in *IEEE IROS*, 2019, pp. 1315–1322.

[5] C. Gruijthuijsen *et al.*, "Leveraging the fulcrum point in robotic minimally invasive surgery," *IEEE RAL*, 2018.

[6] M. Kok *et al.*, "Using inertial sensors for position and orientation estimation," *Foundations and Trends in Signal Processing*, 2017.

https://doi.org/10.31256/Zy6Yv5Z

Validating the use of off-the-shelf sensors for biometric data collection in affective computing

1st Liz Felton
Institute of Artificial Intelligence
De Montfort University
Leicester, United Kingdom
elizabeth.felton@dmu.ac.uk

2nd Dr Pamela Hardaker
Computing, Engineering, and Media
De Montfort University
Leicester, United Kingdom
pamela.hardaker@dmu.ac.uk

3rd Professor Yingjie Yang
Institute of Artificial Intelligence
De Montfort University
Leicester, United Kingdom
yyang@dmu.ac.uk

***Abstract*—Affective computing, or computing with mood and emotion, is likely to become an integral part of home robotics in the near future. Affective computing solutions have been developed across multiple sensor modalities, of which a popular, non-invasive solution is wearable biometric sensors. There are purpose-built devices for this task, however their price-point is largely prohibitive to their adoption in large, multi-user affective systems. This paper aims to address the issues with access to these devices by validating the use of off-the-shelf sensors for use in affective systems, with a mood prediction problem.**

***Index Terms*—affective computing, wearable computing, sensors, smart living**

I. Introduction

Affective computing is a field of artificial intelligence concerned with translating human moods and emotions into machine-understandable data [1]. It is a relatively recent field in artificial intelligence and as such it is difficult to find any reports on acceptable standards for components used in affective systems. Therefore, the validation of off-the-shelf components for building reproducible and affordable affective systems is important.

Affective computing systems are likely to become an important part of home robotics, particularly in smart living spaces (assisted or otherwise [2]) and for the operation of "helper" or therapeutic robots. Most commonly, biometrics-based affective systems use galvanic skin response (GSR) to measure changes in electro-dermal activity to help determine mood; GSR is a sympathetic nervous system response which is not consciously controllable and has been directly correlated to mood [3]. The other two common sensors used in wearable biometric devices are skin temperature and heart rate [4].

The system presented here is capable of high accuracy using generic off-the-shelf sensors. This is established through an analysis of the time-series' regression values and root mean squared errors.

II. Experimental Setup

A. Sensors and Modalities

Three sensors were used to collect data from two participants: a blood-volume pulse (BVP) sensor for monitoring heart rate, a temperature sensor (negatively-correlated thermistor type) for monitoring skin temperature, and a two-finger GSR sensor. The BVP sensor was attached to the index finger of the left hand, the temperature sensor to the inner forearm, and the GSR sensor was attached via the built-in finger-tip sleeves to the index and middle fingers of the right hand. A simple script was written for the Arduino which read from the sensors when the system was switched on, and a Processing script took that data and wrote it to a CSV file for later use.

B. Participants

The two participants were both female, aged 25-30 years old, and both were UK nationals and postgraduate students. All three sensors were attached to a participant whilst they undertook the experiment, which recorded BVP, GSR, and skin temperature for the length of the experiment.

C. Affective Photographs

The experiment to collect affective data used a series of images from the Geneva Affective Picture Database (GAPED, [5]) across positive, negative, and neutral affect. Each image in the database is assigned a valence and arousal value based on the circumplex model of emotion, scaled to the axes as in Fig. 1. A series of six randomly-selected images from each emotion type (total of 18 images) were put into a PowerPoint presentation, one image per slide, and were shown to the participant whilst they were wearing the three biometric sensors and the system was recording the data from the sensors. The distribution of the valence-arousal values of the images selected is presented in Fig. 2. The participants were aware of the emotion type but not of the exact valence-arousal value of the image they were being shown.

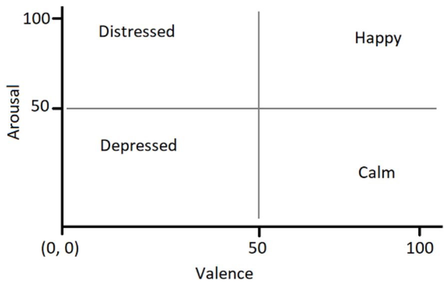

Fig. 1. Valence-Arousal axis for GAPED images

D. Classification System

The biometric data recorded, as well as the valence-arousal coordinate labels provided by the GAPED database, were used build a classification system. The data was pre-processed before being used to train a nonlinear autoregressive with extraneous input net (NARX-Net) time-series. The raw data from the sensors was split into 18 segments (one per image, based on timestamps) with each segment containing 83 data samples (each data sample consisting of three normalised values for BVP, GSR, skin temperature). To create targets for the NARX-Net, the valence-arousal of each image was used to produce an emotion vector consisting of 83 points which moved from (50, 50) (neutral in the valence-arousal model used by GAPED) to the target emotion's (valence, arousal). A time-series was chosen due to the dynamic nature of emotions, as a time-series would preserve the idea that an emotion changes over time.

For classification, an individual NARX net was trained for each class of emotion. Training examples were presented to the nets with a 15% hold-out for validation purposes. These time series were trained on the normalised data streams from the sensors; a feature set was tested, but due to the short period of time biometric data was recorded for reducing the raw signals to a feature set did not leave enough data for a classification system to be built (the nets showed high levels of inaccuracy across all emotion classes after training, indicating the data was not suitable).

III. Results and Discussion

Regression graphs were plotted after training and gave correlation coefficients (R-values) thus: negative-emotion R-value of 0.88; neutral-emotion R-value of 0.99; positive-emotion R-value of 0.98. The final root mean square error (RMSE) of each of the networks was as follows: negative-emotion RMSE 1.30e-8; neutral-emotion RMSE 9.65e-10; positive-emotion RMSE 9.71e-15.

The R-values and RMSE values combined reflect an accurate model built from biometric readings and valence-arousal values, using generic components. This forms a strong base for future work in off-the-shelf sensor validation for affective computing use, as well as providing justification for systems using generic components. This should make affective computing more accessible for home use.

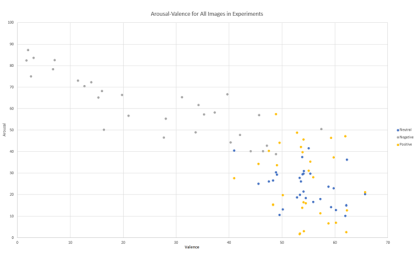

Fig. 2. Valence-Arousal distribution for images selected for the experiment

IV. Future Work

Future work should focus on validating generic components, as presented here, against purpose-built affective research devices, by using the same experimental design as other work in order to form a direct comparison between the sensors' fidelity. Work may also be done in validating a wider range of sensor modalities where a generic sensor is available, e.g. electromyogram sensors or cameras for facial recognition, and comparing results to those from other affective computing experiments.

V. Conclusion

In this paper, an affective system using affordable, mass-produced, off-the-shelf sensors was built to collect biometric data for use in an emotion classification system. A classification system was built from this data, which means these sensors are of high enough fidelity for use in both research and commercial affective systems. Future work may build on this base by repeating experiments done with currently available affective sensing systems, and directly comparing the accuracy of developed sensors to generic components.

References

[1] S. Poria, E. Cambria, R. Bajpai, and A. Hussain, "A review of affective computing: From unimodal analysis to multimodal fusion," *Information Fusion*, vol. 37, pp. 98–125, sep 2017.

[2] A. Costa, J. A. Rincon, C. Carrascosa, V. Julian, and P. Novais, "Emotions detection on an ambient intelligent system using wearable devices," *Future Generation Computer Systems*, vol. 92, pp. 479–489, 2018. [Online]. Available: https://doi.org/10.1016/j.future.2018.03.038

[3] C. A. Torres-Valencia, H. F. Garcia-Arias, M. A. Lopez, and A. A. Orozco-Gutierrez, "Comparative analysis of physiological signals and electroencephalogram (EEG) for multimodal emotion recognition using generative models," in *2014 19th Symposium on Image, Signal Processing and Artificial Vision, STSIVA 2014*, 2015.

[4] E. Reinertsen and G. D. Clifford, "A review of physiological and behavioral monitoring with digital sensors for neuropsychiatric illnesses," *Physiological Measurement*, vol. 39, no. 5, may 2018.

[5] E. S. Dan-Glauser and K. R. Scherer, "The Geneva affective picture database (GAPED): a new 730-picture database focusing on valence and normative significance," *Behavior Research Methods*, no. 43, pp. 468–477, 2011.

https://doi.org/10.31256/Ut2Qg2T

End-Effector Mobility for Manipulators in Confined Spaces

Kathryn Styles Wood
Bristol Robotics Laboratory
University of Bristol, UK
kat.styles@bristol.ac.uk

Thomas B. Scott
Interface Analysis Centre
University of Bristol, UK
T.B.Scott@bristol.ac.uk

Antonia Tzemanaki
Bristol Robotics Laboratory
University of Bristol, UK
antonia.tzemanaki@bristol.ac.uk

***Abstract*—A robotic manipulator operating within a confined space ideally positions its end-effector with minimal spatial displacement of each link. Achieving certain poses can require a large overall displacement of the hardware. This work investigates the effect of an additional degree of freedom (DOF) at the end-effector of a KUKA LBR iiwa14 arm by assessing the space occupied by the arm during 6 manipulation tasks and the dexterity of the arm within its workspace.**

***Index Terms*—Dexterous Manipulators, Path Planning, Workspace Analysis, Constrained Motion**

I. Introduction

While a commercial robotic arm can reach many poses when operating in free space, the path required to reach these poses can require a large motion of its links, especially when attempting a change in end-effector orientation [1]. This large motion could be problematic when operating in confined spaces, for example, when picking an item from within a cluttered cupboard. Although the required pose to pick the item may be achievable by the arm, the path the arm must travel through to reach that pose could be blocked by the cupboard walls or other items on the shelf. Existing robotic kitchen systems [2] are able to cook pre-defined recipes when operating within a standardised environment. However, most domestic spaces are optimised for the robot workspace. Previous studies have been performed implementing a robotic arm for domestic use within cluttered environments which found difficulty in successfully achieving grasp poses [1] [3]. Performance could be improved by minimising the motion required of the robotic arm when positioning the end-effector, in order to lower the occurrence of object collision. To achieve this, additional DoF could be provided in the end-effector of the kinematic chain [4] [5]. This paper investigates the impact of an additional revolute joint at the wrist of the end-effector when carrying out a series of tasks within a restricted workspace. Herein, we simulate an additional joint at the interface between a KUKA LBR iiwa14 7DoF robotic arm [6], Fig. 1 and a Franka Emika parallel gripper [7].

II. Methodology

The analysis is performed by simulating the arm in two kinematic configurations, for comparison. First, with a rigid link between the arm and the gripper and, subsequently, with

This work was supported by EPSRC EP/S021795/1.

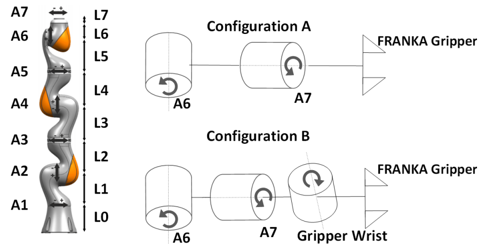

Fig. 1. Left: KUKA robot joint axis (A) and links (L) [6], Right Top: Fixed Gripper Configuration A, Right Bottom: Mobile Gripper Configuration B

an additional revolute joint (the gripper's wrist) positioned between the arm and the gripper, as shown in Fig. 1. The arm model is the IIWA STACK metapackage [8] which has been simulated in Gazebo [9], controlled using ROS [10] and Moveit! [11]. The added gripper wrist joint has a range of -90° to +90°, with its axis of rotation perpendicular to KUKA axes A6 and A7. This provides a 3-axis rotation at the end-effector. No model mesh has been created for this joint; as a simplification, it is assumed that the gripper is attached directly to the final joint of the KUKA arm (A7) without interfacing hardware, meaning that no additional length is considered at the interface in either configuration A or B, Fig. 1. Two experiments have been explored regarding the impact of the gripper's added wrist joint on: a) the spatial displacement of the arm's links (manipulation task) and b) the workspace of the arm when planning Cartesian motion (path planning task). The arm is controlled in end-effector space and the joint angles are found by Movit! default kinematics solver KDL.

A. Manipulation Task

The spatial displacement of the arm has been analysed for 6 object manipulation tasks: 2 pick-rotate-and-place tasks (rotates as it moves), 1 pick-and-pour task (rotate about an edge) and 3 wrenching tasks (rotate about a centre point). For each task, the end-effector follows the same path in both the fixed (A) and mobile (B) gripper configurations. During motion, the centre line of each link of the arm sweeps out a surface, Fig. 2. The area of this surface is calculated for each task. In comparing the two configurations, a smaller total swept area indicates a more effective motion.

B. Path Planning Task

The workspace is sampled at 10cm intervals within the +X+Y+Z quadrant for a total of 1400 goal positions. The arm

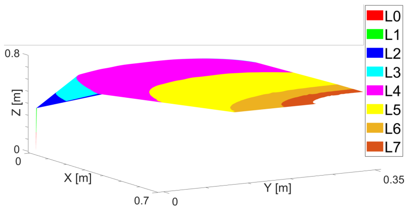

Fig. 2. Surface swept by each robot link, L, during a wrenching motion

is commanded to place the end-effector at each position in six different orientations to give a total of 8400 goal poses. The ability to plan a simple point to point straight line path from an arbitrary start pose to each of these goal poses is assessed in both the fixed (A) and mobile (B) gripper configurations. The start pose is arbitrarily selected: A1=20°, A2=20°, A3=0°, A4=-40°, A5=0°, A6=70°, A7=0°, Gripper Wrist Joint=0°. To validate the sampling interval, the workspace is sampled at 1cm intervals for one orientation. This showed similar (success rate to within 0.5%) results to 10cm sampling for the same orientation. For computational efficiency, the interval of 10cm is then used for all poses.

III. Results

Table I presents the results of the manipulation task. The total area of the surfaces swept by the links of the KUKA arm are presented for each of the six object manipulation tasks. Although the impact of the gripper's added wrist joint was low for the pick, rotate and place tasks (a reduction in swept area of <10%) the optimisation achieved for the wrenching tasks, where the object is rotated about it's centre point, was much more substantial (>50%). This suggests that for changes in end-effector orientation occurring over smaller distances, the optimisation of movement is more significant than for movements occurring over larger distances. Table II presents the results of the path planning task. The number of positions successfully reached by the Cartesian point-to-point planner is shown according to the number of orientations successfully reached at each position. Whilst the added wrist joint has low impact on the number of positions reached in at least 1 orientation (improved from 64% to 68% of the workspace sampled), it has impacted the end-effector dexterity at those positions. With the added wrist, 42% of the sampled workspace positions are reached in at least 4 orientations and 23% are reached in all 6 orientations. Without the wrist, no points in the workspace are reached in 5 or 6 orientations and only 4% are reached in 4 orientations.

TABLE I
MANIPULATION TASK RESULTS

Motion	Total Swept Area [m^2]		Mobile Gripper Swept Area Reduction
	Fixed Gripper	*Mobile Gripper*	
Pick, Rotate in X and Place	0.29	0.27	6.8%
Pick, Rotate in Y and Place	0.31	0.28	7.6%
Pick and Pour	0.24	0.21	14.3%
Wrench about X	0.21	0.10	50.1%
Wrench about Y	0.35	0.17	52.4%
Wrench about Z	0.33	0.13	60.8%

TABLE II
PATH PLANNING TASK RESULTS

Orientations Reached	Fixed Gripper Configuration		Mobile Gripper Configuration	
	Positions achieved	*% of sampled workspace*	*Positions achieved*	*% of sampled workspace*
At least 1	895	64	956	68
At least 2	605	43	822	59
At least 3	349	25	717	51
At least 4	60	4	582	42
At least 5	0	0	473	34
All 6	0	0	319	23

IV. Conclusion

The addition of a single degree of freedom at the end-effector reduces the space occupied by the robot arm and improves point-to-point path planning success for motions where a large change in orientation occurs over a smaller distance. Reduced improvement is shown for motions with a smaller change in orientation or where the orientation change occurs during motion over a longer path. Within a confined space however, it is more likely to be necessary to maneuver over small distances and to need to perform larger orientation changes. The added wrist joint allows the goal pose to be achieved whilst minimising the spatial displacement of the preceding links of the robot arm.

This work is a preliminary investigation into the potential improvement in performance achievable with a robot arm of increased end-effector mobility. Future work will account for the interfacing hardware and design of the wrist joint. Although this experiment has been performed using a specific commercial robot arm and gripper, it is expected that the findings would be applicable to all similar setups.

References

[1] W. Ruotolo, R. Thomasson, J. Herrera, A. Gruebele and M. Cutkosky, "Distal Hyperextension Is Handy: High Range of Motion in Cluttered Environments," IEEE Robotics and Automation Letters, vol. 5, no. 2, pp. 921-928.
[2] Moley Robotics, 'The world's first robotic kitchen'. [Online]. Available: https://moley.com/. [Accessed:19/03/2021].
[3] D. Wang, C. Kohler A. ten Pas, M. Liu, H. A. Yanco and R. Platt Jr, "A Scooter-Mounted Robot Arm to Assist with Activities of Daily Life," CoRR, vol. abs/1809.09541, 2018.
[4] R. R. Ma and A. M. Dollar, "On dexterity and dexterous manipulation," 2011 15th International Conference on Advanced Robotics (ICAR), Tallinn, Estonia, 2011, pp. 1-7.
[5] F. Negrello, S. Mghames, G. Grioli, M. Garabini and M. G. Catalano, "A Compact Soft Articulated Parallel Wrist for Grasping in Narrow Spaces," IEEE Robotics and Automation Letters, vol. 4, no. 4, pp. 3161-3168.
[6] KUKA Roboter GmbH, 'LBR iiwa LBR iiwa 7 R800, LBR iiwa 14 R820 Specification'. [Online]. Available: http://www.oir.caltech.edu/twiki_oir/pub/Palomar/ZTF/KUKARoboticArmMaterial/Spez_LBR_iiwa_en.pdf. [Accessed:19/03/2021].
[7] FRANKA EMIKA, 'Introducing the Franka Emika Robot'. [Online]. Available: https://www.franka.de/. [Accessed:19/03/2021]. [Accessed:19/03/2021].
[8] C. Hennersperger, B. Fuerst, S. Virgaand, O. Zettinig, B. Frisch, T. Neff, and N. Navab, "Towards MRI-based autonomous robotic US acquisitions: a first feasibility study," IEEE Transactions on Medical Imaging, vol. 36, no. 2, pp. 538-548, Feb. 2017.
[9] N. Koenig and A. Howard, "Design and use paradigms for Gazebo, an open-source multi-robot simulator," 2004 IEEE/RSJ International Conference on Intelligent Robots and Systems (IROS) (IEEE Cat. No.04CH37566), Sendai, Japan, 2004, pp. 2149-2154 vol.3.
[10] Stanford Artificial Intelligence Laboratory, 'Robotic Operating System'. (ROS Noetic) [Online]. Available:https://www.ros.org. [Accessed:19/03/2021].
[11] I. A. Sucan and S. Chitta, 'MoveIt', [Online] Available:moveit.ros.org. [Accessed:19/03/2021].

https://doi.org/10.31256/Fa9De1K

Using a Video Game to Collect Harvesting Data for Learning from Demonstration

Zhuoling Huang
Department of Informatics
King's College London
London, UK
zhuoling.huang@kcl.ac.uk

Elizabeth I Sklar
Lincoln Institute for Agri-Food Technology
University of Lincoln
Lincoln, UK
esklar@lincoln.ac.uk

Simon Parsons
Lincoln Centre for Autonomous Systems
University of Lincoln
Lincoln, UK
sparsons@lincoln.ac.uk

***Abstract*—We created a video game in order to collect data for an application of learning from demonstration during the Covid-19 pandemic. The game simulates the arrangement of strawberries on a farm, and the game requires players to make decisions about harvesting. The data we collected from players indicates that there is a pattern to human behaviour when planning the sequence in which strawberries are harvested.**

***Index Terms*—agricultural robotics, human robot interaction, harvesting sequence, learning from demonstration**

I. Introduction

The cycle time for picking fruit is one of the major bottlenecks in current robotic harvesting [1]—current cycle times are too high—but so far very little research has been devoted to cycle time optimization compared to other robotic harvesting tasks [2]. Cycle times can be improved by optimizing the harvesting sequence [3]. For robotic harvesting of sweet peppers, experimental results indicate that planning the sequence of tasks using the traveling salesman paradigm (TSP) results in a 12% cost reduction [2]. In robotic grape-harvesting, an energy optimal method for computing the harvesting sequence in path planning has been proved to improve the general performance [4]. For strawberry harvesting, [5] suggested that the robot sorts all of the strawberries from low position to high to suit the working mode of the gripper.

This previous work leaves room for improvement in planning the harvesting sequence, especially when the environment around the target fruit is complex. As the number of targets and the number of obstacles around the targets, increases, using exhaustive search to find an optimal harvest sequence within reasonable time is not feasible and heuristic approaches must be sought. Here we describe steps towards learning from human patterns of harvesting. We used a virtual environment, a feasible approach to collect data for such research [4], and a convenient one during restrictions on doing experiments face-to-face on campus due to Covid-19.

II. Experimental Platform Design

Strawberry plant model. The strawberry plant model used in the video game ignores leaves and only presents the distribution of strawberries, both ripe and unripe. The model is derived from a dataset that includes 1143 images of Driscoll's Amesti Strawberry taken by a robot in 2019 in polytunnels at Riseholme, Lincoln. The images—186 taken from bottom of the plant and 957 from the side—contain labels for 2997 ripe strawberries and 34101 unripe strawberries in total. The arrangement of fruit in 3D is simulated from the distribution of strawberries in elevation and plan views respectively (Fig.1 (b)). The number of ripe and unripe strawberries follows the pattern in which they appear in each image. The strawberry models were created using Blender, and can be easily distinguished from each other by colour as shown in the game interface in Fig.1 (c). Overall, the model is designed to represent scenes that a robot might view when harvesting period of Amesti strawberries. Deriving the model from field data means that the data collected from the game will be representative of real harvesting tasks.

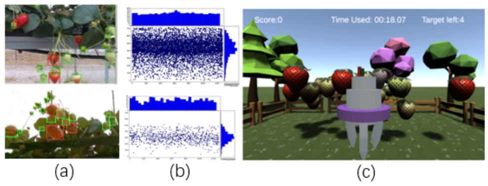

Fig. 1. (a) and (b) Dataset and distribution of red stawberry in plan and elevation view; (c)interface of the game.

Video game design. The video game is a WebGL project created with Unity [6]. It is available online [7], so users can play the game easily with their own device even during social restrictions. The operation data for each player who played the game, including score (percentage of ripe strawberries collected), time used, player movement, locations of all strawberries and the order in which strawberries are chosen, is collected anonymously and sent to a cloud database after each round of the game, and is cleared from the cloud storage, and moved to local storage at intervals.

The game provides three different modes: training mode, easy mode and hard mode. In all modes the user can shift their viewpoint in the game, which we refer to as moving the "camera", remembering that the viewpoint is that of a robot. Training mode introduces the game. Easy mode simulates human strawberry picking by requiring the user to click on the ripe strawberry to "harvest" it. Hard mode simulates harvesting

Supported by the China Scholarship Council (CSC).

by a robot gripper. Thus the user needs to move the gripper with keyboard to a suitable area above the target strawberry and then press a key to harvest. The user needs to collect all the ripe strawberries to win the game. To help select good demonstrations for further research, if a user collects unripe strawberries by mistake, they will lose points.

III. Experiment Design

To analyse user preferences when collecting strawberries, anyone above 18 is welcome to take part in the experiment. [1] To create more robust results, users are encouraged to finish the training mode first, and then play easy mode or hard mode as much as they wish.

For each round of the game, the record will include the sequence of collecting strawberries, the trajectory taken (the camera in easy mode, and the gripper with camera in hard mode), the map of all the strawberry positions and the score. In each game, ripe strawberries are collected in sequence. When a ripe strawberry is selected, it is considered to be "better" than all the others in that situation. We call each situation in which such a choice is made a *scene*. To simplify the description of each scene, the selected strawberry in a certain scene is then paired with all the other ripe strawberries in the same scene. The choice made by the user means there is always a preference between each pair of strawberries. Using such preferences, we can construct a preferred harvesting sequence. The score is checked for each game. As game records with mistakes are not considered to be good demonstration, only game records with a full score are used in our analysis.

To describe the strawberry and the environment more precisely, the following parameters are considered. **Distance:** the distance from the player to the target in 3D; the distance from previous collected strawberry to the target in 3D; and the distance from player to the target in 2D (no depth information). The location of the player for the purpose of these distance calculations is the position of the camera in easy mode, and the position of the gripper in hard mode. **Visibility:** if the target is in the field of view of the camera; the number of obstacles between player and the target; and the percentage of target that is covered. **Space around target:** the space around the target is divided into 27 cuboids (3x3x3, the centre cuboid contains the target), and the type of strawberries as obstacles in each cuboid is recorded.

The parameters for the two strawberries in a pair are placed in a vector, and the vector is labelled depending on the ordering of the two strawberries. A basic neural network (NN) with two fully connected hidden layers was trained on the data.

IV. Experimental Results

Information on the datasets collected from the game to date is shown in Table I. The results are trained and tested on similar sized samples of the datasets. We consider data from easy mode games that had just 2 and 3 ripe strawberries (2-b and 3-b) as separate from data gathered from other easy mode games (EM). The accuracy of the NN trained on each dataset is shown in Table II. The highest accuracy is 98.80%, both trained and tested on 2-strawberry easy mode game results. Comparing different rows, it is noticeable that the 2-b dataset is the best choice to train a robust classifier. There is also a clear difference between easy mode results and hard mode (HM) results, as classifiers trained on 2-b work very differently on hard mode dataset comparing with other easy mode datasets.

TABLE I
DATASETS.

	Games	Pairs	Fruit selected
2 strawberry (2-b)	499	499	998
3 strawberry (3-b)	137	411	411
Other easy mode (EM)	102	726	1241
Hard Mode (HM)	36	347	243

TABLE II
RESULTS FOR NN TRAINED ON DIFFERENT DATASETS

		Tested on				
		2-b	3-b	EM	HM	All
Trained on	2-b	98.80%	90.75%	90.22%	74.35%	82.47%
	3-b	86.17%	92.73%	74.98%	76.66%	80.56%
	EM	81.36%	82.73%	80.19%	74.79%	75.53%
	HM	78.96%	77.13%	82.92%	80.36%	74.40%

V. Summary

We described a video game simulating strawberry harvesting to collect human demonstrations. The experiment suggests that human harvesting follows a pattern that can be retrieved from the data collected. We plan to use this in future research on task allocation in harvesting. And this sequence sorting pattern will be compared with other sequence sorting algorithms. The low accuracy of the classifier trained on the HM dataset may be due to the small dataset, so we plan to collect more data to provide clear conclusions. about human working patterns.

[1]Ethical approval was granted by the King's College London IRB, reference MRSP-20/21-21386.

References

[1] J. Hemming, C. W. Bac, B. A. van Tuijl, R. Barth, J. Bontsema, E. Pekkeriet, and E. Van Henten, "A robot for harvesting sweet-pepper in greenhouses," *Intl Conf of Agricultural Engineering*, 2014.
[2] P. Kurtser and Y. Edan, "Planning the sequence of tasks for harvesting robots," *Robotics & Autonomous Systems*, vol. 131, p. 103591, 2020.
[3] Y. Edan, T. Flash, U. M. Peiper, I. Shmulevich, and Y. Sarig, "Near-minimum-time task planning for fruit-picking robots," *IEEE Trans on Robotics & Automation*, vol. 7, no. 1, pp. 48–56, 1991.
[4] L. Luo, H. Wen, Q. Lu, H. Huang, W. Chen, X. Zou, and C. Wang, "Collision-free path-planning for six-DOF serial harvesting robot based on energy optimal and artificial potential field," *Complexity*, 2018.
[5] Y. Xiong, C. Peng, L. Grimstad, P. J. From, and V. Isler, "Development and field evaluation of a strawberry harvesting robot with a cable-driven gripper," *Computers & Electronics in Agriculture*, vol. 157, 2019.
[6] A. Juliani, V.-P. Berges, E. Teng, A. Cohen, J. Harper, C. Elion, C. Goy, Y. Gao, H. Henry, M. Mattar *et al.*, "Unity: A general platform for intelligent agents," *arXiv preprint arXiv:1809.02627*, 2018.
[7] Z. Huang, "Strawberry hunter game," Available at https:// hypoxanthine plus.itch.io/ strawberry-hunter-demo-v3 (06/Apr/2021).

https://doi.org/10.31256/Pj6Cz2L

Assessing the probability of human injury during UV-C treatment of crops by robots

Leonardo Guevara, Muhammad Khalid, Marc Hanheide and Simon Parsons
Lincoln Centre for Autonomous Systems,
University of Lincoln, UK
{lguevara, mkhalid, mhanheide, sparsons}@lincoln.ac.uk

***Abstract*—This paper describes a hazard analysis for an agricultural scenario where a crop is treated by a robot using UV-C light. Although human-robot interactions are not expected, it may be the case that unauthorized people approach the robot while it is operating. These potential human-robot interactions have been identified and modeled as Markov Decision Processes (MDP) and tested in the model checking tool PRISM.**

***Index Terms*—agricultural robotics, UV-C treatment, hazard analysis, human-aware navigation, model checking**

I. Introduction

In commercial growing operations, crops are sprayed with various pesticides in order to keep diseases at bay. To help reduce the use of chemicals, our collaborators at SAGA robotics have developed a robot that can dose strawberry plants with UV-C light to treat powdery mildew. The robot configuration used during the UV-C treatment is presented in Fig.1, where the robot straddles the tables on which the strawberries grow so that the UV-C emissions are directed inwards. The UV-C dose is carefully calibrated to not damage the strawberry plants but it can harm any other living thing that come closer than 7m to the robot. Thus, even though human-robot interaction during the UV-C treatment is unlikely, it is always possible that an untrained human decides to approach the robot to have a look. For these situations it is crucial that the robot incorporates an on-board safety system with the aim of detecting the approach of a human, alerting the human of the danger and stopping operations if it is required.

In this context, this paper summarizes the potential risks and failure modes identified during a hazard analysis of the UV-C treatment scenario. These failures are then used to construct a model of the human-robot interaction which can be translated into a Markov Decision Process (MDP) to be tested by the PRISM model checking tool [2]. Some preliminary results assessing human injuries are given, pointing some important safety requirements that must be considered during the design and validation of a safety system architecture for the robot.

II. Methodology

A. Hazard identification

For the hazard analysis, we followed the systematic technique called Failure Mode and Effects Analysis (FMEA) [3], which involves identifying and evaluating potential hazards in a system, their occurrence frequency, and determining the severity of the consequences. [4]. In this context, Table I gives a list with the three main risk situations that may occur during UV-C treatment according to a cognitive walkthrough. The consequences of identified failures correspond to potential injuries from UV-C light (F2 and F3), and the risk that people are not getting aware of the danger and continue approaching (F1 and F4) which later contribute to the F2 and F3 occurrence.

This project is supported by the Assuring Autonomy International Programme, a partnership between Lloyd's Register Foundation and the University of York.

Fig. 1: The robot configuration for the UV-C treatment.

B. Safety requirements

The hazard identification is used as input for a Functional Hazard Analysis (FHA) in order to define safety requirements which reduce the severity and/or occurrence of the failures F1-4 described in Table I. In our case, the following two requirements were proposed:

SR1: The robots must incorporate an Audiovisual Alert System (AAS) to signal their current behavior and potential danger. The alerts are triggered any time a human is detected (hopefully above 7m), but also are programmed to be activated periodically in case a human was not detected on time.

SR2: The robots must implement a robust Human Detection System (HDS) based on LiDARs and/or cameras that can detect human presence above 7m. In this way, the robot can stop operations before the human get closer than 7m.

III. Preliminary Results

A. Modelling

The human-robot interactions during UV-C treatment and the behavior of the safety systems (i.e HDS and AAS), were modeled as Markov Decision Processes (MDP) in which the

TABLE I: List of possible risky situations and failure modes during UV-C treatment.

Possible situations	Code	Possible failures	Potential effect	Consequence	Severity	Ocurrence
Robot moving along the row while a human is approaching frontally	F1	Robot fails to detect human farther than 7m	Robot audiovisual alerts are not activated	Human is still approaching to the robot	critical	occasional
	F2	Robot fails to detect human closer than 7m	Robot safety stop is not activated	Human is injuried by the UV-C light	catastrophic	occasional
Robot at the end of the row while a human is approaching laterally	F3	Robot is aware of the human presence only when they are too close	Robot safety stop is not activated	Human is injuried by the UV-C light	catastrophic	probable
Robot detects a human and activate audiovisual alerts	F4	Human was not trained to interpret the alerts	Human is not getting aware of the danger	Human is still approaching to the robot	marginal	remote

transition between states is non-deterministic and modeled by probability distributions. To implement the MDP model in PRISM, a single module was created with 5 local variables which define the states of the robot, human, HDS, and AAS. Ten constants were used to define the transition probabilities of the human decisions, and to characterize the effectiveness of HDS beyond 7m and the effectiveness of the AAS to make the human aware of the danger. Additional auxiliary variables were used to synchronize the transition of states in a specific order. Full details may be found in [1].

B. Model checking

The MDP was analyzed through model checking. Figure 2 gives preliminary results showing how the probability of human injury varies according to the occurrence of failures F1-4. During the experiments, the probability of each failure was varied from 0 to 1 while keeping the probability of remaining failures constant at 0.1 (i.e. failures are always present, but the aim is to analyze which failure influences the most on human injuries). In all the plots, the potential human injuries were also evaluated according to the probability of a human deciding to approach the robot. This probability was varied from 0 to 1 and is shown on the x-axis as the probability of human-robot interaction. The riskiest situation is shown in Fig. 2(c) where, under the assumption that the robot is completely unaware of the human when they approach from the side, the probability of injury is 0.52. The remaining plots showed a much lower chance of injury, with the probability of human injury being less than 0.1. These preliminary results suggest that more effort should be put on robustify the HDS when the robot is at the end of the rows than where the robot is moving along the row. Moreover, pre-programmed explicit voice messages may be activated each time the robot is going to leave a row in order to get the human (trained or not) aware of the robot presence on time.

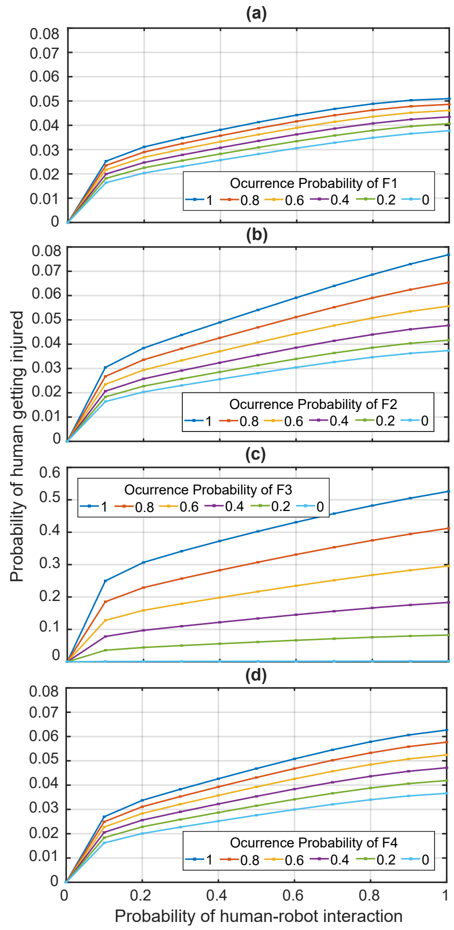

Fig. 2: Probability of a human getting injured by the UV-C light when varying the occurrence probability of a) F1 b) F2 c) F3 d) F4. The three remaining failures which are not analyzed on each case are assumed with a fixed occurrence of 0.1.

IV. Conclusions

This paper presented a preliminary assessment of potential human injuries during UV-C treatment operations. Based on the failures identified during a traditional hazard analysis, we have constructed a probabilistic model to evaluate the effectiveness of any proposed safety systems. The results of the model checking gives the user guidelines on how to improve the current safety systems effectiveness either through improving detection algorithms, adding new sensors to overcome possible hardware limitations, or by including new safety policies related to the workspace.

References

[1] L. Guevara. Probabilistic modelling and formal verification using PRISM; As case study in agricultural robotics. Technical report, School of Computer Science, University of Lincoln, 2021.

[2] M. Kwiatkowska, G. Norman, and D. Parker. PRISM 4.0: Verification of probabilistic real-time systems. In G. Gopalakrishnan and S. Qadeer, editors, *Proc. 23rd International Conference on Computer Aided Verification (CAV'11)*, volume 6806 of *LNCS*, pages 585–591. Springer, 2011.

[3] Diomidis H Stamatis. *Failure mode and effect analysis: FMEA from theory to execution*. Quality Press, 2003.

[4] Roger Woodman, Alan F.T. Winfield, Chris Harper, and Mike Fraser. Building safer robots: Safety driven control. *The International Journal of Robotics Research*, 31(13):1603–1626, 2012.

https://doi.org/10.31256/MI6Ik7G

Assuring autonomy of robots in soft fruit production

Muhammad Khalid, Leonardo Guevara, Marc Hanheide and Simon Parsons
Lincoln Centre for Autonomous Systems (L-CAS), School of Computer Science
University of Lincoln, Lincoln, LN6 7TS, UK.
{mkhalid, lguevara, mhanheide, sparsons}@lincoln.ac.uk

***Abstract*—This paper describes our work to assure safe autonomy in soft fruit production. The first step was hazard analysis, where all the possible hazards in representative scenarios were identified. Following this analysis, a three-layer safety architecture was identified that will minimise the occurrence of the identified hazards. Most of the hazards are minimised by upper layers, while unavoidable hazards are handled using emergency stops. In parallel, we are using probabilistic model checking to check the probability of a hazard's occurrence. The results from the model checking will be used to improve safety system architecture.**

***Index Terms*—agricultural robotics, human-robot interaction, hazard analysis.**

I. Introduction

The UK food supply chain network, from farm to fork, has an average total worth of £108 billion every year and employs around 4 million people (close to 12% of the workforce). The current relatively low level of productivity can be enhanced using Robotics and Autonomous System (RAS) [3]. RAS, in combination with other digital technologies, can have a very positive impact on overall food production by enabling higher production [4]. This is because RAS can work for longer than human workers, and can deal with weather conditions that humans find unpleasant [5]. This increased productivity means that the use of RAS could potentially add £58 billion to the food sector of the UK economy [5]. In the current, post Brexit, scenario in the UK, the food production industry anticipates, and indeed has already experienced, a shortage of labour. This has led to increased demand for RAS equipment [2] while also meaning that, unlike in other sectors, there is no significant danger of increased automation displacing human workers.

Soft fruit makes up 21.3% of the value of all the fruit and vegetables grown in the UK, with strawberries contributing almost 12.5% (£274 million). Soft fruit is thus an important part of the horticulture sector in the UK. Soft fruit production is also very labour-intensive — see for example [1] — and these higher labour costs, compared to other areas of horticulture, mean that RAS can be particularly beneficial. It is for these reasons that we are focussed on the use of robots in soft fruit, particularly strawberry, production.

The use of RAS can increase production, but for the near future, RAS in soft fruit production will have to work alongside humans, and in the agricultural environment [5] this means that there is considerable risk. We believe that the risks involved in using RAS for soft fruit production can be minimised by through a process of hazard identification and mitigation, and that is the work that we are engaged in.

This project is supported by the Assuring Autonomy International Programme, a partnership between Lloyd's Register Foundation and the University of York (2020-2022).

Fig. 1: A Thorvald robot as used in our work

II. Overview

Our work is designing techniques that can contribute to the safe autonomy robots that assist in strawberry production, particularly focusing on safe human-robot interaction. The robots used in this work are Thorvalds, robots that are medium-sized, see Figure 1, but large enough to potentially cause damage to a human co-worker.

We are focusing on four scenarios in a farm setting that is sketched in Figure 2:

- **UV treatment**: Robots deploy UV light to kill powdery mildew. The UV treatment is performed at night time when there are no farm workers in action. As UV light is dangerous for humans no humans should have access to the polytunnels where the plants are during the UV treatment. There is no close interaction with the robot during UV treatment.
- **Logistics**: Robots bring empty trays to fruit pickers, collect full trays and take them to the collection point. The pickers have close interaction with the robot during logistic operations, putting full trays on robot etc.
- **Scouting**: In scouting, the robot traverses the polytunnels to collect data (photos of plants) using RGB cameras. This data helps in predicting yield, making treatment decisions and helping to plan harvesting.
- **Automated picking**: The robot, equipped with a picking arm will be used either for fully automated picking or work alongside other pickers. The robot may come in close interaction with a human during fruit picking.

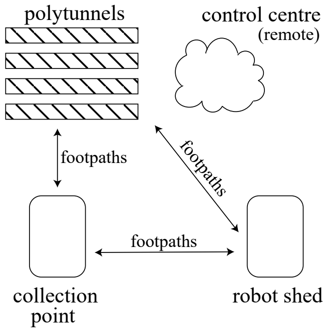

Fig. 2: The major components of a typical fruit farm.

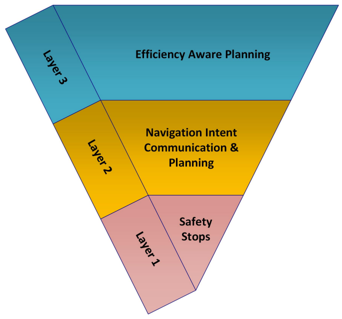

Fig. 3: The safety system architecture.

III. Progress

A. Hazard analysis and mitigation

The first step in our work was to identify all hazards in the four scenarios and categorise them [7]. Having identified the hazards, we could start to design mitigation strategies to avoid the hazards or, at least, minimise their occurrence. It quickly became clear that mitigation would depend upon three key functionalities — the ability to detect people, identify their intentions and predict their motion [6].

B. Functionalities

Detecting the presence of humans is the keystone of safety in a farm context. While the robots are equipped with a mechanical stop, meaning that they will not hurt a human co-worker through collision, activating this will shut the robot down, hurting efficiency. Detecting people at range using 2D and 3D LiDAR will allow the robot to perform a more graceful avoidance, meaning the mechanical stop does not need to be invoked. In addition, in UV treatment, any human within 7m of the robot may suffer UV burns, so detection at range is essential. Having detected people, reliably predicting their motion allows the robot to more efficiently navigate around them rather than stopping and waiting for them to move away, and being able to determine human intentions — signaled using gestures — will further improve robot efficiency.

C. Safety architecture

Assuming the ability to detect people and predict motion, the safety architecture in Figure 3 can help to ensure safety. The architecture is made up of three connected layers where, each layer is designed to address safety interaction at a different level, and higher layers aim to reduce the activation of lower layers. The aim of layer three is to plan routes which minimize the probabilities of interaction with human workers which share the work space. If an interaction is detected, this layer will re-plan in order to avoid the robot having to pause for a long time. In case an interaction occurs, layer two introduces human-to-robot and robot-to-human communication to both make the robot behaviour more comprehensible to the humans and to allow the robot to infer more precisely human intentions in order to increase the fluency of planned interactions and prevent the human and robot getting too close to one another. When a close interaction is about to happen, layer two is also responsible for ensuring a safety by reducing robot speed, performing evasive maneuvers or pausing operations. Finally, if layer two fails to ensure a safe close interaction, the layer one will activate emergency stops in case of imminent physical contact. These stops can be activated by LiDAR readings or by anomalies detected though soft sensors mounted on the robot structure.

D. Probabilistic model checking

In order to validate and enhance the safety features of the robot we are using the probabilistic model checker PRISM to model the human-robot interactions as Markov Decision Processes. The resulting probability models of each agricultural scenario predict the probabilities of the failures identified during the hazard analysis help us to assess the effectiveness of the robot safety system architecture. This analysis will be complemented with experiments in a soft-fruit farm setting.

IV. Conclusions

We have performed a hazard analysis on four scenarios that span the soft fruit production process, and based on this analysis are designing a safety system architecture that provides a layered approach to dealing with these hazards. Probabilistic model checking allows us to quantify the risks faced in deployment.

References

[1] L. Chen. Study on picking system for strawberry harvesting robots. *Beijing: Chinese Agriculture University*, 2005.

[2] F. Chiacchio, G. Petropoulos, and D. Pichler. The impact of industrial robots on eu employment and wages: A local labour market approach. Technical report, Bruegel working paper, 2018.

[3] T. Duckett, S. Pearson, S. Blackmore, B. Grieve, W.-H. Chen, G. Cielniak, J. Cleaversmith, J. Dai, S. Davis, C. Fox, et al. Agricultural robotics: the future of robotic agriculture. *arXiv preprint arXiv:1806.06762*, 2018.

[4] J. Maier. Made smarter—review 2017. *Department for Business EIS. The Stationery Office. London*, 2017.

[5] S. B. R. Maul and W. Maul. Taking control: Robots and risk, emerging risk report. *Lloyd's of London.*, 2019.

[6] A. Rudenko, L. Palmieri, M. Herman, K. M. Kitani, D. M. Gavrila, and K. O. Arras. Human motion trajectory prediction: A survey. *The International Journal of Robotics Research*, 39(8):895–935, 2020.

[7] R. Woodman, A. F. Winfield, C. Harper, and M. Fraser. Building safer robots: Safety driven control. *The International Journal of Robotics Research*, 31(13):1603–1626, 2012.

https://doi.org/10.31256/Is2Kk7K

Task Allocation with Manipulative Dynamic Auctioneering for Multi Robot Systems

Roopika Ravikanna
School of Computer Science
University of Lincoln
Lincoln, United Kingdom
roopikaravi@gmail.com

Alan G. Millard
School of Computer Science
University of Lincoln
Lincoln, United Kingdom
amillard@lincoln.ac.uk

***Abstract*—This research proposes to improve standard auctioneer systems in Multi Robot Task Allocation (MRTA) with a novel auctioneering strategy called 'Manipulative Dynamic Auction System' (MDAS), which is inspired by the 'Leaky Integrate and Fire' neuron model of the human brain. This model is developed and simulated as an extension of MRTeAm, a ROS based software framework built to test MRTA auctioneering strategies. The performance of MDAS is compared against a simpler version of Dynamic Auctioneering named 'Simple Dynamic Auctioneering System', as well as a standard Stationary Auctioneering System called the 'Ordered Single Item Auction', using a range of experiments. It is observed that MDAS is faster and more efficient than the Simple Dynamic Auctioneering System. Also, it is more sophisticated in its allocation of tasks to robots, when compared to Stationary Auctioneering Systems, due to its consideration to the behavior of robots during the auction process. Potential for future research lies in building a Hybrid Auctioneering system using a combination of both Stationary and Dynamic Auctioneering Strategies for task allocation.**

***Index Terms*—Multi Robot Task Allocation, Auctioneer Systems, Multi Robot Systems, Fleet Management, Dynamic Auction**

I. INTRODUCTION

Challenging application domains like space and underwater exploration, search and rescue, and agricultural robotics can benefit from Multi-Robot Systems, as they often deal with tasks that are difficult to solve with a single robot, or too critical to rely on a single robot. The complexities of task allocation in Multi-Robot Systems has led to specialisation of the area called Multi-Robot Task Allocation (MRTA) [1]. MRTA is usually an NP-hard Optimization problem that is modelled in the form of a Fair Division, Optimal Allocation, or Travelling salesman problem [2]. Each of the techniques used for task allocation has its own advantages and disadvantages. The complexity of MRTA increases with the number of robots and tasks, heterogeneity in robot capabilities, coalition requirement for tasks, time constraints in tasks, and unpredictability in the appearance of tasks.

The advancement of autonomous Multi- Robot systems raised the problem of task allocation from that of simple scheduling to optimisation, involving several different constraints like the capabilities of the robot, distance from task area, and time efficiency in task completion. The research presented in this paper proposes a novel methodology for MRTA using Manipulative Dynamic Auctioneering System. This idea is inspired by the Leaky Integrate and Fire neuron model based on the working of human brain [3]. The proposed method is implemented in a simulated multi-robot environment, and its performance is analysed and inferred over a range of experiments by varying core parameters of the system.

EPSRC Centre for Doctoral Training in Agri-Food Robotics

II. LEAKY NEURON MODEL INSPIRATION FOR TASK ALLOCATION

A notable drawback observed with any competitive robot model, including most of the conventional market-based methods and some of the optimisation methods, is the enormous increase in computational load with the increase in the number of robots. To understand this shortcoming better, imagine a large fleet of robots competing for the same task. It is highly probable that with increasing numbers of robot competitors, there is an increase in close competition between some of the robots. To address this problem while leveraging the advantages of a decentralised optimisation approach, a novel idea for MRTA is discussed below.

The logic behind a popular neuron model of the human brain called 'Leaky Integrate and Fire' (LIF) can be adapted for the MRTA problem. The LIF neuron model is based on the assumption that the postsynaptic currents of the neurons competing in the brain have to cross a set threshold in order to fire [4]. After a competing set of neurons fire, it is theorised that the winning neuron of that round, not only increases its own current (self-excitation), but also sends a small inhibitory current to the other neurons in competition to diminish their value. This behavior is observed over a number of distinct time intervals, and it is seen that at the end an ultimate winner is selected after the postsynaptic current of all the remaining neurons reach zero [5].

By modelling the inhibitory behavior, it is expected that the computation complexity of task allocation will be reduced, speeding up the process. A simple outline of this MRTA problem would be to allocate the robots of varying capabilities to a variety of tasks that require the service of one or more robots. Taking agricultural robotics as an example, while tasks such as tilling/ploughing might require just a single robot, some other tasks like harvesting might require one robot for the harvest action, and an accompanying trailer robot on the side for grain collection. This might even involve an additional problem of synchronisation [6]. To evaluate the suitability of the robots, a simple score/weight can be assigned for every task based on the degree of requirements they satisfy. Based on these weights, the robots compete to be allocated with a task. These robots are modelled based on the neuron behavior suggested in the 'Leaky Integrate and Fire' approach. The relative performance of this model in terms of time and computational complexity is expected to improve with the increase in the number of robots and tasks, when compared against other traditional models without an inhibitory action in their auctioning or competing system.

III. Manipulative Dynamic Auctioneer System

Manipulative Dynamic Auctioneer System (MDAS) builds on the Simple Dynamic Auctioneer (SDA) System by strategically altering the bid values of robots in each round of the bidding. In Figure 1, it can be observed that after the bids are collected from the robots, a positive increment is given to the highest bid and the rest of the bid values are decremented.

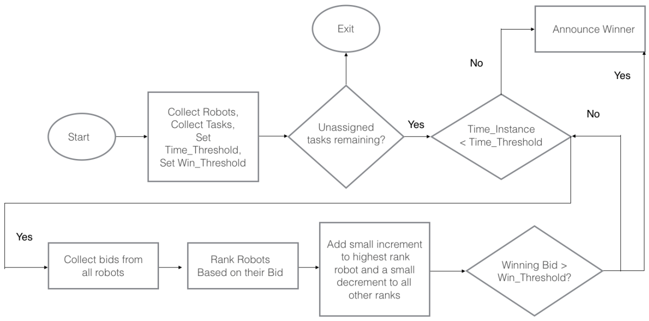

Figure 1. System Diagram for Manipulative Dynamic Auctioneer System

If the altered highest bid is greater than the 'Win Threshold', the winner is announced right away, else all of the altered bid values are retained and are added to the bid of the respective robots in the subsequent bidding rounds, and the process is repeated. The auction for each task is carried out until one of the bids surpass the 'Win Threshold' value or after the bids have been collected for the specified 'Time Threshold'. In either case, the robot with the highest bid at the end of the auction round is announced as the winner.

IV. Results

The performance measure Bid Count is an indicator of the time taken for assigning a task to a robot. Bid Count denotes the number of auction rounds taken before assigning a task. Figure 2 shows the graphs of Bid Count for the three auctioneering strategies used in the experiments. It can be inferred from the results of the experiments that Manipulative Dynamic Auctioneering Strategy is an improvement on the Stationary Auctioneering Strategies like Ordered Single-Item (OSI), due to the consideration it gives to the heterogeneity of the robots and its pattern of travel across the experiment site,

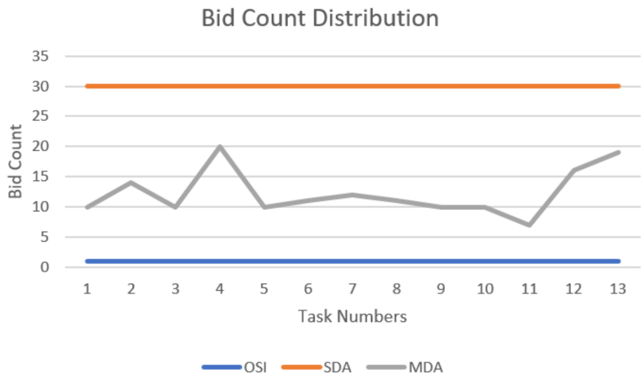

Figure 2. Bid Count comparison amongst diffrent auctioneering strategies

while not consuming as much time as taken by the Simple Dynamic Auctioneering Strategy. From these observations, one of the main objectives of this research, to showcase the sophistication of Manipulative Dynamic Auctioneering Strategy inspired by the LIF neuron model of the human brain has been met.

V. Conclusion

While the decision-making process is very basic in Stationary Auctioneering Strategies like the OSI, one cannot overlook the rapid speed at which task allocations are carried out in such methods. The strength of MDAS is its potential to handle the allocation of unexpected tasks that crop up while the robots in the environment are already at work. A system that combines both these strategies in such a way that pre-defined tasks are handled by the Stationary Auctioneering System, and unexpected tasks via Manipulative Auctioneering System, should perform well for autonomous Multi-Robot environments. This idea could be an interesting research possibility in optimisation of Auction Mechanisms for Multi-Robot Systems.

References

[1] T. Arai, E. Pagello, L. E. Parker *et al.*, "Advances in multi-robot systems," *IEEE Transactions on robotics and automation*, vol. 18, no. 5, pp. 655–661, 2002.

[2] A. Khamis, A. Hussein, and A. Elmogy, "Multi-robot task allocation: A review of the state-of-the-art," *Cooperative Robots and Sensor Networks 2015*, pp. 31–51, 2015.

[3] H. Scharstein, "Input-output relationship of the leaky-integrator neuron model," *Journal of mathematical biology*, vol. 8, no. 4, pp. 403–420, 1979.

[4] J. M. Bower and D. Beeman, *The book of GENESIS: exploring realistic neural models with the GEneral NEural SImulation System*. Springer Science & Business Media, 2012.

[5] L. A. Coward, "Towards a theoretical neuroscience," in *Towards a Theoretical Neuroscience: from Cell Chemistry to Cognition*. Springer, 2013, pp. 389–393.

[6] A. G. Millard, R. Ravikanna, R. Groß, and D. Chesmore, "Towards a swarm robotic system for autonomous cereal harvesting," in *Annual Conference Towards Autonomous Robotic Systems*. Springer, 2019, pp. 458–461.

https://doi.org/10.31256/Dg2Zp9Q

Auction-based Task Allocation Mechanisms for Managing Fruit Harvesting Tasks

Helen Harman
Lincoln Institute for Agri-food Technology, University of Lincoln, Lincoln, UK
hharman@lincoln.ac.uk

Elizabeth I Sklar
Lincoln Institute for Agri-food Technology, University of Lincoln, Lincoln, UK
esklar@lincoln.ac.uk

***Abstract*—Multi-robot task allocation mechanisms are designed to distribute a set of activities fairly amongst a set of robots. Frequently, this can be framed as a multi-criteria optimisation problem, for example minimising cost while maximising rewards. In soft fruit farms, tasks, such as picking ripe fruit at harvest time, are assigned to human labourers. The work presented here explores the application of multi-robot task allocation mechanisms to the complex problem of managing a heterogeneous workforce to undertake activities associated with harvesting soft fruit.**

***Index Terms*—Task Allocation Mechanism, Multi-Agent System, Agent-Based Simulation**

I. Introduction

Multi-robot task allocation (MRTA) problems address situations in which a group of robots must work together to complete a set of tasks. A key challenge is to decide which *tasks* should be assigned to which robots so that a *mission* is accomplished by using resources efficiently and maximising rewards. Auctions are a popular approach because they offer the ability to be flexible and adapt to changes in the environment, as well as balance priorities when multiple criteria need to be considered in the allocation of resources.

As mentioned within the literature [1]–[4], auctions are executed in “rounds” that are typically composed of three phases: (1) tasks are announced to a set of agents, (2) the agents bid on the tasks and (3) an agent is rewarded the task with the winning (e.g. lowest) bid. A prominent strategy in the literature is the *sequential single-item (SSI)* method [5]. SSI is fast (the auction runs in polynomial time in the worst case) and efficient, while also being able to produce an allocation that is close to or within a guaranteed factor away from optimal.

Applying multi-robot teams to *agricultural robotics* [6] has recently been gaining attention. This extremely challenging application domain presents many opportunities to consider not only traditional problems faced in robotics around (e.g.) control, sensing and manipulation, but also emerging issues around human-robot collaboration. One of these challenges is to allocate fruit harvesting tasks to human (and in the near future robotic) labourers efficiently.

This work was supported by Research England [Lincoln Agri-Robotics] as part of the Expanding Excellence in England (E3) Programme.

II. Method

We have developed a simulation of the harvesting process on a small strawberry farm in which tasks are allocated to workers by applying an auction-based mechanism. Harvesting fruits involves two types of tasks and two types of agents that address those tasks: *pickers* harvest fruit in the field and place the produce in punnets; and *transporters* collect full punnets and deliver them to a centralised location called a pack house.

Our simulation (developed in MASON [7], which is a lightweight, multi-agent simulator) is shown in Fig. 1. The coloured patches represent the picking tasks; the colour indicates the number of ripe fruits: red indicates a relatively high number of ripe fruits and green a low number. Each patch contains information on how many ripe fruits are occluded by the canopy (leaves). This illustration was created based on the yield of one day during the 2020 season. Pickers are represented as grey triangles, starting at the left edge of the field, and transporters are represented as grey circles, starting in the pack house.

We compare three different auction-based mechanisms [8], for allocating picking and transporting tasks: *Round Robin* (RR) assigns the first task to the first agent, the second to the second agent and so forth. After one task has been assigned to each agent, the process is re-iterated to assign each agent another task. This process continues until all tasks have been assigned to an agent. In *Ordered Single Item* (OSI), all agents bid on the first task and the agent with lowest-cost bid is assigned the task. The subsequent task is then auctioned. When all tasks are assigned, the process concludes. For *Sequential Single Item* (SSI), in each round all unassigned tasks are bid on by all agents. The task of the lowest-cost bid is assigned to the agent who placed that bid.

Pickers are defined by the tuple $p = \{v, l, S^p\}$, where

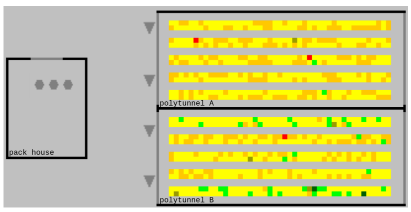

Fig. 1. Our strawberry farm within the simulation. See text for explanation.

l is the agent's initial location and v its navigation speed; $S^p = \{s^o, s^u\}$, the agent's occluded (s^o) and unoccluded (s^u) fruit picking speed. The cost of a picking bid is the number of timesteps it takes the picker to navigate to the picking location, pick the ripe occluded and unoccluded fruits, and, when necessary, wait for a transporter. After a picker has filled a punnet with strawberries, it cannot pick any further fruits, and so a transport task is generated.

Transporters have a navigation speed and an initial location, i.e., $r = \{v, l\}$. The cost of a transporting bid is the time it takes the agent to navigate to the picker, collect the filled punnet and take the punnet to the pack house. Three different modes were implemented for allocating tasks to transporters. For all 3 modes, implementations of RR, SSI and OSI were developed. To differentiate between these and the mechanisms implemented for allocating picking tasks, each adds a prefix to the mechanism name (e.g. WRR):

- *Whilst scheduling picking* (W): Transporters can be scheduled as soon as a transport task is created. This enables a picker's bid to include the time spent waiting for the transporter.
- *Post scheduling picking* (P): The transporters can be scheduled after all transport tasks have been created (i.e. all picking tasks have all been assigned). This could result in the creation of a closer to optimal schedule for the transporters (but potentially at the expense of the pickers).
- *whilst Executing picking* (E): Alternatively, transporters can be scheduled during execution, which facilitates delays (e.g., due to collision avoidance) to be accounted for within the transporters' schedules.

The aisles (i.e. the spaces between the crop rows) are too narrow for agents to pass side-by-side; therefore, two agents of the same type cannot be within the same aisle, and transporters can only enter an aisle if the picker they are assisting is performing the task they require assistance with. If an agent cannot enter an aisle, it waits beside the aisle. These rules can cause deadlocks to occur as transporters and/or pickers could be delayed and blocked from entering an aisle. To prevent deadlocks, a transporter swaps its current task with a task that appears later in its own, or another transporter's, schedule. Collisions in open spaces are avoided by the agents making adjustments to their paths or waiting.

III. Results

We performed a series of experiments, with four different picker configurations (i.e. picking speeds and initial locations) and two random assignments of ripe fruits (that were counted during the 2020 picking season) to fruit patches. These experiments employed 4 pickers and 3 transporters. We compare the three auction mechanisms used for scheduling pickers (RR, OSI and SSI) and nine mechanisms for scheduling transporters ($\{\mathsf{RR}, \mathsf{OSI}, \mathsf{SSI}\} \times \{\mathsf{W}, \mathsf{P}, \mathsf{E}\}$). The results were analysed using factor analysis in order to determine the influence of picker or transporter mechanisms individually or in combination. As expected, SSI results in the shortest execution time (i.e. time it takes to perform the mission). Figure 2a illustrates that there are statistically significant differences for the execution time. Figure 2b shows the ablated results for all combinations of transport task scheduling modes and auction mechanisms, demonstrating that ESSI and EOSI results in the shortest execution times. ESSI and EOSI are equivalent since only one task is available to auction each time the auction is run. Overall, when the results for each picker scheduling mechanism and each transporter scheduling mechanism and mode are ablated, SSI is the superior auction mechanism for assigning picker tasks and E with OSI or SSI is the superior mode for assigning transporter tasks.

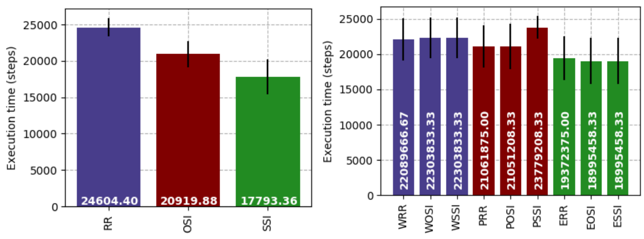

(a) Picker scheduling mechanisms ($H = 150.04, p = 0.00$).

(b) Transporter scheduling modes and mechanisms ($H = 45.40, p = 0.00$).

Fig. 2. Factor analysis. The statistical significance (H and p statistics), calculated by running Kruskal-Wallis tests [9], are reported in the captions.

IV. Conclusion

The experiments presented here explore the application of auction-inspired task-allocation mechanisms to assigning strawberry harvesting task to pickers and transporters. A data-backed simulation of a real-world soft fruit farm is presented. Our current work involves scaling the results to larger farms, using data recently obtained from two commercial farms with over 500 pickers at each farm in the height of the season. Early results indicate that the trends seen here will hold.

References

[1] M. B. Dias, R. Zlot, N. Kalra, and A. Stentz, "Market-based multirobot coordination: A survey and analysis," *Proceedings of the IEEE*, vol. 94, no. 7, 2006.

[2] B. Heap and M. Pagnucco, "Sequential single-cluster auctions for robot task allocation," in *AI 2011: Advances in AI*, D. Wang and M. Reynolds, Eds. Springer, 2011.

[3] N. Kalra, R. Zlot, M. B. Dias, and A. Stentz, "Market-based multirobot coordination: A comprehensive survey and analysis," Carnegie-Mellon University, Tech. Rep. CMU-RI-TR-05-16, 2005.

[4] E. Schneider, "Mechanism selection for multi-robot task allocation," Ph.D. dissertation, University of Liverpool, 2018.

[5] S. Koenig, C. Tovey, M. Lagoudakis, V. Markakis, D. Kempe, P. Keskinocak, A. Kleywegt, A. Meyerson, and S. Jain, "The power of sequential single-item auctions for agent coordination," in *AAAI*, 2006.

[6] T. Duckett, S. Pearson, S. Blackmore, B. Grieve, and M. Smith, "Agricultural Robotics White Paper: The Future of Robotic Agriculture," https://www.ukras.org/wp-content/uploads/2018/10/UK_RAS_wp_Agri_web-res_single.pdf (last accessed 10-Mar-2020), 2018.

[7] S. Luke, C. Cioffi-Revilla, L. Panait, K. Sullivan, and G. Balan, "MASON: A Multiagent Simulation Environment," *Simulation*, vol. 81, no. 7, 2005.

[8] E. Schneider, E. I. Sklar, S. Parsons, and A. T. Özgelen, "Auction-based task allocation for multi-robot teams in dynamic environments," in *TAROS*. Springer, 2015.

[9] W. H. Kruskal and W. W. Wallis, "Use of Ranks in One-Criterion Variance Analysis," *Jrnl of American Statistical Association*, vol. 47, no. 260, 1952.

https://doi.org/10.31256/lc8Et3X

Safety Assessment of a Robotic Arm Motion including Human Factors

Mohammed Rezwan Rahman
Centre for Automation & Robotics Research
Sheffield Hallam University
Sheffield, United Kingdom
Mohammed.R.Rahman@student.shu.ac.uk

Lyuba Alboul
Centre for Automation & Robotics Research
Sheffield Hallam University
Sheffield, United Kingdom
L.Alboul@shu.ac.uk

Louis Nisiotis
School of Sciences
University of Central Lancashire, Cyprus
Larnaca, Pyla, Cyprus
LNisiotis@uclan.ac.uk

Jacques Penders
Centre for Automation & Robotics Research
Sheffield Hallam University
Sheffield, United Kingdom
J.Penders@shu.ac.uk

Alessandro Di Nuovo
Centre for Automation & Robotics Research
Sheffield Hallam University
Sheffield, United Kingdom
A.Dinuovo@shu.ac.uk

***Abstract*—Human-Robot Collaboration (HRC) requires not only technical safety but also a level of comfort for humans to ensure that humans and robots work and interact safely in the daily process flow. This paper presents a review of preliminary design considerations on how a robot arm can be controlled to explore various safe and personified movements in order to assess and improve legibility of robot performance in the presence of moving humans at home, industry, or any other environment.**

Keywords— human-robot collaboration (HRC), perceived safety, robot manipulation, motion planning, workspace, fetch

I. Introduction

Human-Robot Collaboration (HRC) is a rapidly developing area of robotics. Several research studies have shown that spontaneous and continuous human-robot collaborations can be achieved in industrial settings [1]. The robots considered are ranged from simple robotic manipulators [2] to complex humanoid robots [3], which are expected to help human co-workers in various tasks that may require coordination for a safe, successful, and efficient execution. HRC implies that a robot enters the personal workspace and comfort zones of a human co-worker, causing safety concerns. Technical safety is largely accounted for by the robot supplier and it has been a central point in HRC research [4].

Recent research in HRC is focusing on human factors and human-centred design [5]. Of particular research interest is the mutual understanding and anticipation of each other's intentions. To this end, robots should be capable of interpreting several communication mechanisms similar to mechanisms involved in human-to-human interaction [6]. However, human related aspects like perceived safety, emotional and teamwork are less investigated and needs further exploration.

This paper presents an assessment study on safe robotic arm motion trajectories and how human factors could play a role in safe collaborative manipulation tasks in an industrial HRC environment. The main focus of our study is the development of a custom model for safe robot arm movements in an industrial HRC scenario. In addition, coordination methods based on human-human collaboration will be examined for their application on fluent and effective human-robot collaboration. This will provide information for further development in design standards for robot arm manipulation and contribute to human-robot co-working quantitative models.

II. Investigational Approach

This study could help in the development and implementation of tracking and fetching algorithms for collaborative robots. However, in real scenarios, external factors, such as, unanticipated obstacles, mechanical failures [4], may affect the performance of robot motion. Therefore, several experiments will be conducted to investigate those challenges. For manipulation tasks, the exchange of objects between a human and a robot is a basic way to coordinate movements and jointly perform useful work. For coordinated manipulation, it will explore the approach presented in [7], which demonstrated the technical feasibility of exchanging objects when a robot and a human work together.

The proposed approach to the robot arm manipulation tests can be simply explained as illustrated in figure 1 by a basic pick & place process. Figure 1(a) shows how a robot arm rotates with its arm entering directly into the personal space of the human co-worker, thus, causing human-robot collision. In figure 1(b) it can be seen; a single addition of a retractable step helps to avoid collision with the human. The robot arm retracts (joints J2 and J3) before rotating and extends again to reach the end position. The intrusion action in figure 1(a) compromises a larger volume of the workspace and makes its final destination unpredictable, whereas the rotation in figure 1(b) compromises less volume. This study would reveal a broad spectrum of experimental proposals, which can be examined to determine and implement safe movements around human subjects and evaluate their effectiveness.

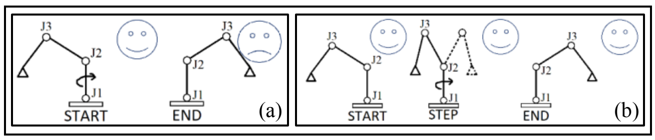

Fig. 1. (a) Robot arm rotating in joint J1 straight to position close to human, (b) Robot arm making intermediate safe step before rotating.

III. Experimental Method And Setup

The experiments will implement a pick and place application setup as well as a human-robot co-assembly task, which comprises the Fetch robot arm and the use of Robot Operating System (ROS). Python and/or MATLAB programming will be used to code the ROS packages. The idea is to achieve different variations of safe robot arm movements around a human user or any obstacles. The motion planning scenarios will be executed through the Gazebo simulator (to rapidly test algorithms, design robots and train AI system using realistic scenarios) and RVIZ 3D visualization tool (tool for ROS applications which provides a view of the robot model, captures and visualises sensor information and shows ROS topics communication). The use of simulation and visualisation software allows to develop and assess the intended ideas and prototype implementations of this study in risk free virtual environments, with the ability to edit, retry and adjust configurations and algorithms safely. Based on the kinematics, the motion formation will be designed to construct the robot arm workspace and configuration space.

The software will be programmed to enable the robot arm to read its sensors data (speed, acceleration, time constraints, potential fields, etc) and make itself aware of the workspace and make motion decisions, i.e., avoiding obstacle while in motion. The main task would be to complete an action, for example, a pick and place motion and move its end-effector from point 'A' to point 'B', as exemplified in figure 3, while avoiding any obstacles. To investigate perceived safety, human participant experiment will be devised where both the robot and the human user will perform a collaborative task within a shared workspace. Dragan et al. [8] investigated both positive and negative impacts of different planning motions on human comfort by comparing multiple robot motion trajectories and controlling the robot with varied velocities. Our tests will be designed for the robot to be able to gradually adjust its arm speed according to the separation distance between the participant and the robot. Participants will be provided with a questionnaire for feedback on human-robot closeness, robot response speed and human comfort. These participant responses will play a significant role in improving human comfort and achieve safe motion trajectory.

Fetch Robot

The Fetch mobile manipulator is designed to be robust and of high-performance [9]. Fetch is equipped with a single 7 degrees-of-freedom arm which supports up to a 6 kg payload, including the gripper. The head of the robot is capable of two motions: pan and tilt. Torso has a lift actuator which makes it possible for the robot to move up and down as shown in the figure 2.

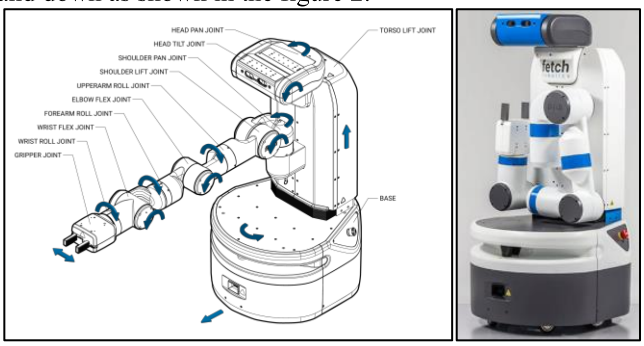

Fig. 2. Fetch Robot illustration [9].

The Fetch also consists of sensors that will be utilised in this study. a) *Base Laser* - SICK TIM571 scanning range finder with a range of 25m, 220° field of view, 15Hz update rate and angular resolution of 1/3°, b) *IMU* - the Gyroscope within the 6-axis inertial measurement unit (IMU) has the capability of measuring +/-2000 degrees per second, while the accelerometers are capable of measuring +/-2g, c) *Head Camera* - Primesense Carmine 1.09 short-range RGBD sensor best calibrated in the 0.35-1.4m range, d) *Gripper Sensors* - in addition to the position and effort feedback of the gripper joint, the gripper incorporates a 6-axis IMU.

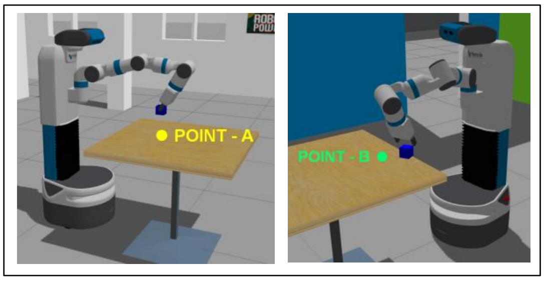

Fig. 3. Gazebo Simulation - 'Pick up' object at Point A and 'Place' at Point B.

Main Tasks

1) Identify and locate obstacles, 2) Apply motion planning algorithm, 3) Calculate the path avoiding the obstacles, 4) Based on the path, calculate robot arm joint configurations (these data will be used in simulation for testing and verification), 5) Finally, evaluate the joint positions to move safely and reach the goal.

IV. Discussion And Future Work

To evaluate the proposed approach, simulation experiments will be carried out based on existing path and trajectory planning methods to distinguish between the two and then implement the motion configuration. Immediate future work includes the development of several simulations to help preparing the physical experimentation setting(s) to implement and test the algorithms and the proposed solution.

References

[1] S. Robla-Gomez, V. Becerra, J.R. Llata, E. Gonzalez-Sarabia, C. Torre-Ferrero and J. Perez-Oria, “Working Together: A review on safe human-robot collaboration in Industrial Environments” IEEE Access, vol. 5, pp. 26754–26773, 2017.

[2] A. Albu-Schaffer, S. Haddadin, C. Ott, A. Stemmer, T. Wimbock and G. Hirzinger, “The DLR light-weight robot: design and control concepts for robots in human environments”, Industrial Robot: An International Journal, vol. 34(5), pp. 376–385, 2007.

[3] Tsagarakis et al., “Walk-man: A high performance humanoid platform for realistic environments”, in Journal of Field robotics, 2016.

[4] M Dohi, K. Okada, I. Maeda, S. Fujitani and T. Fujita, “Proposal of Collaboration Safety in a Coexistence environment of human and robots”, IEEE International Conference on Robotics and Automation, 2018, pp. 1924–1930.

[5] N. Wang, C. Chen and A. Di Nuovo, "A Framework of Hybrid Force/Motion Skills Learning for Robots," in IEEE Transactions on Cognitive and Developmental Systems, vol. 13, no. 1, pp. 162-170.

[6] B. Curuklu, G. Dodig-Crnkovic and B. Akan, “Towards Industrial Robots with Human-like Moral Responsibilities”, 5th ACM/IEEE International Conference on Human-Robot Interaction, pp. 85–86, 2010.

[7] A. Edsinger and C.C. Kemp, “Human-Robot Interaction for Cooperative Manipulation: Handing Objects to One Another”, in 16th IEEE International conference on Robot and Human Interactive Communication, August 26-29, 2007.

[8] A.D. Dragan, S. Bauman, J. Forlizzi and S.S. Srinivasa, “Effects of robot motion on human-robot collaboration”, in proceedings of the 10th ACM/IEEE International conference on Human-Robot Interaction, USA, pp. 51-58, 2015.

[9] M. Wise, M. Ferguson, D. King, E. Diehr and D. Dymesich, “Fetch Robotics Inc, Fetch & Freight: Standard Platforms for Service Robot Applications”, USA, 2016.

https://doi.org/10.31256/Ts2Po9M

Using Plan Libraries for Improved Plan Execution

Ionut Moraru
Dept. of Informatics
King's College London
London, UK
ionut.moraru@kcl.ac.uk

Gerard Canal
Dept. of Informatics
King's College London
London, UK
gerard.canal@kcl.ac.uk

Simon Parsons
Lincoln Centre for Autonomous Systems
University of Lincoln
Lincoln, UK
sparsons@lincoln.ac.uk

***Abstract*—The difficulty of task planning for robotic agents arises from the stochastic nature of their environment and the high cost of a failure during execution meaning frequent replanning is required. One way to address this problem is to make use of a pre-defined plan library. In this paper, we present work that combines a plan library with task planning. Initial results show that such an approach alleviates the computational burden of synthesising plans, while providing the same level of autonomy as using a planner that starts from scratch.**

***Index Terms*—Task Planning, BDI, Case-Based Reasoning, Plan Library, ROSPlan**

I. Introduction

In order for robots to become helpful in dynamic and stochastic environments, their reasoning about their actions must combine two qualities: autonomy and speed. Autonomy to decide for themselves how to achieve their goals, regardless of the situation they are placed in [1] and speedy reasoning so that they can perform in dynamic environments where plans can become unusable if a robot takes too long to synthesise them. One way to ensure that the robot has a high degree of autonomy is by reasoning directly about the state of the environment. Most systems that do this are based on STRIPS [2], and help the robot to come up with a sequence of actions (i.e. plans), from a set of available operators that would satisfy a set of explicit goals given in a planning task. The downside of this approach is that it is PSPACE-complete in the simplest versions (propositional planning), and becomes more difficult the more expressive the models become [3].

One approach to deal with this computational complexity is to make use of pre-defined plans that a robot then looks up rather than having to plan from scratch. Several examples within this paradigm have been based on the Belief-Desire-Intention (BDI) model [4], such as Jason [5], which has a predefined Plan Library. The downside to this approach is that the robot is limited to the prescribed behaviours, trading some autonomy for computational efficiency. Meneguzzi [6] describes the approaches that try to combine BDI with state based planning, but in a limited manner as plans are not added into the Library.

Here we describe a complementary approach. It starts with no plan library, carries out task planning to achieve goals, stores the plans that are generated, and reuses them where possible. We implemented this idea by introducing a Plan Library node in ROSPlan [7], a middle-ware layer between task planners and the Robot Operating System (ROS). This Plan Library node checks if the current planning task has already been solved. If it has, rather than invoking the *planner*, the previous plan is sent to the *acting component*.

II. Plan Library for ROSPlan

The Plan Library is a proxy for the Planner Interface from the default ROSPlan framework. Previously solved problems together with their plans (stored on in YAML format), are loaded as a dictionary during initialisation.

When the node receives a planning task as a PDDL file from ROSPlan's Problem Interface, it parses it into three parts: *types* indicating the types of instances involved in the problem, *init* defining the predicates in the initial state, and *goal* integrating the variables from the goal state. Next, the node iterates over the Plan Library, matching its initial state and goal elements with those of the problem it needs to solve. If there is a match, the iteration is interrupted and the plan from that Plan Library element is sent to the Parsing Interface.

If no problem from the Plan Library is found to match, then the problem is sent to the planner via the Planner Interface node. If it returns a solution to the problem, then it will be added as a new entry to the Plan Library along with the tasks *types*, *init*, and *goal*. The proposed methodology is PDDL agnostic, accepting all planning languages available in ROSPlan.

III. Empirical Evaluation

We used the temporal domain Office, consisting of a robot-assistant operating in a dynamic office setting. The robot is tasked with navigating the environment and bringing different office resources (e.g.: mugs, post or papers) to the people in it, asking humans for help when needed. We created 10 problems, increasing in planning difficulty — taking from 3 to 20 seconds to compute, and varying in length between 40 and 140 actions. Each of these problems was then solved and its robot execution simulated. Each action had varying probabilities of failing during execution (between between 0.5 and 0.9). When an action failed, a new plan was computed from that state. We ran each problem 40 times sequentially, meaning that the plan library was not cleared between these iterations, allowing the robot to learn through additions to the plan library. We compare our method with a standard version of ROSPlan without a Plan Library. We used the POPF planner

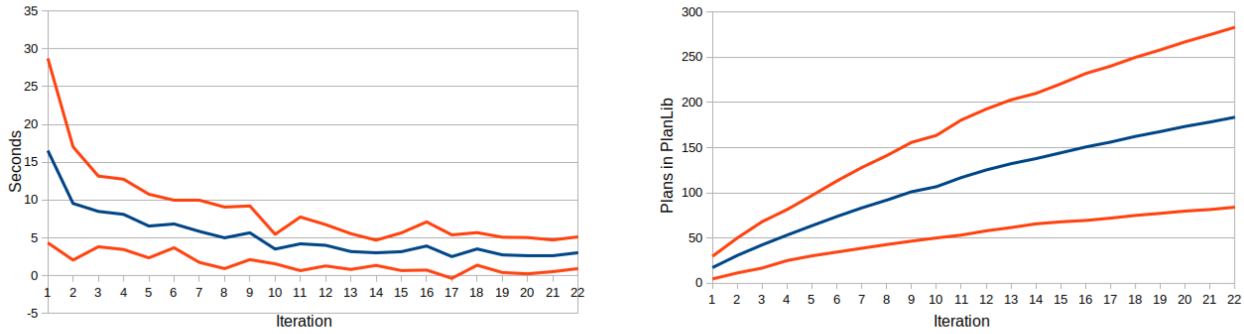

(a) (b)

Fig. 1: Summary plots averaged across all action failure probabilities on (a) Total planning time in seconds; (b) Number of plan in the plan library. Average values in blue, with ± 1 std deviation (red).

[8] with a timeout of 30 seconds to compute the plans. The overall system was given 500 seconds for each problem to be solved and reach the goal.

Over the course of our experiments, the modified version of ROSPlan reached the goal 1403 times out of the 2000 problem instances it faced (timing out the remaining times). The system spent an average of 0.022 seconds (7.2% of the total planning time) searching for plans in the Plan Library. The problem requested from the system was found in the Plan Library 64.6% of the times in total. In comparison, the standard version of ROSPlan managed to reach the goal 1645 times, performing better than the Plan Library version in the problems with more actions (100+). This is due to the fact that the Plan Library was being used blindly, exploiting only the plans it had solved already, with no exploration, meaning that if it got a poor plan in a prior run, it had a higher chance of getting stuck in it. This, together with higher action probability, would lead the agent into states that would need more than the allocated planning time (30 seconds) to solve, causing it to fail to reach the goal.

In Figure 1, we can see how the plan library performed overall. In short, across all the problems and probabilities of action failure, the plan library works effectively. Figure 1a shows that, over successive runs, the cost of planning falls, while Figure 1b exhibits that the plan library grows, but showing signs that the size of the library will plateau. The second of these is exactly what we would expect, and the first is exactly what we would hope.

IV. Conclusion & Future Work

Our results show that for a dynamic environment and medium length tasks, our approach manages, after a short number of runs, to gain enough experience for a considerable speed-up in deliberation to emerge.

Our experiments make the big assumption that all actions fail with the same probability. Once Covid allows, we will run experiments in real world environments, where action failure is a property of the world instead of it being defined in our simulation. This will give us a better idea of how often a Plan Library can be used, and how fast it can accumulate knowledge about the environment. Seeing if we can balance exploitation of past plans with exploration to discover new plans would be complementary to this work.

Knowing that the time spent searching for a plan is short (7.2% of all planning time), we will investigate if it is possible to add planners [9] that search for better quality plans. Comparisons between different types of heuristics [10] will tell us if using a Plan Library, makes it possible to use classical optimal planners in planning for robotics.

Finally, we are investigating if having a library of the robot's abilities would increase the explainability of its reasoning process. Given such a library, the robot would be able to keep track of its executions, giving a more in-depth explanation for its decision based on its *experiences*.

Acknowledgements

This research was partly funded by a PhD studentship from the Faculty of Natural and Mathematical Sciences at King's College London, and by EPSRC EP/R033722/1 Trust in Human Machine Partnerships.

References

[1] F. Ingrand and M. Ghallab, "Deliberation for autonomous robots: A survey," *Artificial Intelligence*, vol. 247, pp. 10–44, 2017.
[2] R. E. Fikes and N. J. Nilsson, "Strips: A new approach to the application of theorem proving to problem solving," *Artificial intelligence*, vol. 2, no. 3-4, pp. 189–208, 1971.
[3] M. Fox and D. Long, "PDDL2.1: An extension to PDDL for expressing temporal planning domains," *JAIR*, vol. 20, pp. 61–124, 2003.
[4] M. Bratman *et al.*, *Intention, plans, and practical reason*. Harvard University Press Cambridge, MA, 1987, vol. 10.
[5] R. H. Bordini, J. F. Hübner, and M. Wooldridge, *Programming multi-agent systems in AgentSpeak using Jason*. John Wiley & Sons, 2007.
[6] F. Meneguzzi and L. De Silva, "Planning in BDI agents: a survey of the integration of planning algorithms and agent reasoning," *The Knowledge Engineering Review*, vol. 30, no. 1, pp. 1–44, 2015.
[7] M. Cashmore, M. Fox, D. Long, D. Magazzeni, B. Ridder, A. Carrera, N. Palomeras, N. Hurtos, and M. Carreras, "ROSPlan: Planning in the robot operating system." in *ICAPS*, 2015, pp. 333–341.
[8] A. J. Coles, A. I. Coles, M. Fox, and D. Long, "Forward-chaining partial-order planning," in *ICAPS*, 2010.
[9] M. Martinez, I. Moraru, S. Edelkamp, and S. Franco, "Planning-PDBs planner in the IPC 2018," *IPC-9 Planner Abstracts*, pp. 63–66, 2018.
[10] I. Moraru, S. Edelkamp, S. Franco, and M. Martinez, "Simplifying automated pattern selection for planning with symbolic pattern databases," in *Künstliche Intelligenz*. Springer, 2019, pp. 249–263.

https://doi.org/10.31256/Px3Rq7M

Towards 5G-Enabled Education: Remote Laboratory and Training Prototype

Burak Kizilkaya*, Zhen Meng*, Guodong Zhao*, Liying Li†, and Muhammad A. Imran*
*School of Engineering, University of Glasgow, UK
† Department of Mathematics, Physics and Electrical Engineering, Northumbria University, UK
Email : b.kizilkaya.1@research.gla.ac.uk

***Abstract*—Advanced technologies have significant impacts on every aspect of education, where digital connectivity is the foundation to support the way people learn. Current Internet and pre-5G cellular communication networks can deliver visual and auditory data, which enable distance/virtual learning. However, remote physical interaction between students and learning facilities, which is an essential part of a new education paradigm is still missing. The 5G cellular network with impressive latency and reliability performance would be a game changer by enabling students to attend remote physical learning environment. In this paper, we introduce our prototype of real-time remote laboratory which enables students to attend remote physical environment and have interactive laboratory session with help of robotics.**

***Index Terms*—5G, prototype, remote lab, education**

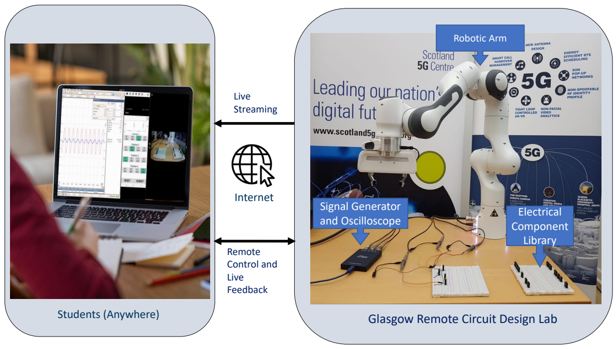

Fig. 1. The structure of the remote circuit design Lab

I. Introduction

The Covid-19 pandemic has affected 1.5 billion learners in 185 countries [1] and accelerated the transition from traditional education towards ubiquitous, personalised education that is part of the connected digital ecosystem [2]. Traditional education relies on face-to-face teaching in classrooms with hard copy materials. All assessments and examinations are paper based with space and time limited laboratory sessions. Mobile and digital connectivity will revolutionize education and make knowledge easily accessible.

Unfortunately, there are several aspects of higher education that require physical interaction between the student and laboratory facilities. This makes remote access to physical laboratories one of the vital requirements of future education. In order to enable remote access to the physical laboratories, the communication network needs to be able to deliver information with very high communication performance in terms of latency, reliability, and data rates. The fifth generation of cellular communications (5G) will enable new opportunities for future education. 5G has outstanding performance and capability [3] which are the foundations to support emerging technologies in future education. For example, Ultra-Reliable Low-Latency Communications (URLLC) would be the game changer since it enables the exchange of physical skills over the mobile communications [4], [5]. Enhanced Mobile Broadband (eMBB) supported Virtual Reality (VR) [6] and 360° video streaming would provide immersive experience to students in virtual classes. Massive Machine Type Communications (mMTC) supported smart campus would allow students to check the availability of facilities such as classrooms, laboratories, and sport equipment and provide remote booking and scheduling services.

In this paper, we focus on remote laboratory and training, which would be the first time in education sector that allows students to physically interact with remote laboratory environment. We demonstrate our remote laboratory prototype in Glasgow, UK and discuss future directions. Our main purpose is to provide first prototyping efforts on remote laboratory and training which will lead new directions and opportunities.

II. Remote Laboratory and Training Prototype

In this section, we present one of the earliest prototypes of remote laboratory and training[1] as seen in Fig. 1. It offers an unrivaled experience of remote interaction to students all around the world. Physically, the lab is located at James Watt School of Engineering, University of Glasgow, UK. It is now accessible to students from all around the world where students take control of a robotic arm to conduct circuit design experiments remotely over internet connection. The robotic arm is capable of assembling electrical circuits according to students' control commands by precisely placing electronic components (e.g. resistors, capacitors, etc.) on circuit boards. In addition, the remote lab prototype enables remote measurement of real circuit to complete lab task in circuit design courses. Specifically, remote lab consists of three main components:

This work is in part supported by EPSRC IAA (EP/R511705/1) Project.

[1]The demonstration video can be found at https://youtu.be/RCR5l72HVuM

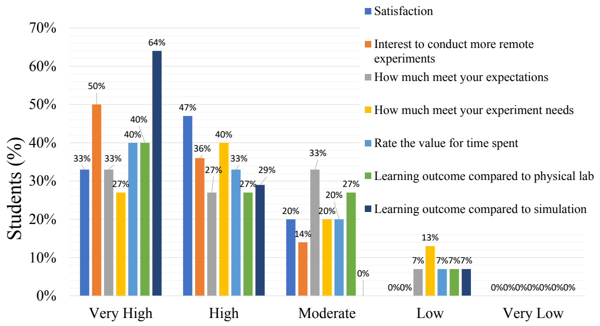

Fig. 2. Student survey results on the prototype of the remote circuit design lab.

- **Robotic Arm:** Franka Emika Panda robotic arm is used as a remote teleoperator. Robotic arm is programmed for assembling electrical circuits according to high-level user commands using Franka Control Interface(FCI) [7].
- **Communication Network:** Conventional internet access is used to communicate control commands and video feedback packets.
- **Control Interface:** A custom control interface is developed to be used in remote lab prototype which provides high level commanding interface to users.

Using aforementioned components, remote lab enables three main capabilities. First, students can observe the remote lab environment via high quality video streaming, which provides more engagement to remote environment. Secondly, students can control the remote robotic arm using custom design control interface. Lastly, students are able to control lab equipment (digital signal generator and oscilloscope) to take remote measurements.

A. Teaching and Learning Perspective

So far, more than 30 students in UK and China have used our remote lab prototype in their circuit design courses and we have conducted a survey to collect feedback from them. In Fig. 2, the survey results show that the majority of the students are satisfied with the remote lab and interested in conducting more remote lab experiments.

In addition, the remote lab prototype provides vast amount of advanced resources such as robot aided circuit design lab to more students with more flexible way which is not always possible because of space and time limitations in traditional lab environment. It also provides game based teaching with the help of advanced technology which in turn grasps more attention of students and enables more effective learning.

B. Discussion

The remote lab prototype is crucial in terms of two very important aspects. First, it is critical for collecting students' responses to real life remote laboratory experience. Second, it is vital for demonstrating the communication requirements of remote laboratory use case with real life testbed implementation to further emphasize the necessity of the 5G cellular communications. In this prototype, we have used conventional internet connection to conduct remote laboratory experiments in UK and China. We recorded communication latency of between $50 - 300$ ms in the UK and up to 2 seconds in China. Latency values are not stable and change depending on locations, internet speed, or other uncontrollable conditions in the internet. Students are asked for feedback after every session and as shown in Fig. 2, 20% and 14% (considering moderate, low, and very low) of students are not satisfied and unwilling to further engage with the remote lab experience, respectively, with latency being the main contributing factor. Students expect more smooth interaction with remote environment. In addition, high latency also affects the quality of experience of students which could lower interest and motivation in the subject. Another important aspect is the reliability of the communication network. Similar to other industrial robots, the robot is sensitive to packet loss which affects the control performance. For example, it can compensate for up to 20 consecutive packet drops then the control process stops. This implies that packet loss rate is very crucial in ensuring stable control which cannot be guaranteed with current communication networks. These results show the current capabilities as well as exigency of 5G and beyond cellular communications.

III. Conclusions

The future of education system will be enabled by a collection of emerging digital technologies which will create ubiquitous, immersive, adaptive and personalized learning experience. 5G is the key enabler of this ecosystem by supporting stringent communication requirements as well as providing high quality of experience for both the learners and tutors. In this study, we introduce our remote circuit design laboratory prototype and discuss teaching and learning perspectives, and emphasize the necessity of 5G for future education. As a future work, we will extend the capability of the remote lab by using 5G and Mobile Edge Computing to meet the stringent requirements of this use case based on advanced 5G and robotics platforms in University of Glasgow.

References

[1] G. Marinoni, H. van't Land, and T. Jensen, "The impact of covid-19 on higher education around the world," *IAU Global Survey Report*, 2020.
[2] Y. Siriwardhana, C. De Alwis, G. Gür, M. Ylianttila, and M. Liyanage, "The fight against the covid-19 pandemic with 5g technologies," *IEEE Engineering Management Review*, vol. 48, no. 3, pp. 72–84, 2020.
[3] M. A. Imran, Y. A. Sambo, and Q. H. Abbasi, *Enabling 5G Communication Systems to Support Vertical Industries*. John Wiley & Sons, 2019.
[4] A. Aijaz and M. Sooriyabandara, "The tactile internet for industries: A review," *Proceedings of the IEEE*, vol. 107, no. 2, pp. 414–435, 2018.
[5] K. Antonakoglou, X. Xu, E. Steinbach, T. Mahmoodi, and M. Dohler, "Toward haptic communications over the 5g tactile internet," *IEEE Communications Surveys & Tutorials*, vol. 20, no. 4, pp. 3034–3059, 2018.
[6] E. Bastug, M. Bennis, M. Médard, and M. Debbah, "Toward interconnected virtual reality: Opportunities, challenges, and enablers," *IEEE Communications Magazine*, vol. 55, no. 6, pp. 110–117, 2017.
[7] *Franka Control Interface Documentation*, Franka Emika, April 2017, https://frankaemika.github.io/docs/.

https://doi.org/10.31256/On8Hj9U

The need for speed: How 5G communication can support AI in the field

Adrian Salazar Gomez[1], Tsvetan Zhivkov[1], Junfeng Gao[1], Elizabeth I Sklar[1], and Simon Parsons[2]

[1]*Lincoln Institute for Agri-food Technology, University of Lincoln*, UK
Email: {asalazargomez, tzhivkov, jugao, esklar}@lincoln.ac.uk

[2]*Lincoln Centre for Autonomous Systems, University of Lincoln*, UK
Email: sparsons@lincoln.ac.uk

***Abstract*—Using AI for agriculture requires the fast transmission and processing of large volumes of data. Cost-effective high speed processing may not be possible on-board agricultural vehicles, and suitably fast transmission may not be possible with older generation wireless communications. In response, the work presented here investigates the use of 5G wireless technology to support the deployment of AI in this context.**

***Index Terms*—robotics, 5G, computer vision, agriculture**

I. Introduction

The agricultural workforce in the UK is both ageing and shrinking in numbers threatening food security of the UK. One response is increased automation, employing robotics and AI to lighten the load on UK farmers [2]. This has the advantage of increasing sustainability, since it allows for more precise targeting of fertilizers, herbicides and pesticides.

For example, herbicide is used to control weeds in fields with young crops. The herbicides are selective, so do not damage the crop, but kill the weeds. Currently, entire fields are sprayed to ensure all weeds are treated. This is wasteful, spraying areas that do not contain weeds. Advances in computer vision mean sprayers can be equipped to only spray where there are weeds to kill. Such an approach is estimated to save up to 90% [6] of the herbicide currently used.

Applications of AI in agriculture, which include the use of robots for fruit harvesting and yield estimation as well as weed and pest control, use cameras as their primary sensors. State-of-the-art methods for processing these images are based on *deep learning*. They therefore have heavy computational demands which may not be met by the relevant vehicles, either because of the power required, or because it is not cost-effective to equip every vehicle with a suitable computer. As a result, the computation may be delivered better through edge or cloud computing. However, this creates a further demand: that of transmitting the data from farm vehicles to the processing. For a field sprayer with a standard 24 meter boom, a spray nozzle per meter and HD cameras associated to each nozzle to scan the ground below it, this can involve transfer rates approaching 1 GBit/s which are beyond WiFi and 4G wireless links.

Research is supported through a UKRI Research England E3 grant, Lincoln Agri-Robotics; and through Ceres.

In the remainder of this paper we present pilot results from work to demonstrate how 5G wireless can handle such a load.

II. Networking experiments and results

As an experimental platform, we are using a Leo Rover robot (illustrated in figure 1) equipped with a Raspberry Pi 4 and two 5G-SA (stand-alone) enabled mobile phones. The experiments were split into two parts, to evaluate WiFi and 5G network performance. The WiFi network used the 2.4GHz band and the 5G network used the N78 band, which was provided by the 5G mobile phones located on top of the robot platform. In the experiment setup, the Rover (under human control) followed a fixed path while streaming a video of a sequence of images (at a resolution of 1920x1080 and running at 30 frames-per-second) using a wireless connection. The video stream was compressed over the network (H.264) and the throughput was on average 7.64Mbps for WiFi and 6.86Mbps for 5G. The throughput for 5G is 10% better than for WiFi. Due to the H.264 traits, the more unstable the connection the worse the compression algorithm performs [5].

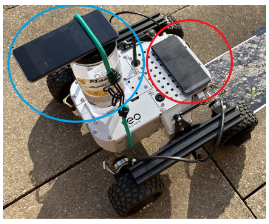

Fig. 1: The Leo Rover setup for 5G. The item in the orange circle is a 5G mobile phone enabled with 5G-SA connectivity.

During the trials, the WiFi station was at a distance of ≈10 meters from the robot, and the 5G antenna was on the roof of a building at a distance of ≈130 meters. For both connections, we evaluated the latency; latency is the time taken for data to travel to the destination and get back to the sender device. To do so, we measured, in milliseconds (ms), the difference between the time when a data packet was sent and the time when the sender got the packet acknowledgement. Figure 2 shows the latency results of the WiFi and 5G networks. The average latency for 5G is ≈18ms and WiFi is ≈227ms, which is over 12 times greater. The lower latency average and the

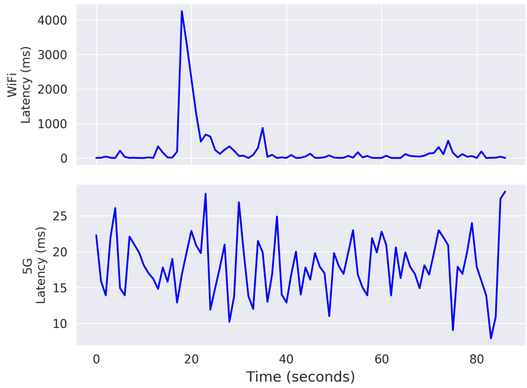

Fig. 2: Latency plot. Note the different y-axis scales between the top (WiFi) and bottom (5G) plots. The maximum latency for 5G is two orders of magnitude lower (better) than for WiFi.

smaller standard deviation for 5G over WiFi indicates that 5G communications are more stable and consistent.

III. Vision Results

As an example task, we are considering spraying for weeds, as described above. From a machine vision perspective, this means running an object detector on image data from the vehicle. However, fast and accurate detectors require GPUs with high specifications, which, in most of the times, cannot be mounted on autonomous systems because high-end GPUs require a lot of energy and need to remain steady. As discussed above, a potential solution is to place the necessary GPU on a remote server at risk of the transmission medium being too slow or unreliable and limiting the vehicle's mobility. However, our experiments suggest that a robot can communicate with a GPU processor without significant issues with latency, and hence reliability, if we are using 5G.

Another potential issue is the speed with which the object detector can operate. We evaluated this using an object detector to identify weeds within a sugar beet crop. The object detector was YOLO5l, which is a one-stage object detector based on a YOLOv4 [1] architecture with a backbone based on CSPNet [7], a PA-NET neck [4], mosaic data augmentation, and auto learning bounding box anchors. The size of the model on the GPU is 3.9GB We trained this detector using the dataset provided in [3], which contains pictures of sugar beets and field bindweed with their corresponding ground truth bounding boxes (fig 3.a). The dataset split was 70% for training, 10% for validation, and 20% for testing. The detector was trained over 300 epochs using a batch size of 16, an SGD optimiser with a learning rate of 0.0001 and a momentum of 0.95, and a image resizing strategy where the shortest image side is converted to 640 pixels and the longest size is resized to keep the original image ratio. The resulting trained model couldn't run on the robot's Raspberry Pi 4, because the Pi's RAM does not meet the memory requirements of the model (3.3GB). However, the model can run suitably quickly on a GPU. Based on the speed with which a single image frame is processed, this model locates sugar beets and weeds at a speed of 104 fps (frames per second) on a GTX1050 Ti and 196 fps on a RTX2080 Ti.

(a) Ground truth data (b) Prediction example

Fig. 3: Sugar beet images with (a) ground truth bounding boxes and (b) predicted bounding boxes. Note that since this work was too early in the season for sugar beet to be growing, our initial experiments involved a simulated field made up of photographs from [3].

We tested the trained model over wireless connections using the setup in section II, where the images contained sugar beets and weeds, and the remote device receiving the video stream had a GeForce GTX1050 Ti to operate the detection model. During the WiFi and 5G trials, the detector identified items on the video frames at a speed of 50 fps. Fig. 3.b shows an example of the bounding boxes inferred by the detector. These results confirm that, with high-end GPUs, vision systems need not be a bottleneck in the detection of items in a video stream as long as the data transmission is fast enough.

IV. Conclusions and Future Work

Robot communication over 5G networks is faster and more reliable than WiFi communications. Using 5G, we provided a successful example of how the vision that is critical for agri-robotics can be carried out on a remote computer.

Future experiments will test whether 5G networks can handle more information (larger images, depth information) from a single camera and information from multiples sources (more cameras and more robots roaming the fields). A particular challenge is scaling up to the number of cameras required on a commerical sprayer.

References

[1] A. Bochkovskiy, C.-Y. Wang, and H.-Y. M. Liao. YOLOv4: Optimal speed and accuracy of object detection. *arXiv preprint:2004.10934*, 2020.

[2] T. Duckett, S. Pearson, S. Blackmore, B. Grieve, W.-H. Chen, G. Cielniak, J. Cleaversmith, J. Dai, S. Davis, C. Fox, et al. Agricultural robotics: the future of robotic agriculture. *arXiv preprint arXiv:1806.06762*, 2018.

[3] J. Gao, A. P. French, M. P. Pound, Y. He, T. P. Pridmore, and J. G. Pieters. Deep convolutional neural networks for image-based Convolvulus sepium detection in sugar beet fields. *Plant Methods*, 16(1):1–12, 2020.

[4] S. Liu, L. Qi, H. Qin, J. Shi, and J. Jia. Path aggregation network for instance segmentation. In *Proceedings of the IEEE Conference on Computer Vision and Pattern Recognition*, pages 8759–8768, 2018.

[5] I. E. Richardson. *H. 264 and MPEG-4 video compression: video coding for next-generation multimedia*. John Wiley & Sons, 2004.

[6] E. Tona, A. Calcante, and R. Oberti. The profitability of precision spraying on specialty crops: a technical–economic analysis of protection equipment at increasing technological levels. *Precision Agriculture*, 19(4):606–629, 2018.

[7] C.-Y. Wang, H.-Y. M. Liao, Y.-H. Wu, P.-Y. Chen, J.-W. Hsieh, and I.-H. Yeh. CSPNet: A new backbone that can enhance learning capability of CNN. In *Proceedings of the IEEE/CVF conference on computer vision and pattern recognition workshops*, pages 390–391, 2020.

https://doi.org/10.31256/Qb8Xt6P

Wearable Sensor Tools for Efficient Human Robot Interaction

Max Workman
Intlligent Automation Centre
Loughborough University
Loughborough, UK
m.j.workman-18@student.lboro.ac.uk

Ali Al-Yacoub
Intelligent Automation Centre
Loughborough University
Loughborough, UK
a.al-yacoub@lboro.ac.uk

Ella-Mae Hubbard
Intelligent Automation Centre
Loughborough University
Loughborough, UK
E.Hubbard@lboro.ac.uk

Abstract— **Human-robot interaction (HRI) technology is growing rapidly, with many products being designed to operate outside the industry, such as in the home. However, controlling robots in a domestic setting is challenging due to high variations in such environments. Also, human behaviour varies, and the same individual might behave differently in similar situations. In this paper, the design of a wearable data acquisition system, comprised of wearable sensors and a control box that communicates wirelessly with sensors on the robot to improve safe human-robot collaboration on tasks, is revised. The literature review identifies factors that affect the robotic system's wearability and leads to the production of a Product Design Specification (PDS), against which the original and subsequent designs of the set-up are evaluated. Several iterations are assessed, and how limitations in the original design are overcome are explained with reference to the system's location, ergonomics, and wearability. The final prototype is then tested on human users using 'range of motion' and 'representative task' experiments to assess its improved wearability. The potential applications of the device in the domestic environment are explained and suggestions for the future scope of the research made.**

Keywords—Human-Robot Interaction, wearable technology, robots, product design, wearability, user friendliness

I. Introduction

Human-robot wearable technology has developed to manage the communications between a human and a robot, to allow them to collaborate safely and efficiently. This paper reviews human wearable technology that is being developed for an industrial setting and explores how it could be used domestically. The focus was to revise the design of the data acquisition box that uses wearable sensors to monitor a human's physical and physiological state and then wirelessly communicates with a robot's sensors to control its movement better, creating improved human-robot collaboration on tasks. How the system can be modelled to be aesthetic, ergonomic and comfortably located to enhance the user's experience is explored and tested. The system investigated was produced by an Engineering and Physical Sciences Research Council (EPSRC) DigiTOP project.

II. Literature review

A. Significance of Wearable technology

In an industrial setting Human-Robot Collaboration (HRC) needs to work effectively to maximise efficiency and minimise risks, requiring situational awareness by the human and active avoidance of contact by the robot. Stress in humans can lead to a reduced situational awareness, which in turn can increase the likelihood of accidents [1]. Wearable technology is the communication interface between man and machine. Kasier et al. [2] found the ergonomic design of the wearable technology significantly impacts the user and therefore the effectiveness of the human-robot collaboration.

B. Design of Wearable Technology

Findings from an industrial setting can be applied in a domestic environment, where design factors such as aesthetics may prevail. Thomas et al. argues that when designing a wearable device emphasis must be put on human factors [3].

This includes **aesthetics**, which means a design that is more attractive than functional, shows improved desirability [4]. Potential hazards can be mitigated through **ergonomic** design, creating opportunities to produce a welcoming environment for use. To achieve comfort levels that enable humans to acclimatise quickly to the wearable technology, it must have acceptable temperature, shape, texture, weight and tightness [5], enabling normal movements without physical or psychological constraint.

Contextual awareness affects comfort, which can vary significantly in different social contexts [6]. **Ease of use** and simplicity can increase engagement level which can also have a positive effect on productivity [7]. **Reliability** is a key factor, and includes safety, precision and effectiveness [8]. **Wearability** involves physical shape and its active relationship with the human form and is a key aspect to the user's engagement and satisfaction [9].

C. Location of Wearable Technology

The Institute of Complex Engineered Systems (ICES) has developed six parameters for wearability [9] which affect the location on the body chosen for wearable technology products, and these include **attachment**: how forms are fixed to the body, **size;** cross section variation of the human body, **human movement**; how body form changes with motion, **unobtrusivity**; less obtrusive areas for wearable products, and **body motion**; areas with low movement/flexibility are shown by Langer lines, which define the direction within the skin that has the least flexibility.

III. Design, Methodology and Approach

The design approach was to develop a PDS and analyse the original design, and new iterations of the data acquisition system.

Liaising with the DigiTOP team, the changing electronic needs were addressed, hardware improvements were made to accommodate the updated Printed Circuit Board (PCB) and other design changes were identified. The original design favoured functionality over human-centred design, so was not as user friendly and the body attachment was not optimal. Also, the original location was obtrusive, made movement difficult and ergonomically was not comfortable. Loose connections were causing electrical noise and wires outside the box caused issues as they interfered with the user's movements. [10].

New design iterations were developed and assessed against the PDS until the most viable solution was created. The new prototype system was then tested by human users to assess its improved wearability using 'range of motion' and 'representative task' experiments.

The location on the body of the acquisition box affected other design factors and was therefore addressed first. The lower back area is one of the least intrusive places on the body, interfering minimally with prominent moving parts such as the arms and shoulder blades. The device is used primarily on standing pose, so this location does not interfere with a worker's physical movement.

Additionally, locating the device on the lower back allows wires to travel up the spine, making them unobtrusive and keeping them away from the user's limbs, as shown in Fig. 1. The existing solution used a belt to secure the device, but there was no place to contain the wires effectively. After exploring different options, a vest type garment was identified as the most suitable. This allowed the device to be held securely in the desired location and provided a suitable means of containing the wires. The wires could also travel up the spine, contained in an enclosed section of the vest, avoiding complications surrounding the user's movement.

Next, the inner workings were considered. The new location influenced the layout of electronics significantly, allowing the wires to exit the top of the box and travel up the spine, as shown in Fig. 2. This meant the PCB was oriented on top of the Raspberry Pi with the battery and charging board positioned to the side. To reduce electrical noise the sensor connections to the electronics in the box are clamped within the box frame reducing movement.

All design refinements were then tested to check they made the product more wearable, user friendly and effective. The new location allowed improved, uninterrupted movement and the improved wire layout avoided interference with the user as they were working. The vest meant the device could also be set up more quickly and easily.

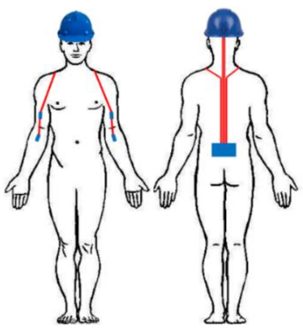

Fig. 1: Location of device, sensors and wires

Fig. 2: Box location on vest

IV. Results and Findings

The data acquisition system was designed for an industrial setting. However, programming service robots to intuitively perform a domestic task can be achieved by capturing human action in a structured environment using the proposed design. Then, using artificial intelligence and machine learning algorithms, this data can be utilised to program robots to carry out domestic tasks with human-like behaviour. The redesign of this wearable technology system improved the control box location, wires layout, electrical noise level, ease of use, obtrusivity, comfort, wearability and housing of the internal electronics. All these improvements reduced any effect wearing the device might have on human behaviour whilst interacting with robots. As a result, improved classification of human intentions and activities during human-robot collaboration can be made; and hence robots can actively adapt to ensure human safety while addressing the required actions.

V. Research Limitations and Implications

This research was limited to the informed redesign of the control box, the route of the wiring and how these are worn by the human. By improving the wearability of the system, which is used to allow humans and robots to work collaboratively on tasks, the redesigned prototype has improved many features that give it the potential and suitability to work in the domestic environment even though the DigiTOP system is designed for an industrial setting.

Acknowledgment

This work was funded by the EPSRC as part of the DigiTOP project (DigiTOP; EP/R032718/1). The authors of this paper would like to thank the various authors of referenced material for their permission to use figures and tables in this paper.

References

[1] M. R. Endsley, "(PDF) Endsley, M.R.: Toward a Theory of Situation Awareness in Dynamic Systems. Human Factors Journal 37(1), 32-64." https://www.researchgate.net/publication/210198492_Endsley_MR_Toward_a_Theory_of_Situation_Awareness_in_Dynamic_Systems_Human_Factors_Journal_371_32-64 (accessed Nov. 12, 2020).

[2] L. Kaiser, A. Schlotzhauer, and M. Brandstötter, "Safety-related risks and opportunities of key design-aspects for industrial human-robot collaboration," in *Lecture Notes in Computer Science (including subseries Lecture Notes in Artificial Intelligence and Lecture Notes in Bioinformatics)*, 2018, vol. 11097 LNAI, pp. 95–104, doi: 10.1007/978-3-319-99582-3_11.

[3] S. Thomas, "4 main factors that affect hardware design in wearable devices." https://www.einfochips.com/blog/4-main-factors-that-affect-hardware-design-in-wearable-devices/ (accessed Oct. 29, 2020).

[4] Leonardo Angelini, "(PDF) Designing a Desirable Smart Bracelet for Older Adults." https://www.researchgate.net/publication/262187864_Designing_a_Desirable_Smart_Bracelet_for_Older_Adults (accessed Nov. 12, 2020).

[5] W. Tharion, "(PDF) Acceptability of a Wearable Vital Sign Detection System. Vital Signs Detection System (." https://www.researchgate.net/publication/268358384_Acceptability_of_a_Wearable_Vital_Sign_Detection_System_Vital_Signs_Detection_System (accessed Nov. 13, 2020).

[6] D. Siewiorek, A. Smailagic, and T. Starner, "Application design for wearable computing," *Synth. Lect. Mob. Pervasive Comput.*, vol. 3, pp. 1–66, Jan. 2008, doi: 10.2200/S00106ED1V01Y200801MPC003.

[7] J. Hanaysha, "Improving employee productivity through work engagement: Empirical evidence from higher education sector," *Manag. Sci. Lett.*, vol. 6, pp. 61–70, 2016, doi: 10.5267/j.msl.2015.11.006.

[8] G. Cho, "(PDF) Smart_Clothing_-_Technology_and_Applications_(Human_Factors_and_Ergonomics)-Gilsoo_Cho.pdf | Sachin Roy - Academia.edu." https://www.academia.edu/37239520/Smart_Clothing_Technology_and_Applications_Human_Factors_and_Ergonomics_Gilsoo_Cho_pdf (accessed Nov. 13, 2020).

[9] F. Gemperle, C. Kasabach, J. Stivoric, M. Bauer, and R. Martin, "Design for Wearability." Accessed: Nov. 12, 2020. [Online]. Available: http://www.ices.cmu.edu/design/wearability.

[10] A. Al-Yacoub, A. Buerkle, M. Flanagan, P. Ferreira, E.-M. Hubbard, and N. Lohse, "Effective Human-Robot Collaboration Through Wearable Sensors," in *2020 25th IEEE International Conference on Emerging Technologies and Factory Automation (ETFA)*, Sep. 2020, vol. 2020-Septe, pp. 651–658, doi: 10.1109/ETFA46521.2020.9212100.

https://doi.org/10.31256/Sa3Rn8N

Design and Validation of Mobile Robot with Hybrid Wheel-Leg Design

Elizabeth Smith, Eisa Anwar and Ildar Farkhatdinov
School of Electronic Engineering and ComputerScience
Queen Mary University of London
London, United Kingdom
e.smith@se18.qmul.ac.uk, i.farkhatdinov@qmul.ac.uk

***Abstract*—This paper presents a novel concept of a hybrid wheel-legged robot used to navigate uneven or difficult terrain. We present the design prototype and validation testing where the onboard sensors' data is used to navigate around or over obstacles with the wheels or legs. During testing the prototype was found to be able to climb a step of 70 mm using the legs. With further adjustment to the back of the robot this could be increased. It could also detect potential obstacles directly in front of it using only a few sensors.**

Keywords—mobile robot, hybrid locomotion

I. Introduction

Mobile robots with hybrid locomotion are a more recent research area for mobile robotics which offers the flexibility of leg-based movement combined with the efficiency of wheel-based movement. These types of robots have many applications, including remote exploration, assisting rescue operations, and deployment in environments not designed or adapted for wheel-based robots.

Most existing designs fall into one of two categories: wheels fixed to the end of legs and wheels that transform into legs. The designs which feature wheels fixed to the end of legs are diverse: they vary from legs with only one degree of freedom [1] to designs with five actuators per leg [2]. The robots described in these papers tended to be larger than robots in the other category but have smaller wheels. This means when in use they would rely on legged movement more due to the small wheels being unable to reach any height above the radius of the wheel. The higher number of actuators means they are complex and expensive to implement.

The category of designs which had wheels that transform into legs splits into two subcategories: wheels that transform into legs ([3] and [4]) and rotating legs that protrude outwards and rotate with the wheel ([5] and [6]). These designs are simpler than the ones discussed above but most still use several actuators per wheel/leg unit. Few designs have any physical validation or implementation.

A further limitation of previous works is that they do not discuss how the robots could transition between wheeled and legged mode based on the environment (with the exception of [6], which uses an environment-based trigger to transition between wheeled and legged mode, but only climbing onto an obstacle is discussed, not climbing off). The solution discussed in this paper will feature autonomous transitioning between legged and wheeled mode. This work presents the results obtained during the final year project conducted by the first author.

II. Proposed Solution

Our design is based on a combination of co-axial leg-wheel actuation which requires two actuators per wheel/leg unit and will use sensor information to autonomously transition between wheeled and legged mode. The wheels are 120 mm in diameter and the legs are 125 mm from axis centre to top edge. The robot is shown in Figure 1.

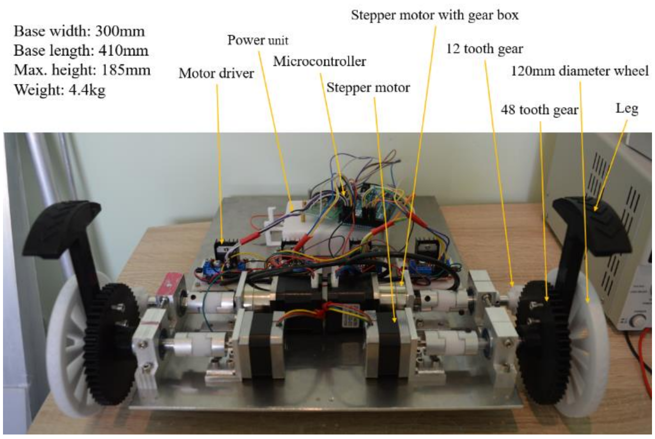

Figure 1: The prototype with hybrid leg-wheel design.

Overall, the robot has two wheels and two legs, and each leg rotates around the same axis as its corresponding wheel. The wheels are rotated using separate motors (for this implementation stepper motors have been used, but brushless DC motors can also be used).

The legs are rotated using separate stepper motors, which are adjacent to the wheel motors. They control the legs via gears; with one gear attached to the motor shaft and the other attached to the leg. The gears have a 4:1 reduction ratio to provide more torque to the legs when lifting the robot.

Although this slows the rotation of the legs to ¼ of the motor speed, the legs only need to do one full rotation in order to bring the wheels up onto the obstacle. In the centre of the leg gear is a bearing which allows the wheel and leg to move independently of one another. During wheeled movement, the legs sit stationary in the upright position (as shown in Figure 1). When engaged they rotate once.

The hook shape on the front end of the leg engages with the (horizontal) surface of the obstacle (ledge or step) to be climbed.

This then lifts the robot onto the obstacle, until the wheels sit directly above the legs in the downwards position. The hooks are curved and wide to provide a smooth movement with enough grip to stop them slipping while the robot is being lifted into position. Once the legs have finished the rotation, the wheels re-engage, "dragging" the back of the robot up onto the ledge. This is shown in Figure 2.

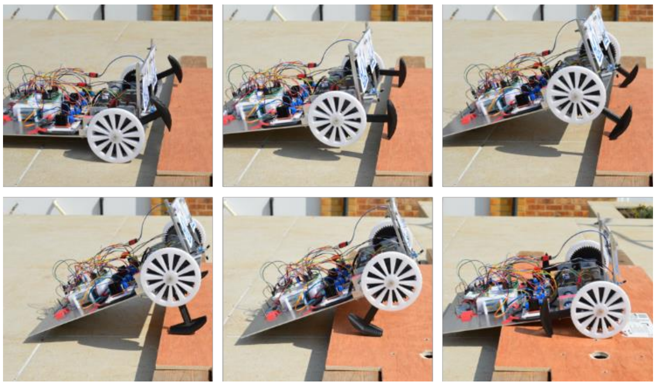

Figure 2: Robot overcoming 60 mm step.

The robot is controlled using an Arduino Mega 2560 microcontroller. For the initial testing of the concept, the controller is connected to a Bluetooth module which in turn is be connected to a smartphone application. The application is used to directly control the hybrid leg-wheel mechanism. Three distance sensors are placed on the front side of the robot: one ultrasound sensor and two infrared sensors. The ultrasound sensor is raised above the base of the robot (placed at a height just under the maximum leg height) and is used to detect open space above an obstacle. It is necessary to use ultrasound rather than infrared in this role because distance data will be needed to determine if there is enough space for the robot to climb onto the obstacle/ledge detected. One infrared sensor is placed on the base of the robot in a horizontal orientation and is used to detect obstacles and walls. The second infrared sensor faces downwards from the base and is used to detect drop offs that are too large for the robot to simply roll off, but rather test the distance with its legs.

III. Testing and Results

The initial testing of the robot investigates the mechanical capabilities of the robot. This includes: the maximum upwards and downwards gradient the robot is capable of traversing; the maximum obstacle height the robot can overcome; the maximum drop off the robot can overcome (using its legs).

The testing will be carried out on the same surfaces throughout. With the sensor placement as described in section II, the following research questions will be answered: can the robot detect and climb over obstacles of up to the maximum height reached in the initial experiments, can the robot determine whether a ledge is of a height that is safe to climb down, and can the robot detect obstacles and stop before impact? An accelerometer and gyroscope sensor will also be mounted on the robot base to provide data about the stability and vibration in the robot during movement. The testing will be performed on the same surfaces as the initial testing. Obstacles will be built from wooden blocks with the same wood piece on the top for each one, so the legs are using the same surface for each experiment. Each experiment will be performed ten times.

During the initial testing it was found that the robot had a maximum climbing height of 70 mm. The limiting factor here was not the length of the legs as expected but the back of the robot, which was too heavy to be lifted higher and the legs slipped along the surface when trying to bring the back up onto the obstacle. The acceleration measurements showed considerable vibration during leg movement. The acceleration peaks observed in the data showed when the legs of the robot were lifting the wheels into the air. At the end of the experiment the back of the robot dropped off the obstacle, resulting in the large impact.

IV. Discussion and Conclusion

Our work has several limitations which will be addressed in the future. We are conducting more tests to explore the performance of the proposed hybrid locomotion mechanism on different types of terrain and obstacles. The design of the robot will be improved to address potential limitations.

The limiting factor of the robot's climbing was its inability to pull the back of the robot up onto an obstacle. This would be addressed in a four wheeled version as it could use the back legs to climb, and it could possibly handle more weight. It may also be possible to decrease the time taken for the robot to climb an obstacle by increasing the speed of the leg rotations. Further experiments can be done to optimise the speed so the robot can both move faster and still lift any specified weight requirements.

Future design versions may support four legged-wheeled configurations for applications such as rescue and remote exploration tasks. Further sensors may also be added to increase the awareness of the robot and improve its response to more complex obstacles. We plan to test the proposed concept combined with human-machine interfaces previously developed in our team [7,8,9]

References

[1] Smith, J., Sharf, I. and Trentini, M., 2006. PAW: a Hybrid Wheeled-Leg Robot. *Proceedings of the 2006 IEEE International Conference on Robotics and Automation*.

[2] Schwarz, M., Rodehutskors, T., Schreiber, M. and Behnke, S., 2016, May. Hybrid driving-stepping locomotion with the wheeled-legged robot Momaro. In *2016 IEEE International Conference on Robotics and Automation (ICRA)* (pp. 5589-5595).

[3] Shen, S.Y., Li, C.H., Cheng, C.C., Lu, J.C., Wang, S.F. and Lin, P.C., 2009, October. Design of a leg-wheel hybrid mobile platform. In *2009 IEEE/RSJ International Conference on Intelligent Robots and Systems* (pp. 4682-4687).

[4] Ning, M., Xue, B., Ma, Z., Zhu, C., Liu, Z., Zhang, C., Wang, Y. and Zhang, Q., 2017. Design, analysis, and experiment for rescue robot with wheel-legged structure. *Mathematical Problems in Engineering, 2017*.

[5] Sun, T., Xiang, X., Su, W., Wu, H. and Song, Y., 2017. A transformable wheel-legged mobile robot: design, analysis and experiment. *Robotics and Autonomous Systems*, 98, pp.30-41.

[6] Wang, X., Wang, X., Yu, H., Wang, H., Lu, L., Vladareanu, L. and Melinte, D.O., 2014, July. Dynamic analysis for the leg mechanism of a wheel-leg hybrid rescue robot. In *2014 UKACC International Conference on Control (CONTROL)* (pp. 504-508).

[7] Farkhatdinov I, Ryu JH, Poduraev J. Control strategies and feedback information in mobile robot teleoperation. *IFAC Proceedings Volumes*. 2008 Jan 1;41(2):14681-6.

[8] Otaran A, Farkhatdinov I. A Short Description of an Ankle-Actuated Seated VR Locomotion Interface. In *2021 IEEE Conference on Virtual Reality and 3D User Interfaces Abstracts and Workshops* (VRW) 2021 Mar 27 (pp. 64-66).

[9] Brown, J, Farkhatdinov I, A Soft, Vibrotactile, Shape-Changing Joystick for Telerobotics, *IEEE Worldhaptics work-in-progress*, July, 2020.